National Library of Canada
Acquisitions and Bibliographic Services Branch
395 Wellington Street
Ottawa, Ontario
K1A 0N4

Bibliothèque nationale du Canada
Direction des acquisitions et des services bibliographiques
395, rue Wellington
Ottawa (Ontario)
K1A 0N4

Your file Votre référence

Our file Notre référence

NOTICE

The quality of this microform is heavily dependent upon the quality of the original thesis submitted for microfilming. Every effort has been made to ensure the highest quality of reproduction possible.

If pages are missing, contact the university which granted the degree.

Some pages may have indistinct print especially if the original pages were typed with a poor typewriter ribbon or if the university sent us an inferior photocopy.

AVIS

La qualité de cette microforme dépend grandement de la qualité de la thèse soumise au microfilmage. Nous avons tout fait pour assurer une qualité supérieure de reproduction.

S'il manque des pages, veuillez communiquer avec l'université qui a conféré le grade.

La qualité d'impression de certaines pages peut laisser à désirer, surtout si les pages originales ont été dactylographiées à l'aide d'un ruban usé ou si l'université nous a fait parvenir une photocopie de qualité inférieure.

Canada

Effects of Buoyancy Forces on Miscible Liquid-Liquid Displacements in Porous Media

by

Tianle Guo

A thesis submitted to
the school of Graduate Studies
in partial fulfilment of the requirements for the
degree of Master of Applied Science
in
Chemical Engineering

DEPARTMENT OF CHEMICAL ENGINEERING
UNIVERSITY OF OTTAWA
OTTAWA, ONTARIO.

UNIVERSITÉ D'OTTAWA
UNIVERSITY OF OTTAWA

Abstract

The effects of gravity forces on the miscible displacement of one fluid (aqueous glycerol solution) by another fluid (pure water) in a vertical consolidated porous medium have been investigated. A set of horizontal displacement experiments was performed for comparison with two sets of vertical -upward and vertical-downward displacements. It was found that gravitational forces (i.e. buoyancy forces) can be an important factor in determining the displacement pattern where fluids having different densities and different flowrates are involved.

In a given porous medium system, the principal variables which affect the displacement efficiency of oil (or any other miscible liquid) by water are the viscosity ratio, density difference, and displacement flowrate. Increasing the viscosity ratio will decrease the oil recovery; however, when the viscosity ratio is close to unity, good oil recovery will be obtained. The injection flowrate is also critical. At low injection flowrates, the effects of gravity become relatively more important. At high flowrates, gravity forces have less effect on the displacement efficiency.

In vertical-upward displacements, buoyancy forces play a negative role since they tend to promote viscous fingering and consequently lower the oil recovery (when $\rho_{oil} > \rho_{water}$). On the other hand, in vertical-downward displacements, buoyancy forces tend to stabilize the displacement process, and high oil recoveries can be obtained. Comparing the horizontal displacement patterns with those of the two vertical displacements, it was found that buoyancy forces can exert very significant effects on fingering phenomena.

Acknowledgement

I would like to thank my research supervisor, Dr. G. Neale, for his invaluable guidance and assistance during the course of the experimental work as well as the preparation of this thesis.

I would like to thank Mr. Louis Tremblay, Mr. Giuseppe Gasperetti and Mr. Adriano Bonaldo for their wonderful assistance during the fabrication and installation of the experimental equipment, and Mr. Youssef Touhami and Mr. Ensheng Zhao for their great help regarding computer work.

Nomenclature

1. Abbreviations

OOIP: original oil-in-place.

EOR: enhanced oil recovery.

IFT: interfacial tension.

2. Greek letters

μ_o : viscosity of displaced fluid [mPa.s].

μ_w : viscosity of displacing fluid [mPa.s].

ρ_o : density of displaced fluid [g/cm^3].

ρ_w (ρ_{water}): density of displacing fluid [g/cm^3].

$\Delta\rho$: density difference between displaced and displacing fluids [g/cm^3].

θ : diffusion time [s].

θ_d : time required by displacing fluid to pass through diffusion zone [s].

Φ : porosity of porous medium [dimensionless].

σ : measurement of the inhomogeneity from original position of

an interface [cm].

3. Symbols

d (d_p) : diameter of particle [cm].

D_l : longitudinal molecular coefficient [cm^2/s].

D_t : transverse molecular coefficient [cm^2/s].

D_o : molecular diffusion coefficient of water in glycerol solution [cm^2/s].

F : formation electrical resistivity factor [dimensionless].

g : gravitation acceleration [cm/s^2].

Ngr : gravity number = $\mu_w V/\Delta\rho g d^2$ [dimensionless].

H : height of porous medium [cm].

K : permeability of porous medium [μm^2].

K_l : total longitudinal dispersion coefficient [cm^2/s].

K_t : total transverse dispersion coefficient [cm^2/s].

L : length of porous medium [cm].

M : viscosity ratio = μ_o/μ_w [dimensionless].

M_{cell} : weight of porous medium cell [g].

$M_{cell\text{-}water}$: weight of cell saturated with water [g].

M_{water} : weight of water in cell [g].

P : pressure [mPa].

Pe : Peclet number [dimensionless].

Q : injection flowrate [ml/hr].

R : fractional oil recovery [dimensionless].

Re : Reynold number [dimensionless].

S : aspect ratio = H/d [dimensionless]

T_{br} : breakthrough time [s].

U : average velocity [cm/s].

U_{st} : stable displacement velocity [cm/s].

U_c : critical displacement velocity [cm/s].

V_{pore} : pore volume [cm^3].

V_{water} : volume of water in cell [cm^3].

V : volume of porous medium [cm^3].

X : distance measured from original position of an interface [cm].

X_{max} : maximum distance from original position of an interface [cm].

Y_l : width of longitudinal mixing zone [cm].

Y_{lmax} : maximum width of longitudinal mixing zone [cm].

Y_{tmax} : maximum width of transverse mixing zone [cm].

CONTENTS

LIST OF TABLES

LIST OF FIGURES

Chapter 1

INTRODUCTION

Conventional methods of oil production that rely on internal reservoir pressure are designated as primary recovery. In the early stages of oil recovery from a new oil field, much of the pressure required to force the oil to the surface is obtained from the confined fluids (caused by hydrostatic pressure of the surrounding aquifer, and /or the pressure of gases dissolved in the oil). However, continued production results in decreased reservoir pressure to a point where it becomes necessary to use pumps to " lift " the oil from the well to the surface. The primary recovery stage typically produces 10 ~ 30 % of the original oil-in-place (OOIP) from conventional reservoirs [1]. Due to the decreasing pressure, a technique called " pressure maintenance " will accomplish this task. It consists of the injection of large volumes of water through another well, the so-called injection well. The injection fluid will force the oil out of the porous rock towards the production well. As shown in Fig.1.1, one can see that the water is injected from the injection well, and the oil comes out of the recovery well. To get better oil recovery efficiency, it is important to study the mechanism of this sort of displacement. However, due to the complexity of this displacement, we will only focus on the effects of buoyancy forces. The effects of buoyancy (gravity) forces on liquid-liquid miscible

displacement processes occurring in porous medium are important in a variety of practical situations, in particular during the displacement of oil from partially-depleted underground reservoirs by means of aqueous solutions. When water displaces oil, the water tends to channel or " finger " through the paths of less resistance, thereby leaving regions of oil uncontacted and hence unrecovered.

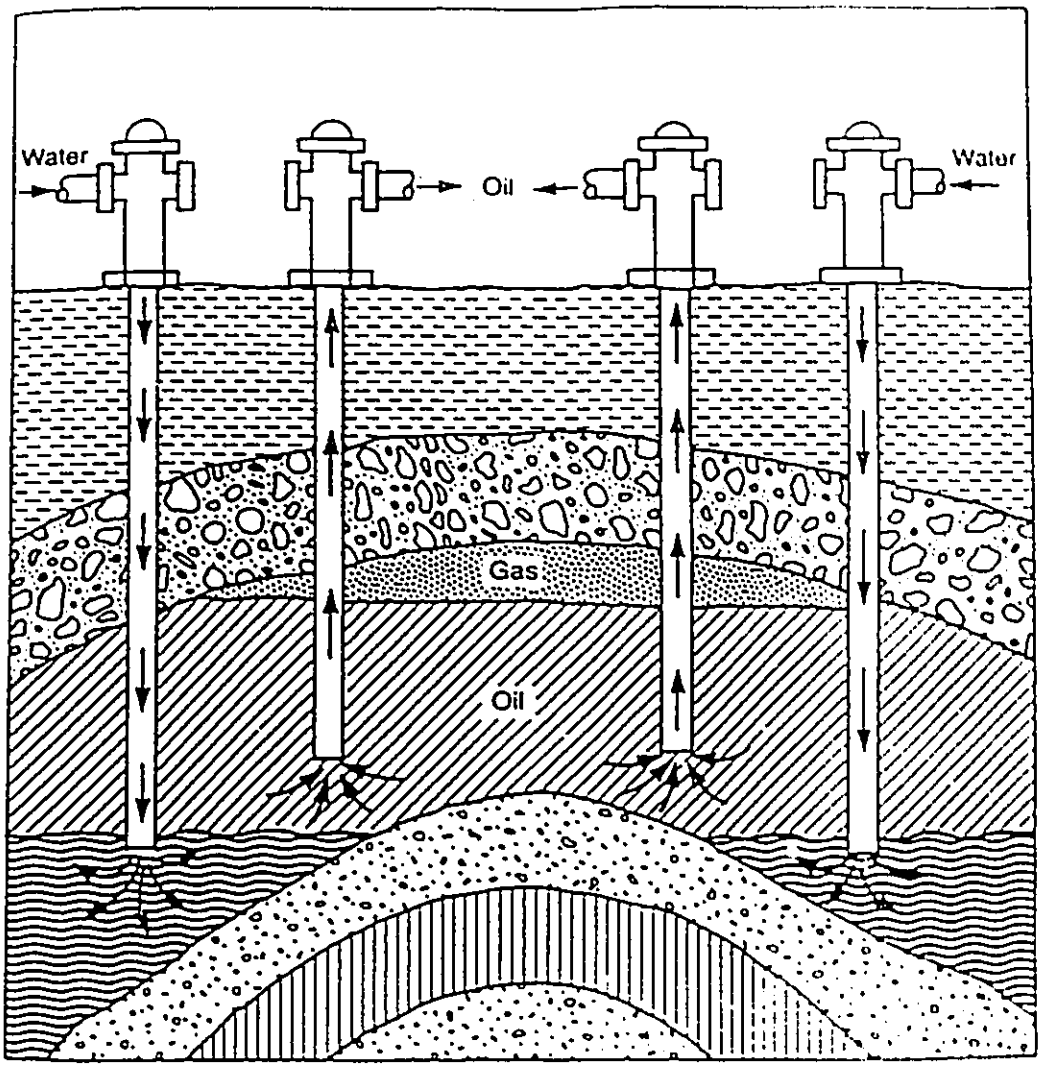

Fig.1.1 Water-Flood Technique [4].

1.1 Viscous Fingering

When a less viscous fluid displaces a fluid of higher viscosity, the less viscous fluid has a tendency to form channels through the more viscous fluid. These channels are referred to as " fingers " [2, 3]. As shown in the simple displacement experiment in Fig.1.2, the displacing fluid diverges at the inlet port and converges at the outlet port of the cell and there is a main finger in the middle of the cell. Many small fingers developed from the original one. The rate of growth of the fingers depends on several physical properties and parameters including;

(a) displacing fluid flow rate;

(b) viscosity ratio of displaced and displacing fluids;

(c) wettability of solid surface;

(d) permeability of porous medium.

Fingering is of great practical interest because it frequently occurs when a displacing fluid is injected into an oil well. The fingering pattern depends significantly on the flow rate, viscosity ratio, density ratio, etc.. The study of the effects of buoyancy forces on fingering is particularly important in EOR research because gravity forces and buoyancy forces are always present. However, buoyancy effects have not received very much attention in the past.

In this study, the main variables are density ratio, viscosity ratio, injection flow rate and flow mode.

Recovery Port

Injection Port

Fig.1.2 Viscous Fingering Phenomena Occurring during the Horizontal Displacement of Aqueous Glycerol Solution by Dyed Water in a Two-Dimensional Porous Medium Cell.

1.2 Objectives of This Study

The principal objective of this study was to investigate the effects of buoyancy forces (or gravity forces) on the recovery of oil from underground oil reservoirs so that the oil recovery efficiency can be improved.

The secondary objective was to explore the effects of density ratio, viscosity ratio, injection flow rate and flow mode on the fingering pattern and on the breakthrough oil recovery for the particular case of miscible displacement.

These objectives will be achieved by performing miscible liquid-liquid displacement experiments in two-dimensional porous medium cells aligned in the vertical plane.

Chapter 2

LITERATURE SURVEY

2.1 Enhanced Oil Recovery (EOR)

EOR has been defined as " all the techniques used to increase the amount of oil obtained after primary recovery" [4]. A broader definition which has been adopted by the Alberta Energy Resource Conservation Board states that EOR is "any oil production via artificial supplementation of natural reservoir energy [5]". By these definitions, EOR methods include:

- Pressure Maintenance And Water Flooding
- Steam Flooding
- CO_2 Injection
- Miscible Fluid Displacement
- Alkaline Injection
- In Situ Combustion
- Steam Stimulation
- Polymer Injection

Fig.2.1 is a classification of these and other related recovery methods. However,

since this research project is only concerned specifically with miscible fluid displacement and the effects of buoyancy forces, we will not discuss those methods which are irrelevant to our study.

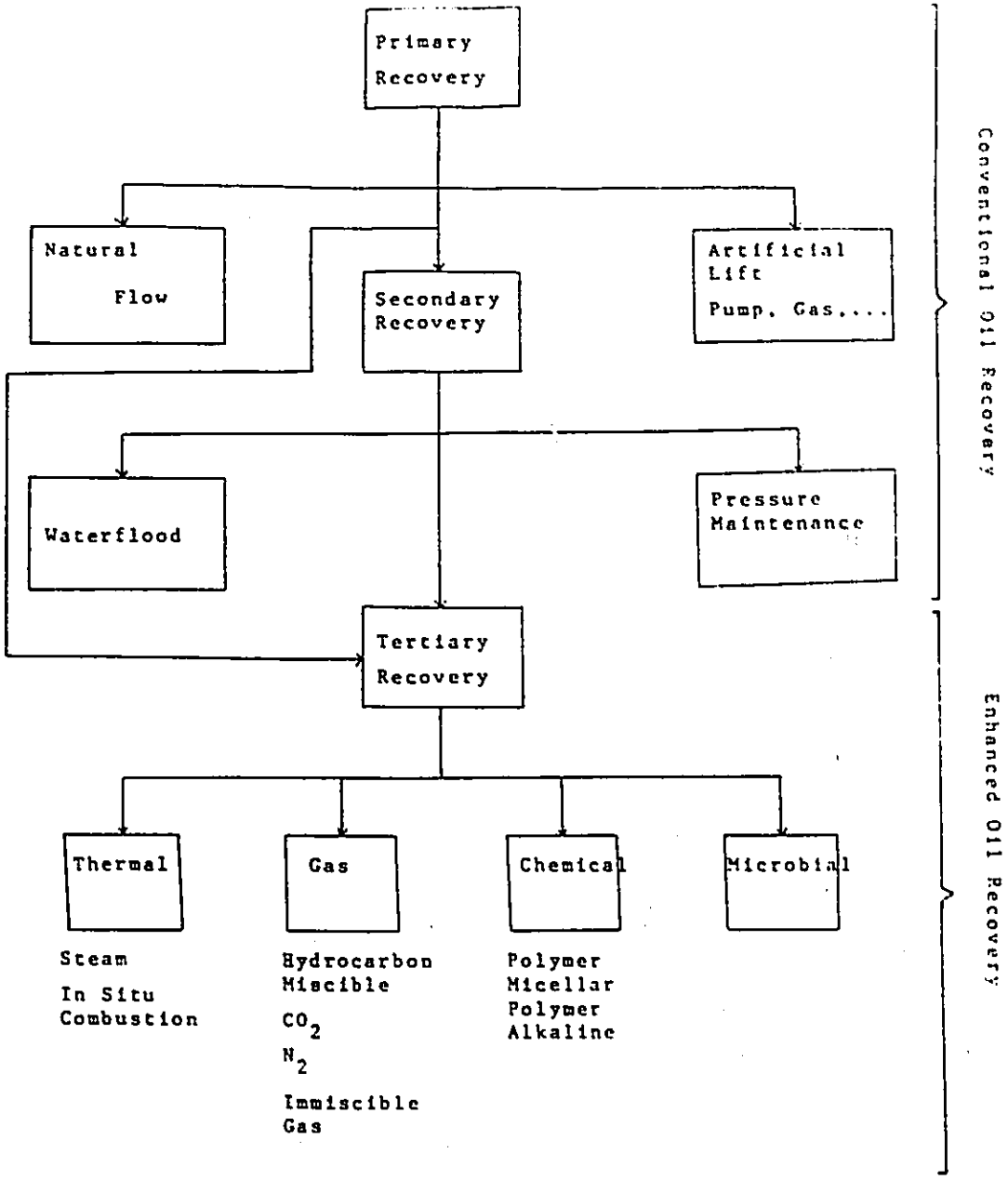

Fig.2.1 Recovery Mechanisms [1]

2.2 Miscible Displacement

The search for an effective and economical solvent along with the development and field testing of miscible-flood processes has continued since the early 1950's. Early focus was on hydrocarbon solvents, and three types of hydrocarbon-miscible processes were developed: 1) the first-contact miscible process; 2) the vaporizing-gas drive process, and 3) the condensing-gas drive process.

Hydrocarbon miscible processes received extensive field testing in the 1950's and 1960's in the U.S. and Canada. More than 150 projects were initiated in this time period; however, most floods were in essentially horizontal reservoirs.

Recent activity in miscible flooding has focused on the CO_2-miscible process. CO_2 has a low viscosity, similar to that of hydrocarbon miscible solvents [6], but there has been limited field testing of the CO_2-miscible process.

In the present study, the first-contact miscible process was adapted. The first contact miscible process implies that some injection fluids can mix directly with reservoir oils. Two fluids are miscible when they can be mixed together in all proportions and all mixtures remain a single phase. Gasoline and kerosene are examples of two liquids that are completely miscible. Because only one phase results from mixtures of miscible fluids, there are no interfaces and consequently no interfacial tension (IFT) between the fluids; therefore, the relevant dimensionless groups for miscible displacement are :

(1) Viscosity Ratio: μ_o / μ_w

(2) Reynolds Number: $Re = \varrho_w U d / \mu_w$

(3) Gravity Number: $Ngr = \mu_w U / \Delta\varrho\, g\, d^2$

An additional important variable is:

(4) Flow Mode (i.e., vertical-upward, vertical-downward, etc.)

Over the years, much work has been done on fluid displacement in porous medium. For the miscible system, the studies were focused on viscous fingering, gravity segregation, transition zone, dispersion, diffusion and so forth.

In 1956, Craig et al. [7] used scaled reservoir models to study the effects of gravity on oil recovery performance in frontal-drive operation, namely water, gas, solvent flocding, in which gravity forces were significant. The difference in density between the reservoir oil and the injection fluid causes their segregation, resulting in a non-uniform advance of the fluid front. In their laboratory flow test, which simulated both five-spot and linear injection operation in flat reservoirs, the viscous, capillary and gravity forces present in these operations were scaled. Dyed fluids were used so that the gross movement of the injected fluid could be observed. The studies covered a range of injection rates, formation thicknesses, and rock and fluid properties normally encountered in field operations. The results of the model tests indicate that the volume of the reservoir contacted by the injected fluid at its breakthrough into the producing well is less than that expected based on information which neglects gravity effects. This difference can often be as much as 80 per cent by gas or water injection in uniform sand bodies. Preliminary flow tests on a non-uniform sand body indicate that uniformity of the flood fronts may in some situations

be influenced to a much greater degree by permeability variations within the rock body than by gravity effects. The magnitude of fluid segregation due to gravity is controlled by the average injection flow rate, rather than by day to day or week to week variations. However, their presentation was only carried out in horizontal, uniform as well as nonuniform systems.

In 1958, Blackwell et al. [8] presented results of an experimental investigation of factors that controlled the efficiency with which oil was displaced from porous media by a miscible fluid. The study was made to elucidate the relevant processes both at the microscopic and macroscopic levels. In their study, they found that the formation of channels was due to viscous fingering, gravity segregation and variation in permeability. With an adverse mobility ratio, it was found for reservoirs of realistic widths that diffusion will not be effective in preventing the formation and growth of fingers, even in homogeneous sands. The study concentrated on the effects of injection flow rate, mobility ratio and model dimensions on the displacement process with equal densities to prevent gravity segregation. Their experimental data are still useful to present researchers; however, gravity forces were negligible in their study.

In 1963, Crane, et al. [9] compared Craig et al.'s and Blackwell et al.'s results. The considerable difference between their results is illustrated in Fig. 2.2 [9], where the breakthrough recoveries are plotted against the mobility ratio; furthermore, Crane et al. conducted experiments to examine how the transition from the one extreme case to the other occurs when the gravity forces are gradually reduced. It

was found that the number of pore volumes which must be injected at a constant rate to displace 98 per cent of the original fluid depends on the gravity forces. For each mobility ratio there is a transition range, and a very significant change in the number of pore volumes required when this range is traversed. This range of the gravity forces is physically linked with the pattern of the viscous fingers. A single finger is predominant for larger gravity forces, while a multiplicity of fingers is formed for smaller gravity forces. Crane et al. also found that four flow regimes are possible at unfavourable mobility ratios, depending on the value of the dimensionless group characterizing the ratio of viscous to gravity forces. Fig.2.3 illustrates conceptually the different flow regimes observed by these authors. At very low values of the viscous/gravity ratio (region I, Fig.2.3a), the displacement is characterized by a single gravity tongue overriding the oil. The geometry of this tongue and vertical sweepout both depend on the particular viscous/gravity ratio of the displacement. At higher values of viscus/gravity ratio, the displacement is still characterized by a single gravity tongue (region II , Fig. 2.3a), but vertical sweepout becomes independent of the particular value of the viscous/gravity ratio until a critical value is exceeded. Beyond this critical value, a transition region is encountered (region III , Fig.2.3b) where secondary fingers form beneath the main gravity tongue. In this region, sweepout for a given value of pore volumes injected increases sharply with increasing values of the viscous/gravity ratio. Finally, a value of viscous/gravity ratio is reached where the displacement is entirely dominated by multiple fingering, and sweepout again becomes independent of the particular value of the viscous/gravity ratio (Region IV,

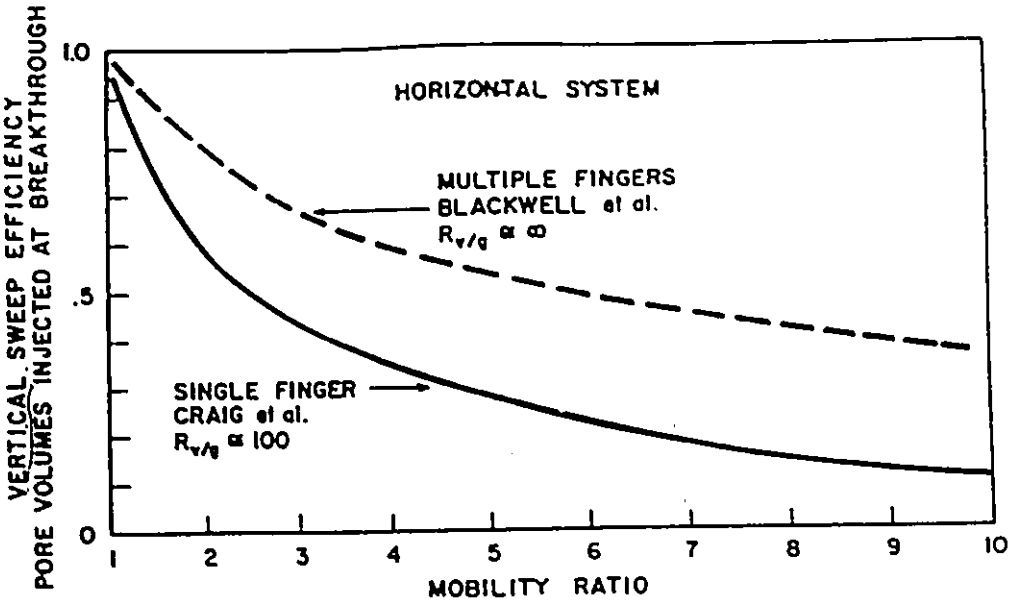

Fig.2.2 The formation of a multiplicity of fingers increases the mixing of the fluids and increases the breakthrough efficiency [9].

Fig.2.3c).

In 1963, Slobod et al. [10] investigated the effects of gravity segregation in a vertical core of unconsolidated sand. Fluids of varying viscosity and density were injected into the top of the core and moved at constant rates by use of a positive displacement pump. The composition of the efflux was analyzed by measurement of the refractive index. The main variables in their studies were the viscosity ratio, the density difference between the displaced and displacing fluids, and the injection flow rate. The experiments fell into four logical groups:

(1) favourable viscosity ratio and favourable density difference;

(2) favourable viscosity ratio and unfavourable density difference;

(3) unfavourable viscosity ratio and favourable density difference;

(4) unfavourable viscosity ratio and unfavourable density difference.

The behaviour of these four systems at various rates of flow was determined by measuring the length of the mixing zone which developed between the displaced and displacing phases. The data indicated that gravity segregation could act to shorten the mixing zone when the displacing material was the less dense phase, and lengthen the zone for a unfavourable density difference. The magnitude of this effect was most marked at slow injection flow rates when a sufficient residence time existed to allow significant flow to occur. The change in the length of the mixing zone with density difference, injection flow rate and viscosity ratio was plotted, and from their graph it became evident that the length of the mixing zone was dependent upon ratio of the viscous forces to the gravity forces. The importance of the ratio of the viscous

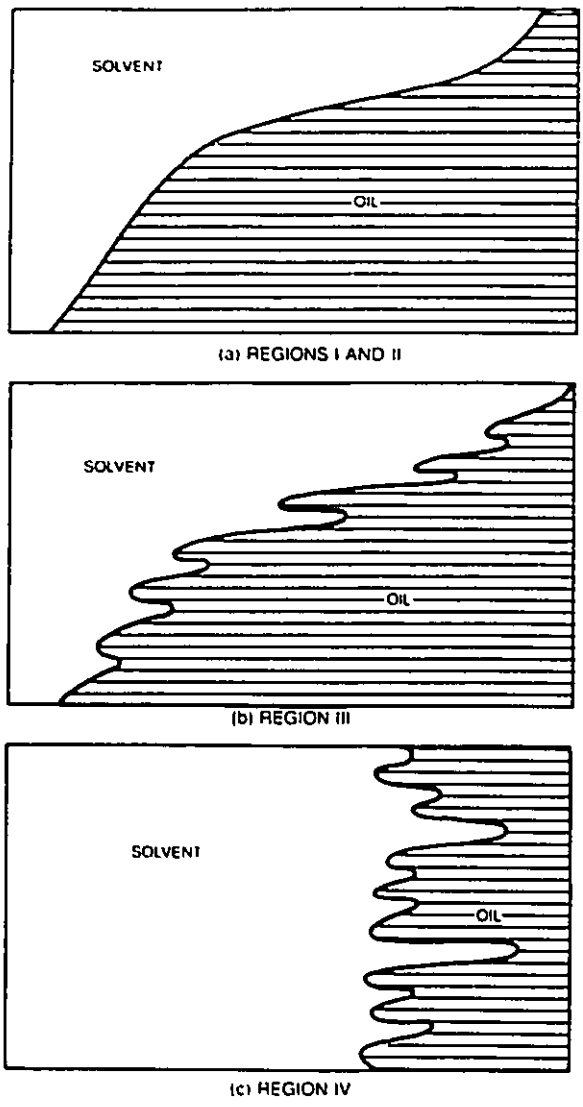

Fig. 2.3 Flow regimes for miscible displacement in a vertical cross section.

forces to the gravity forces was confirmed when analyzing the flow behaviour in the vertical system studied.

In 1964, Dumoré [11] studied the stability situation in downward miscible displacements. In his study the transition zone between the displaced and displacing fluids was neglected, and he developed a criterion for stable displacement by considering a small hypothetical protrusion of one of the fluids into the other. His analysis led to the definition of the well-known critical velocity:

$$U_c = Kg\frac{\Delta\rho}{\Delta\mu} \qquad \ldots\ldots\ldots\ldots (2.1)$$

This result was extended by taking into account the transition zone that develops as a result of diffusion and mixing. A generalization of the previous criterion leads to the definition of another characteristic velocity U_{st} - the stable velocity, which in actual miscible drives will be less than the critical velocity. The expression for the stable velocity is [11]:

$$U_{st} = \frac{(\rho_o - \rho_w)}{\mu_o(\ln \mu_o - \ln \mu_w)} kg \qquad \ldots\ldots\ldots\ldots\ldots (2.2)$$

In such miscible drives, the entire transition zone is stable at rates less than the critical rate. At rates between the stable and critical rates, the displacement is only partly stable, i.e. part of the transition zone adjacent to the displaced fluid is in an

unstable position. From that part of the transition zone viscous fingers will develop. At rates greater than the critical velocity, the entire displacement is unstable and viscous fingers will develop more strongly. Dumoré's results of laboratory experiments are in agreement with the expected behaviour based on the theoretically deduced stability of the displacement.

Unstable miscible and immiscible radial displacement were studied by Hu et al. [12] in 1984. They simplified a theory of fingering in a miscible system presented by Perkins et al. [13] to calculate the total number of fingers in the radial case. In order to eliminate unsatisfactory reproducibility of unconsolidated porous media, a consolidated porous medium was employed.

In 1990, Araktingi and Orr [14] examined the combined effects of gravity segregation, viscous fingering and reservoir heterogeneity in particle-tracking simulations of flow in vertical cross sections. The accuracy of the simulation representation of the physical flow mechanisms was tested in their paper. For homogeneous cross sections, simulator calculations were presented that illustrated the transition from flow in a single gravity-dominated tongue at low viscous to gravity ratios to flow dominated by viscous fingering at high viscous to gravity ratios. Simulation results agreed with experimental results over a wide range of mobility ratios, viscous to gravity ratios, and aspect ratios. Unfortunately, they did not study the effects of buoyancy forces.

Because of the influence of diffusion on miscible displacement processes, diffusion and dispersion phenomena in porous media are of great interest in the oil

industry. Various authors have studied the effects of Peclet number (Pe) on the stability of a miscible displacement. In 1961, Perrine [15] determined the marginal stability criteria for displacements in a semi-infinite porous medium of finite thickness and unbounded width, oriented at some given angle to the vertical direction. In his analysis, D_L and D_T were assumed to be constant. In 1966, Heller [16] undertook a similar study but assumed that the density and viscosity were varying quantities. However, Lee et al. [17] assumed that D_L and D_T depended on U. Most studies so far have been limited to porous media that were unbounded in the direction of flow [18].

Only a few authors have studied viscous fingering phenomena in the presence of buoyancy forces. In 1987, Hornof and Morrow [19] have studied the gravity effects in the displacements of oil by a surfactant solution. However, this study focused on the immiscible displacement. They found that the competition between viscous and capillary forces has a dominant effect on finger behaviour. A more recent consideration of the effects of buoyancy forces in enhanced oil recovery displacement processes was presented by Page et al.[20]. In this preliminary study, miscible displacements in different four flow modes were considered. i.e. horizontal and vertical-upward, vertical-downward and vertical-transverse mode. Significant effects of buoyancy forces on these different flow orientation displacements were observed.

Chapter 3

THEORY

3.1 Driving Force

3.1.1 Pressure Difference Forces

To inject a displacing fluid such as water into a porous medium one must apply a force to realize the process. A pressure difference can be created by a syringe pump between the inlet port and outlet port of the cell, which causes oil to flow from inlet port towards to the outlet port in the model cell.

3.1.2 Buoyancy Forces

Hydrostatic equilibrium is maintained in a fluid by an upward pressure force that exactly balances the weight of the fluid. When part of the fluid volume is replaced by another fluid of different density the remaining fluid continues to exert an upward force whose magnitude is equivalent to the weight of the original volume of the replaced fluid. This upward force is called the Buoyancy Force . If the replacing fluid has a lower density, the net force is upward. On the other hand, if the

replacing fluid has a higher density, the net force is downward [21].

3.1.3 Viscous Forces

An important characteristic of fluids is their viscosity, which is an internal characteristic of a fluid. Because of viscosity, a force is needed whenever one layer of a fluid slides past another, or when one surface slides past another with a layer of fluid between the surfaces. This force is called the Viscous Force . Viscosity plays a vital role in the flow of fluids in porous media, pipes and many other areas of practical importance [22].

3.2 Definitions

3.2.1 Breakthrough and Breakthrough Recovery

Breakthrough occurs when the first finger of the displacing fluid arrives at the exit port. After breakthrough, the fluid which leaves the exit port is a mixture of both the displaced and displacing fluids.

Oil recovery is defined as the ratio of the volume of oil recovered to the volume of initial oil present. The Breakthrough Recovery is the recovery corresponding to the breakthrough condition. Assuming that the displacing and displaced fluids are

incompressible, it may be modified for a miscible system as the ratio of the volume of glycerol solution recovered to the volume of initial glycerol solution present, i.e.,

$$\textit{breakthrough recovery} = \frac{\textit{cumulative volume of glycerol solution displaced}}{\textit{total initial pore volume of porous medium}}$$

It also can become the ratio of the volume of displacing fluid injected to the volume of initial oil or glycerol solution present; therefore, the recovery is:

$$\textit{Breakthrough Recovery} = \frac{QT_{br}}{V_p}$$

Where: Q = injection flow rate;

T_{br} = breakthrough time;

V_p = pore volume of porous medium.

3.2.2 Porosity

The porosity of a porous material is the fraction of the bulk volume of material occupied by voids. The symbol usually employed for this parameter is ϕ [23], where:

$$\phi = \frac{\textit{pore volume of porous medium}}{\textit{bulk volume of porous medium}}$$

3.2.3 Permeability

Permeability is the property of a porous material which characterizes the ease with which a fluid may be made to flow through the material by an applied pressure gradient. Permeability represents the fluid conductivity of the porous material [23].

3.2.4 Homogeneity

Prior to the displacement experiment, a homogeneity test for the cell was conducted by performing a displacement experiment using distilled water as the displaced fluid, and distilled water dyed with methylene blue as the displacing fluid. Because the viscosity ratio is unity and the densities of both fluids are almost the same. A stable unperturbed displacement front should be observed if the porous medium is homogeneous. The flow pattern was indeed observed to be perfectly radial before the front reached the cell exit [24, 25, 26], and no instability or fingering phenomena were observed, thus indicating good homogeneity of the porous medium.

Chapter 4

EXPERIMENTAL STUDIES

4.1 Experimental Design

4.1.1 Elements of a Working System

Displacing and Displaced Fluids

The experimental procedure used was based on the previous work [7, 24, 27, 28]. Aqueous glycerol solution was selected as the displaced fluid and water dyed with methylene blue was chosen as the displacing fluid. To obtain different viscosity and density ratios (please see Appendix A for the viscosity measurement and density measurement), several glycerol solutions of different concentrations were prepared.

Table 4.1. The relationship between concentration, viscosity and density for aqueous glycerol solution at 25 ^{0} C.

Glycerol concentration (Vol.%)	Viscosity (m Pa.s)	Density (g/ml)
86%	147.46	1.23
67%	23.41	1.19
50%	7.40	1.14
30%	3.10	1.09
10%	1.56	1.03

The displacing fluid used in all experiments was distilled water (dyed with methylene blue) having a viscosity of 1.00 mPa.s and density of 1.00 g/ml at 25^{0} C.

The Square Cell

All of the experiments were conducted in a consolidated porous medium. The reason for using a square cell rather than a radial cell is to eliminate the effects of the boundary of the cell so that the pattern of the fingers (gravity tongues) can be shown better in the cell.

4.1.2 Manufacturing and Properties of the Cell

Manufacturing of the Cell

Three consolidated porous medium cells of nominal dimensions 15cm × 15cm × 0.3cm were produced by lightly sintering glass beads (0.345~0.500 mm) between two parallel glass plates at about 650°C. The glass beads had been previously treated with 50% nitric acid in order to remove any possible organic contamination, then washed with distilled water and dried; After annealing and cooling, six holes (inlet/outlet ports) of diameter 0.3 cm were carefully drilled from the upper glass plate into the porous medium. The outer edge of each cell was sealed to prevent the fluids from leaving the cell during displacement [29]. A summary of the physical properties of the cells is given in Table 4.2.

Properties of the Cell

Table 4.2 Properties of the porous medium cells used in this project.

Cell No.	Vp (cm^3)	porosity (%)	thickness (cm)	dimension (LxW) (cm^2)
cell I	21.99	31.73	0.3	15.2 x 15.2
cell II	19.48	28.86	0.3	15.0 x 15.0
cell III	22.29	31.74	0.3	15.0 x 15.0

4.1.3 Specification of System

Table 4.3 Specification of the system used in this project.

NAME	SPECIFICATION
Water	Distilled
Glycerol	BDH
Glass Beads (0.345~0.500 mm)	Rouville Inc.
White Silicon Epoxy	Lepage Inc.
Propanol--2	BDH
Acetone	BDH
Syringe Pump	Sage Instrument Model 341A
Multifit Syringe and Methylene Blue Dye	Fisher Scientific Co.
Timer	Precision Scientific Co.
Camera	Minolta XG--M

4.1.4 Apparatus

Following is a list of the main components used in all experiments:.

1. Porous medium cell.
2. Camera.
3. Constant flow rate syringe pump.
4. 20ml Syringe.
5. 1.65 mm O.D syringe needle.
6. Timer.
7. Vacuum tubing.

In the horizontal displacement model, the camera was located over head and the cell lay above the light source. In the vertical mode, the camera was supported by a tripod and the cell was supported by a wooden holder in the front of the light source. The light source consisted of four fluorescent lights bulbs. The experimental set-up is shown in Fig.4.1 and the different orientations of the cells are shown in the Fig.4.2.

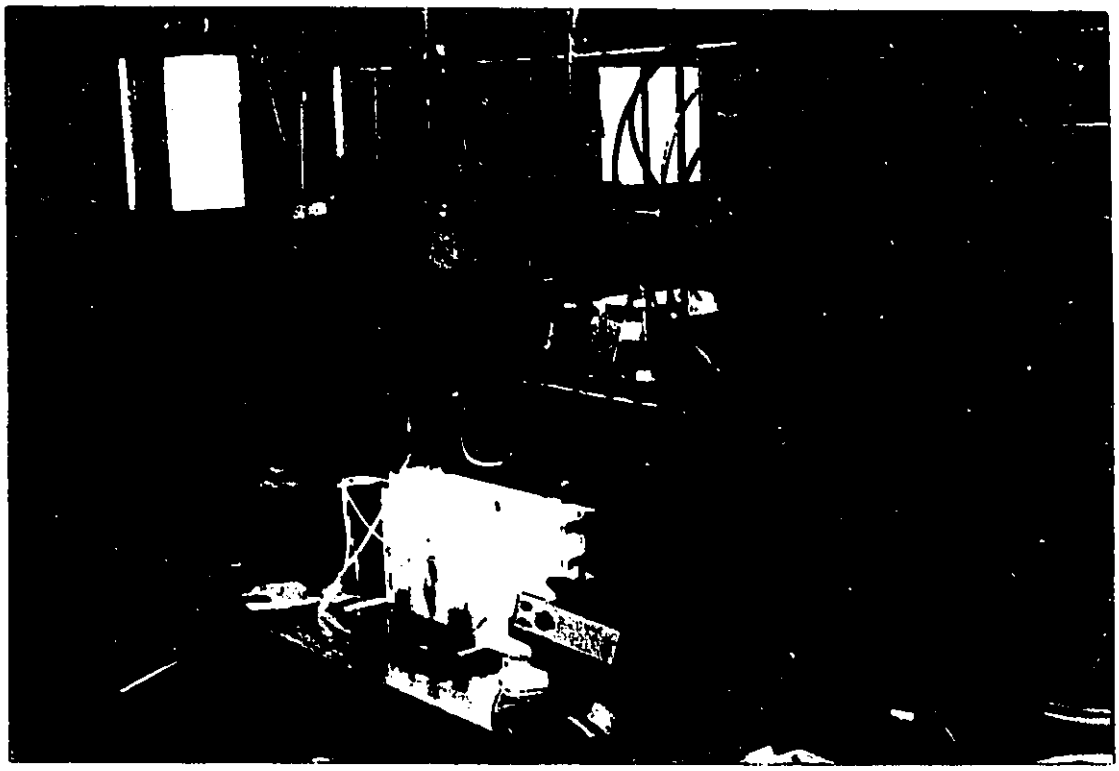

Fig.4.1 Scheme of experimental set-up.

(showing vertical-upward displacement experiment in progress)

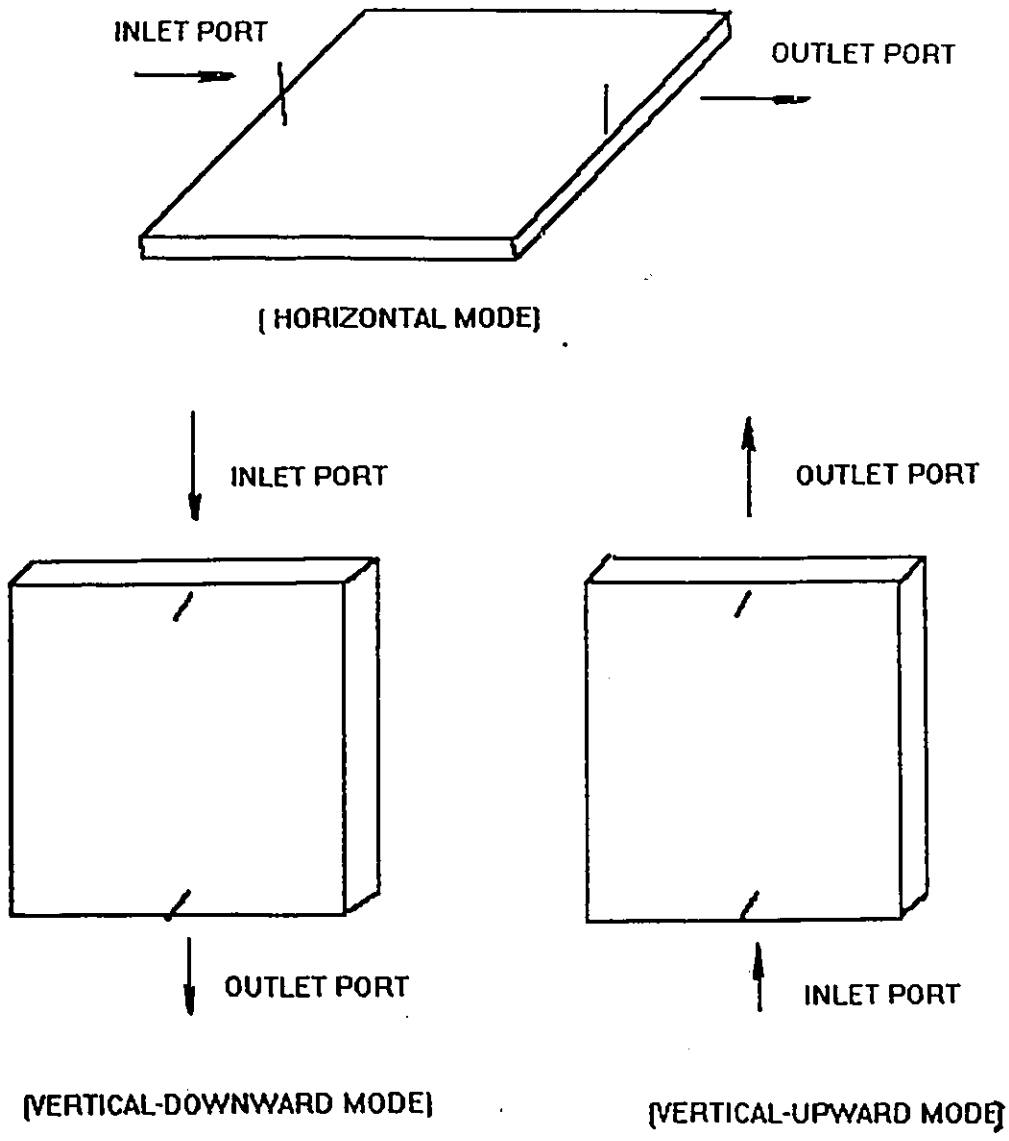

Fig.4.2 Scheme of the orientation of the cell. (a) horizontal mode; (b) vertical-downward mode; (c) vertical-upward mode.

4.2 Experimental Method

4.2.1 Saturation Process

To ensure 100% filling of the cell by a glycerol solution, the cell was firstly connected to a water aspirator , which was used to remove the air in the cell; secondly, after the absolute pressure reached a certain value (30 Psi), the cell was saturated with the glycerol solution by the pressure difference between outlet and inlet ports of the cell. It was observed from the experiment that glycerol solution slowly filled the cell without any bubble appearance.

4.2.2 Displacement Processes

The syringe filled with dyed water and the syringe pump were used to simulate the injection of water station in a real oil field. The cell represented the oil reservoir, and the several inlet/outlet ports represented the production and injection wells. The flow rate selector was set to provide a certain preselected flow rate. During the displacement process, photographs were taken at different times to record the behaviour of the fingering and displacement patterns. Finally, the breakthrough time was recorded as soon as the displacing fluid front arrived at exit port of the cell and the breakthrough recovery was calculated.

4.2.3 Cleaning and Drying Process

After the displacement process was completed, the cell was firstly cleaned with two pore volumes of propanol-2 and two pore volumes of acetone, respectively, following which two pore volumes of water were used. The cell was dried by water aspirator for about ten minutes and then by slowly passing nitrogen gas through the porous medium for another ten minutes. The cell was completely dried during this process.

4.3 Experiment Performed

4.3.1 Reproducibility Experiment

Consolidated porous media possess the inherent advantage that the constituent particles are rigidly fixed and cannot migrate during the displacement process, thereby permitting a wide range of experiments to be carried out within an identical porous medium [20]. Experiments were performed to examine the reproducibility of the displacements. Glycerol solution (30%) and dyed water were used as the displaced (μ_o = 3.10 m Pa.s and ρ_o = 1.09 g/ml) and displacing (μ_w= 1.00 g/ml and ρ_w= 1.00 g/ml) fluids at the flow rate of 16.8 ml/hr. and the experiment was set on the horizontal flow orientation.

4.3.2 Miscible Displacements

All experiments were carried out with glycerol solution (the different volume concentrations selected were in 10%, 30%, 50%, 67%, 86%) as the displaced fluid and dyed water as the displacing fluid. Specifications are presented in Table 4.4.

Table 4.4 Miscible System Experiments Performed

Experiment	*Flow Mode*	*Glycerol Concentration (volume %)*
No. 1	*Horizontal Displacement*	*10 %*
No. 2	*Horizontal Displacement*	*30 %*
No. 3	*Horizontal Displacement*	*50 %*
No. 4	*Horizontal Displacement*	*67 %*
No. 5	*Horizontal Displacement*	*86 %*
No. 6	*Downward Displacement*	*10 %*
No. 7	*Downward Displacement*	*30 %*
No. 8	*Downward Displacement*	*50 %*
No. 9	*Downward Displacement*	*67 %*
No.10	*Downward Displacement*	*86 %*
No.11	*Upward Displacement*	*10 %*
No.12	*Upward Displacement*	*30 %*
No.13	*Upward Displacement*	*50 %*
No.14	*Upward Displacement*	*67 %*
No.15	*Upward Displacement*	*86 %*

Chapter 5

RESULTS AND DISCUSSIONS

5.1 Reproducibility Experiments

The reproducibility experiments were carried out in the horizontal flow mode, where 30% glycerol solution was displaced by dyed water at an injection flow rate of 16.8 ml/hr. The pattern of these displacements is shown in Fig.5.1. As one can observe, these two fingering patterns are almost the same. In the first experiment, the breakthrough time is 1282 seconds and the breakthrough recovery is 27.21% (Fig.5.1a), while in the second experiment the breakthrough time is 1277 seconds and the recovery is 27.10%. The difference in breakthrough time is only 5 seconds, and the difference in breakthrough recovery is only 0.1 %. The reproducibility of these experiments in the horizontal model is entirely acceptable. Moreover, this also confirms that the particle packing of this consolidated porous medium is uniform and homogeneous [24].

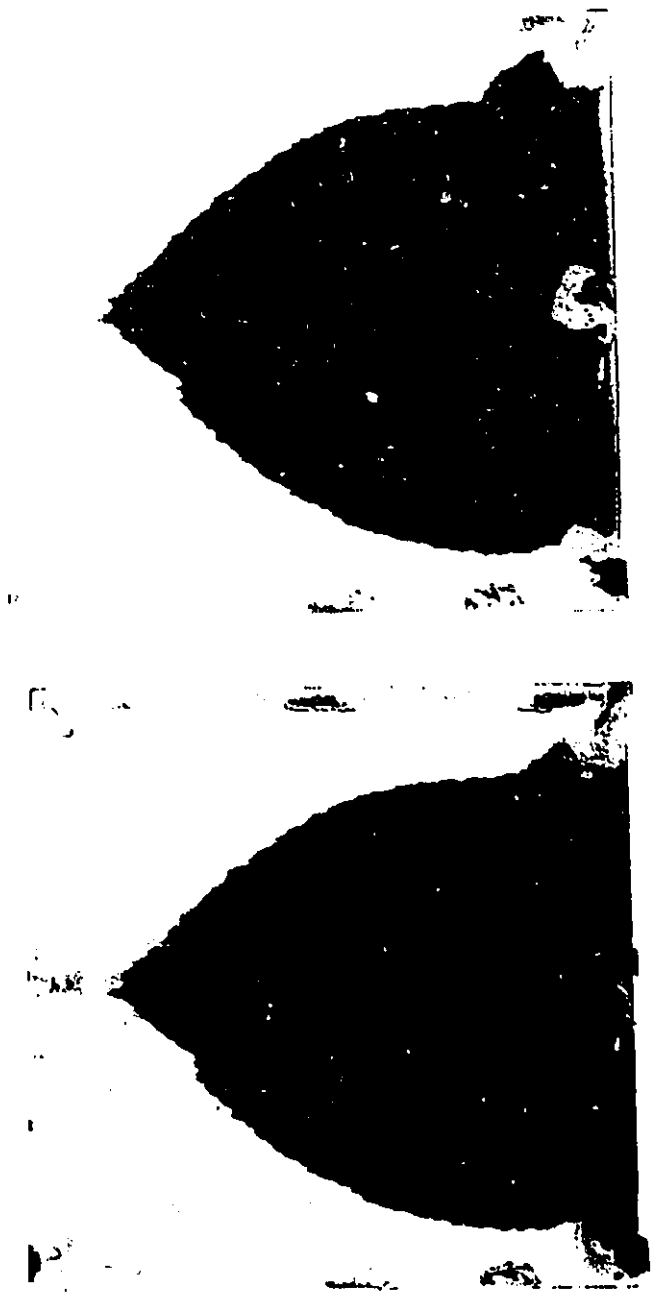

(a)

(b)

Fig.5.1 Results of Reproducibility Experiments for Water Displacing 30 % glycerol Solution. (a) T_{br} = 1282 seconds, R = 27.21 %, Q = 16.8 ml/hr. (b) T_{br} = 1277 seconds, R = 27.10 %, Q = 16.1 ml/hr..

5.2. Effects of Diffusion and Dispersion

Diffusion and dispersion in porous media are of considerable interest to the oil industry. This interest arises because of the effects of diffusion on miscible displacement processes.

In a recovery process utilizing a zone of miscible fluids, there is the possibility of losing miscibility by dissipation of the miscible fluid or by channelling or " fingering " through the miscible zone. Diffusion and dispersion are two of the mechanisms that may lead to mixing and dissipation of the slug. On the other hand, dispersion may tend to damp-out viscous fingers which may be channelling through the miscible slug [30]. Hence, dispersion may be detrimental or beneficial if it prevents fingering through the miscible zone. Therefore, it is doubly important that we understand these processes.

When one fluid is displaced from a porous medium by another miscible fluid (in the absence of fingers), a longitudinal mixed zone will be established. The mixed zone results from two phenomena-diffusion and mechanical mixing (or dispersion). If the average velocity is not too great, the total longitudinal dispersion coefficient is given quantitatively by Eq (5.1) [23]:

$$K_l = \frac{D_o}{F\Phi} + 0.5\, U d_p \sigma \qquad \text{.....(5.1)}$$

and the total transverse dispersion coefficient is given quantitatively by Eq (5.2) [23]:

$$K_t = \frac{D_o}{F\Phi} + 0.0157\ U d_p \sigma \qquad \text{.....(5.2)}$$

The widths of the longitudinal and transverse mixed zones in a linear system are given by Eqs (5.3) and (5.4) [23]:

$$Y_l = 3.625 \sqrt{D_o \frac{X}{F\Phi U} + 0.5 d_p \sigma X} \qquad \text{.....(5.3)}$$

$$Y_t = 3.625 \sqrt{D_o \frac{X}{F\Phi U} + 0.0157\ d_p \sigma X} \qquad \text{.....(5.4)}$$

where

D_o = molecular diffusion coefficient (cm^2 /s).

F = formation electrical resistivity factor (dimensionless).

Φ = porosity (dimensionless).

U = average velocity (cm/s).

d_p = particle diameter (cm).

X = distance measured from original position of an interface (cm).

σ = a measure of the inhomogeneity from original position of an interface (cm).

In this study, we modify Eqs (5.3) and (5.4) by using X_{max} so that the maximum widths of the longitudinal and transverse mixed zones Y_{lmax} and Y_{tmax} can be obtained. Therefore, Eqs (5.3) and (5.4) become:

$$Y_{lmax} = 3.625\sqrt{D_o\frac{X_{max}}{F\Phi U} + 0.0157\, d_p\sigma X_{max}} \qquad \ldots\ldots\ldots\ldots (5.5)$$

$$Y_{tmax} = 3.625\sqrt{D_o\frac{X_{max}}{F\Phi U} + 0.0157\, d_p\sigma X_{max}} \qquad \ldots\ldots\ldots\ldots (5.6)$$

From reference [23], we also have :

$$Y_l = 3.625\sqrt{K_l\theta} \qquad \ldots\ldots\ldots\ldots (5.7)$$

Combining (5.1) , (5.5) and (5.7), the diffusion time can be obtained:

$$\theta = \frac{X_{max}}{U} \qquad \ldots\ldots\ldots\ldots (5.8)$$

Perkins' et al.'s experimental data [31] suggested that σ was 3.5 for a typical random pack [30], and $F\Phi \approx 3.5$. From the reference [32], Blackwell et al. gave different diffusion coefficients from their experimental data (Table 5.1). Also from reference [33], we obtain $D_o = 1.06 \times 10^{-5}\ cm^2/s$ for a very dilute glycerol solution. Comparing this data with Blackwell et al.'s data, we estimate that if D_o is $1.06 \times 10^{-5}\ cm^2/s$, the viscosity of the glycerol solution must be lest than 6 mPa.s, which means that the viscosity ratio between the displaced and displacing fluid

Table 5.1. Relationship between viscosity and diffusivity

Viscosity (mPa.s)	6.1	11.4	22.6
Diffusivity (cm^2/s)	0.266×10^{-5}	0.142×10^{-5}	0.717×10^{-6}

is much closer to each other. Therefore, we take the maximum value of diffusivity so that we can obtain maximum widths of the longitudinal and transverse mixed zones, and d_p = 0.04224 cm and Φ = 0.34. We calculate the width at different average velocities from 0.02 cm/s to 3.98 cm/s. We can also calculate the time required by the displacing fluid to flow through the same distance Y_{lmax} by:

$$\theta_d = \frac{Y_{lmax}}{U} \qquad \text{.....(5.9)}$$

The results were shown in Table 5.2 after all the calculations.

Table 5.2 Results of Calculations of Widths of Longitudinal and Transverse Mixed Zone

velocity (cm/s)	Y_{lmax} (cm)	Y_{tmax} (cm)	θ (s)	θ_d (s)
0.02	1.19	1.03	750.00	59.49
0.03	1.19	1.03	499.99	39.66
0.04	1.19	1.03	375.00	29.75
0.06	1.19	1.03	250.00	19.83
0.15	1.19	1.03	100.00	7.93
0.34	1.19	1.03	44.12	3.50
0.48	1.19	1.03	31.25	2.48
1.03	1.19	1.03	14.56	1.16
1.50	1.19	1.03	10.00	0.79
3.98	1.19	1.03	3.77	0.30

Comparing these two characteristic times, it was found that the diffusion time is much greater than the time required by the displacing fluid, thus proving that the velocity of diffusion is much smaller than the velocity of the displacing fluid. In other words, the effects of diffusion and dispersion do not affect the displacement process very much in this study. Also, as shown in Table 5.2, the Y_{lmax} and Y_{tmax} keep the same value when the average velocity is changed. This is because the diffusivity is very small, so the first terms in the square root in Eqs (5.5) and (5.6) do not affect the total value of the square root. Therefore, it does not affect the widths of the longitudinal and transverse mixed zones. This, again, confirms that the effects of diffusion and dispersion can be neglected.

5.3 Discussion for Horizontal Displacement

Fig. 5.2 shows the effects of the injection flow rate on the cumulative fractional oil (glycerol solution) recovery at the breakthrough condition. Although there is an inevitable scatter in the experimental data presented in Fig.5.2, the relationship between recovery and injection flow rate appears to fall into two distinct regions depending on the dominant displacement mechanism prevailing. These two regions are the so-called gravitational region and viscous region. Fig.5.3 shows the relationship between breakthrough time and injection flow rate. These data are in qualitative agreement with the data given by Ni et al. [29] for immiscible system. The two regions for each curve are located at different flow rate ranges. The first region (for μ_o/μ_w=147.46) occurs at low flow rates, Q < 90.0 ml/hr, where gravitational forces are dominant [9]. In this region, the oil recovery decreases as the flow rate increases. The second region occurs at high flow rates (Q > 90.0 ml/hr), where viscous forces are dominant in the displacements [34]. In the latter region the oil recovery increases as the flow rate increases. It is elucidating to re-plot the data of Fig.5.2 in terms of the so-called gravity number, N_{gr}, instead of the injection flow rate, where:

$$N_{gr} = \frac{U\mu_w}{g\Delta\rho d^2} \qquad \ldots\ldots\ldots\ldots (5.10)$$

which denotes the ratio of viscous to gravity forces. The re-plotted data shown in Fig.5.4 are very similar with those given by Araktingi and Orr [14], Pozzi and Blackwell [35] and Van Der Poel [27]. Calculations were carried out and listed in Table 5.3. It can be seen that recoveries increase sharply when the viscous/gravity ratio (N_{gr}) is greater than 0.0193 (for $\mu_o/\mu_w = 147.46$) (Fig.5.4). As we mentioned before, the viscous forces completely dominate in this region. A large number of fingers results in that displacing fluid displaces more oil (aqueous glycerol solution), consequently, increasing oil recovery. When the viscous/gravity ratio (N_{gr}) is less than 0.0193. We can see that recoveries tend to decrease with increasing injection flow rates. Also, the effects of gravity forces are gradually diminished with injection flow rates. On the other hand, when the viscous/gravity ratio is very small (i.e. $N_{gr} = 0.00039$) a relatively higher recovery can be obtained (Fig. 5.4). The critical value of the viscous/gravity ratio to separate gravity region and viscous region in this study is different from those given by previous investigators because that depends on the geometry of the porous medium and the definition of viscous/gravity ratio (N_{gr}).

As can be seen in Fig.5.4, there are not two regions when the viscosity ratio and density difference are very small (1.56 and 0.03). At this situation, the effects of gravity forces and viscous forces can be neglected and the breakthrough oil recoveries are almost independent of the viscous/gravity ratio. However, with increasing viscosity ratio and density difference, these two regions gradually become obvious.

Table 5.3. Results of Calculations of Gravity Number, N_{gr}

injection flowrate (ml/hr)	average velocity (cm/s)	viscous/gravity ratio N_{gr}				
		μ_o / μ_w =147.46	μ_o / μ_w =23.41	μ_o / μ_w = 7.40	μ_o / μ_w = 3.10	μ_o / μ_w = 1.56
1.8	0.016056	0.00039	0.00048	0.00065	0.00102	0.00306
2.9	0.025212	0.00062	0.00076	0.00103	0.00160	0.00480
4.7	0.041224	0.00102	0.00124	0.00168	0.00261	0.00786
7.2	0.063694	0.00158	0.00192	0.00260	0.00405	0.01214
16.8	0.148620	0.00368	0.00447	0.00607	0.00944	0.02831
38.4	0.339703	0.00842	0.01022	0.01387	0.02157	0.06473
54.6	0.483015	0.01197	0.01453	0.01972	0.03068	0.09204
87.6	0.774947	0.01926	0.02332	0.03164	0.04922	0.14766
116.4	1.029723	0.02551	0.03098	0.04024	0.06540	0.19021
169.2	1.296815	0.03709	0.04503	0.06111	0.09507	0.28521
279.6	2.473461	0.06147	0.07442	0.10099	0.15710	0.35348
449.4	3.975583	0.09851	0.11961	0.16232	0.25251	0.75753

- **The underlined data corresponds to flow in the viscous region.**

5.3.1 The Development of Displacement Pattern

Figs 5.5, 6, 7, 8, 9 show the development of the displacement pattern for a low injection flow rate of 38.4 ml/hr. The time was recorded to show the behaviour of the fingering pattern. During the initial stages of displacement, as shown in Fig.5.5a, b for a low viscosity ratio, a gravity tongue starting from the inlet port can be seen. Actually, there were some smaller fingers appearing when the oil was displaced, but they were suppressed because of the effects of gravitational forces. Diffusion may also serve to reduce fingers [23]. Also, one can observe that the location of the gravity tongue was uniformly distributed over the inlet port. This further confirms that the cell is macroscopically homogeneous. Continuously, when the time was about 522 seconds, it showed (Fig.5.5c) that the distance in longitudinal direction was longer than that in transverse direction. By using Darcy's Law (5.11), we can explain it as following:

$$U = -\frac{K}{\mu}\frac{dP}{dX} \qquad \text{.....(5.11)}$$

As can be seen in Fig.5.10, the distance X_1 is shorter than distance X_2. Under the condition of the same pressure difference ($P = P_1 - P_2$), $dP/dX_1 > dP/dX_2$ can be got, so the displacing fluid tends to flow in the longitudinal direction much faster than that in transverse direction until the breakthrough is reached. As shown in Fig.5.5d, the displacing fluid finally converged at the outlet port of the cell. At the

breakthrough condition, it can be clearly seen that the gravity forces completely controlled the displacement, and the gravity forces was more important in this region than viscous forces.

With the increasing of viscosity ratio, the pattern of the displacements changes gradually, as shown in Fig.5.6, 7, 8, 9. One can observe that at the initial stage some viscous fingers appeared and grew with the value change of viscosity ratio from low to high, and the number of fingers also increased from small to large. During the next stages, the fingering development was mainly in the longitudinal direction rather than in the transverse direction and the displacing fluid was basically filling the invaded areas. This process continued up to breakthrough of the displacing fluid, as shown in Fig.5.6d, 7d, 8d, 9d.

5.3.2 The Effects of Flow Rate

Increasing the injection flow rate in the gravity region tends to decrease recovery and this has two effects. Firstly, due to the effects of the buoyancy forces, the macroscopic interface* between the displacing and displaced fluids is increased (Fig.5.11); therefore, the front of the displacing fluid at the top of the cell goes

* It is the interface between two colourful fluids, this is the purpose to use the distilled water dyed with methylene blue so that we can see the effects of buoyancy forces. Actually, there is no interface between two miscible fluids.

much faster than that at the bottom, and results in a decreased recovery. Secondly, increasing flow rate will increase viscous forces [34], and one can observe (Fig. 5.12, 5.13, 5.14, 5.15, 5.16) that from relatively high viscosity ratio (23.41) to higher viscosity ratio (147.46) some new born fingers appeared from the original ones. This will diminish the width of the big fingers and consequently lower oil recovery. From the results shown in Fig.5.2, it seems that the effect of the second factor is more important, and therefore, the oil recovery decreases with the injection flow rate to the lowest recovery value.

Fig 5.12, 13, 14, 15, 16 show the development of the displacement pattern for a high injection flow rate of 169.2 ml/hr. The behaviour of the displacement pattern is different from that at the low injection flow rates. Fingers do not commence uniformly at the inlet port for the high viscosity ratio. With the displacement continuing , lots of smaller fingers were born from the original ones and the colour density of these fingers was getting more dilute. In addition, comparing this with those at low injection flow rates, these fingering patterns are wider and they cover more areas of the cell when the viscosity ratio is higher, therefore, it results a little higher recovery. However, when the viscosity ratio is lower, the differences of the fingering pattern and the final oil recovery between these displacements are very small because the gravity forces or viscous forces do not affect the displacement very much. All the final stages are shown in Fig.5.12d, 13d, 14d, 15d, 16d.

Increasing flow rate even more will greatly increase the viscous forces. Meanwhile, flow resistance (Ω) will decrease with the amount of pore volume of

solvent injected when M is greater than 1. If M<1, however, Ω will increase with amount of the pore volume of solvent injected [8, 36]. Due to flow resistance decreasing (in this study M>1), the displacing fluid flows through the porous medium very freely, as shown in Fig.5.17a, b, the pattern of the fingers was tree-like, branch fingers developed freely in any direction, and the tree-trunk (darker area) was getting bigger with flow rates, which clearly indicates that viscous forces dominate gravity forces in this region. However, for a decreasing viscosity ratio, the pattern of the fingers seems to remain the same shape at any injection flow rates (see Fig.5.17c, d). Fingers became smaller and displacing fluid could occupy entire cross-section of the cell, therefore, a high oil recovery could be obtained.

One should note the transition zone from gravity region to viscous region should be very smoothly because the effects of viscous forces are comparable with the effects of gravity forces in this zone. Comparing Fig.5.18a, b, fingering patterns are very similar to each other. On the other hand, the width of fingers in Fig.5.18b is a little smaller than that in Fig.5.18a, but the number of fingers in Fig.5.18b is more than that in Fig.5.18a. More fingers appearing will complement the loss caused by buoyancy forces. In addition, when the viscosity ratio was getting small, the pattern of the fingers gradually showed the same shape (see Fig.5.18c, d). As a result, the recovery is basically independent of injection flow rate in this transition zone.

5.3.3 The Effects of Density Differences

Density differences also play an important role in miscible displacements. Decreasing density ratio will eliminate the effects of gravitational forces and diminish the span of macroscopic interface between the displacing and the displaced fluids (Fig.5.11). It is clear that the displacing fluid will occupy more space of the cell at a low density ratio than that at a high density ratio, not only at the top of the porous medium, but the entire space as well. The change of the colour density will also prove this assertion. One can simply find that reducing the effects of the gravitational forces in the horizontal mode will improve oil recovery. As shown in Fig.5.2, one can see that the recovery increases as the density ratio decreases. When the density ratio is close to 1, the recovery is almost independent of injection flow rates, which indicates that the influence of gravitational forces is negligible. Thus, one can conclude that reducing the density difference can greatly improve the efficiency of oil recovery.

5.3.4 Comparison of the Effects of Gravity Forces and Viscous Forces

Comparing Fig.5.7 with Fig.5.14, one can also observe the influences of gravitational forces and viscous forces, respectively. Even though the recoveries are close to each other, the patterns of the fingers are completely different, which strongly proves the explanation about the gravitational region and viscous region we

mentioned before.

HORIZONTAL DISPLACEMENT

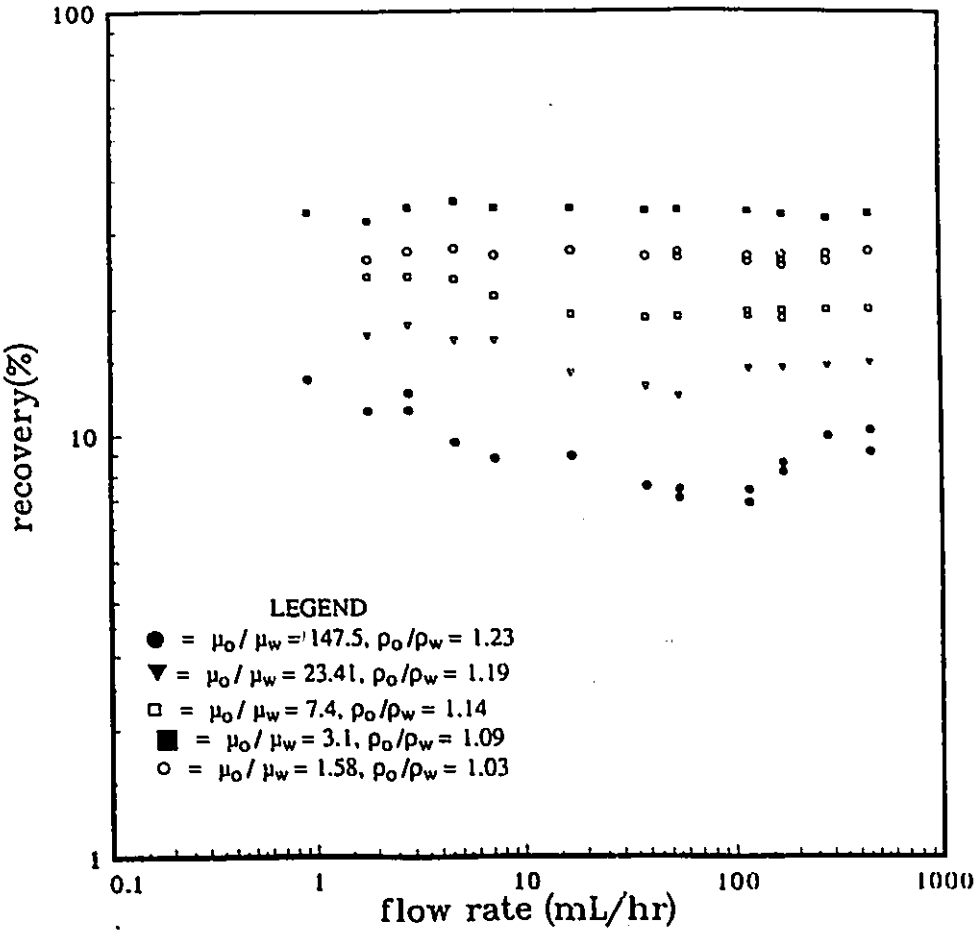

Fig.5.2. Horizontal Mode, the relationship between flowrate and breakthrough.

HORIZONTAL DISPLACEMENT

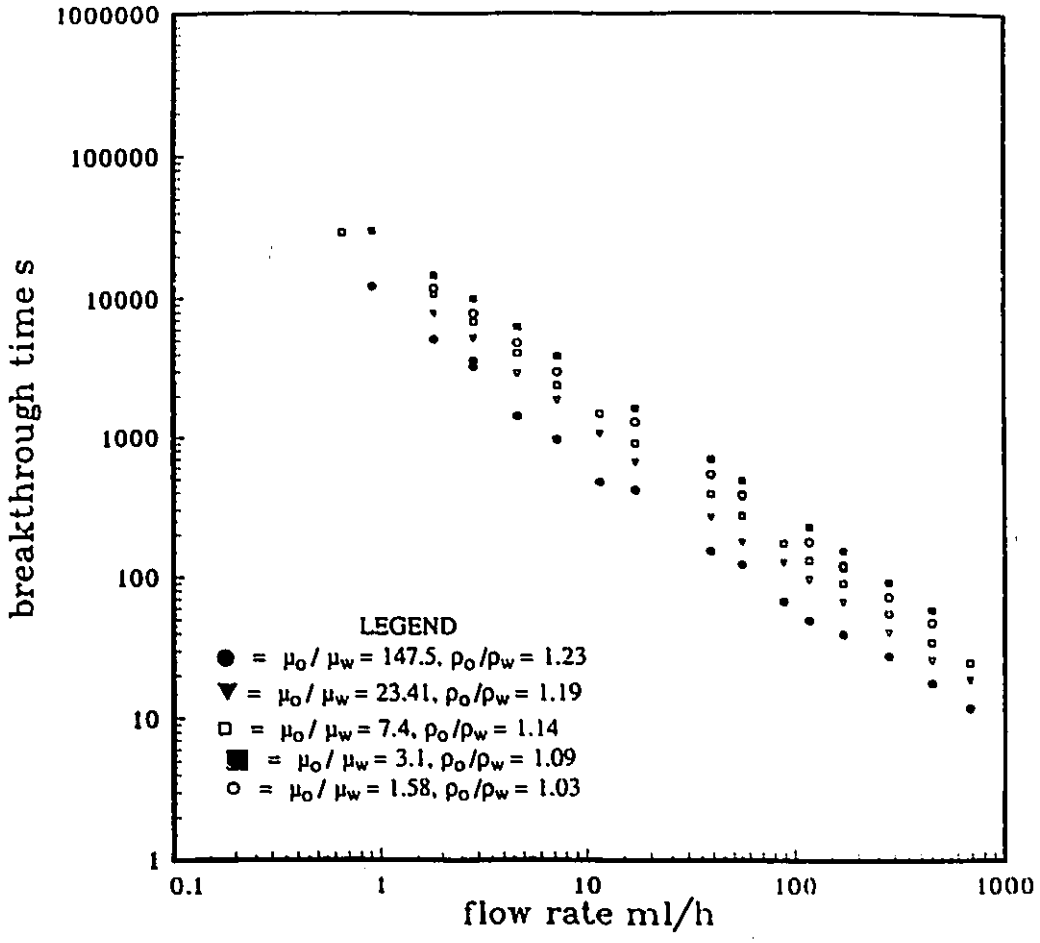

Fig.5.3. Horizontal Mode, the relationship between injection flowrates and breakthrough time.

HORIZONTAL DISPLACEMENT

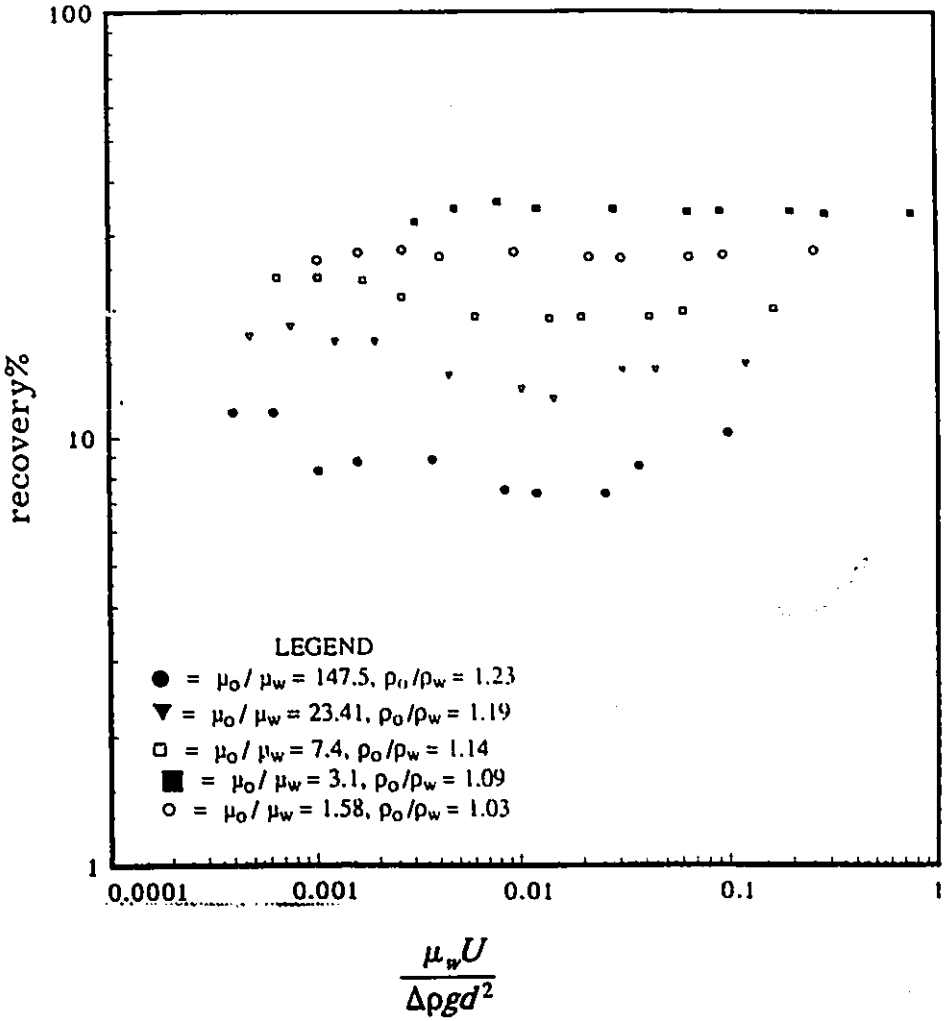

Fig.5.4. Horizontal Mode, the breakthrough recovery behaviour as a function of viscous/gravity ratio.

HORIZONTAL DISPLACEMENT

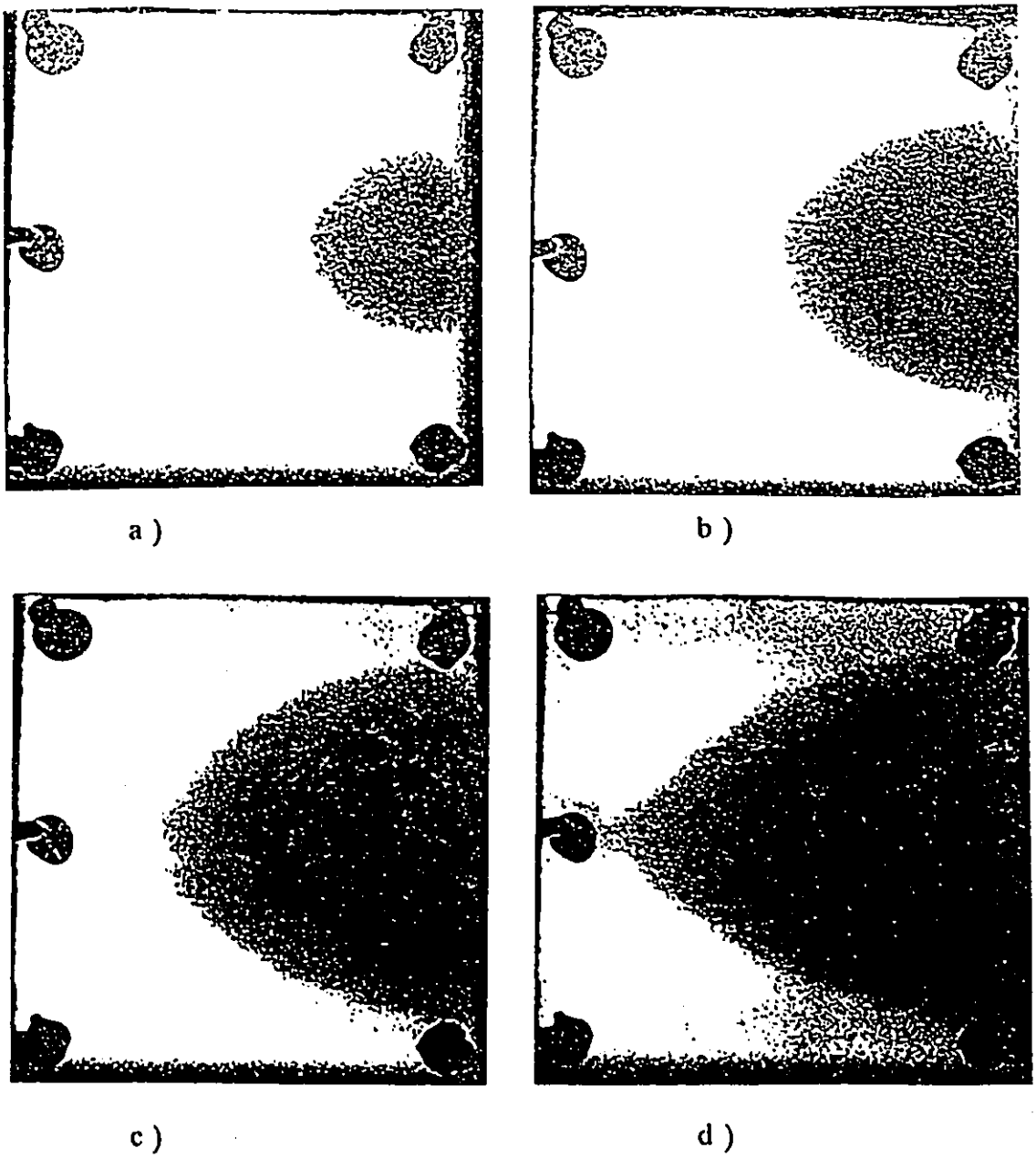

a)

b)

c)

d)

Fig.5.5 The development of the displacement pattern for a low injection flowrate of 38.4 ml/hr. μ_o/μ_w = 1.56, ρ_o/ρ_w = 1.03, (a) time = 122 seconds, (b) time = 287 seconds, (c) time =522 seconds, (d) time = 638 seconds, Recovery = 30.53 %.

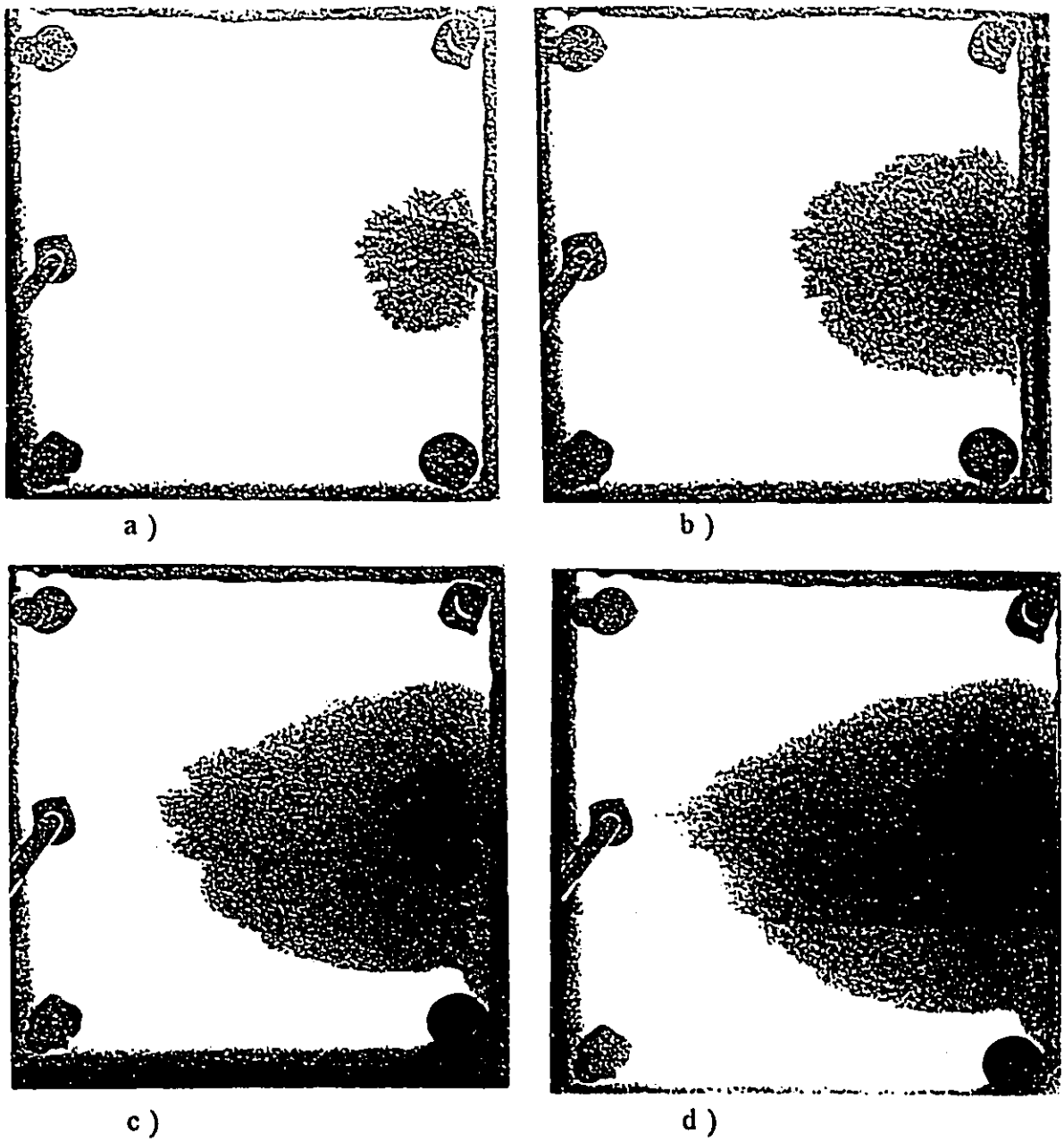

Fig.5.6 The development of the displacement pattern for a low injection flowrate of 38.4 ml/hr. μ_o/μ_w = 3.1, ρ_o/ρ_w = 1.09, (a) time = 58 seconds, (b) time = 112 seconds, (c) time =210 seconds, (d) time = 264 seconds, Recovery = 22.61 %.

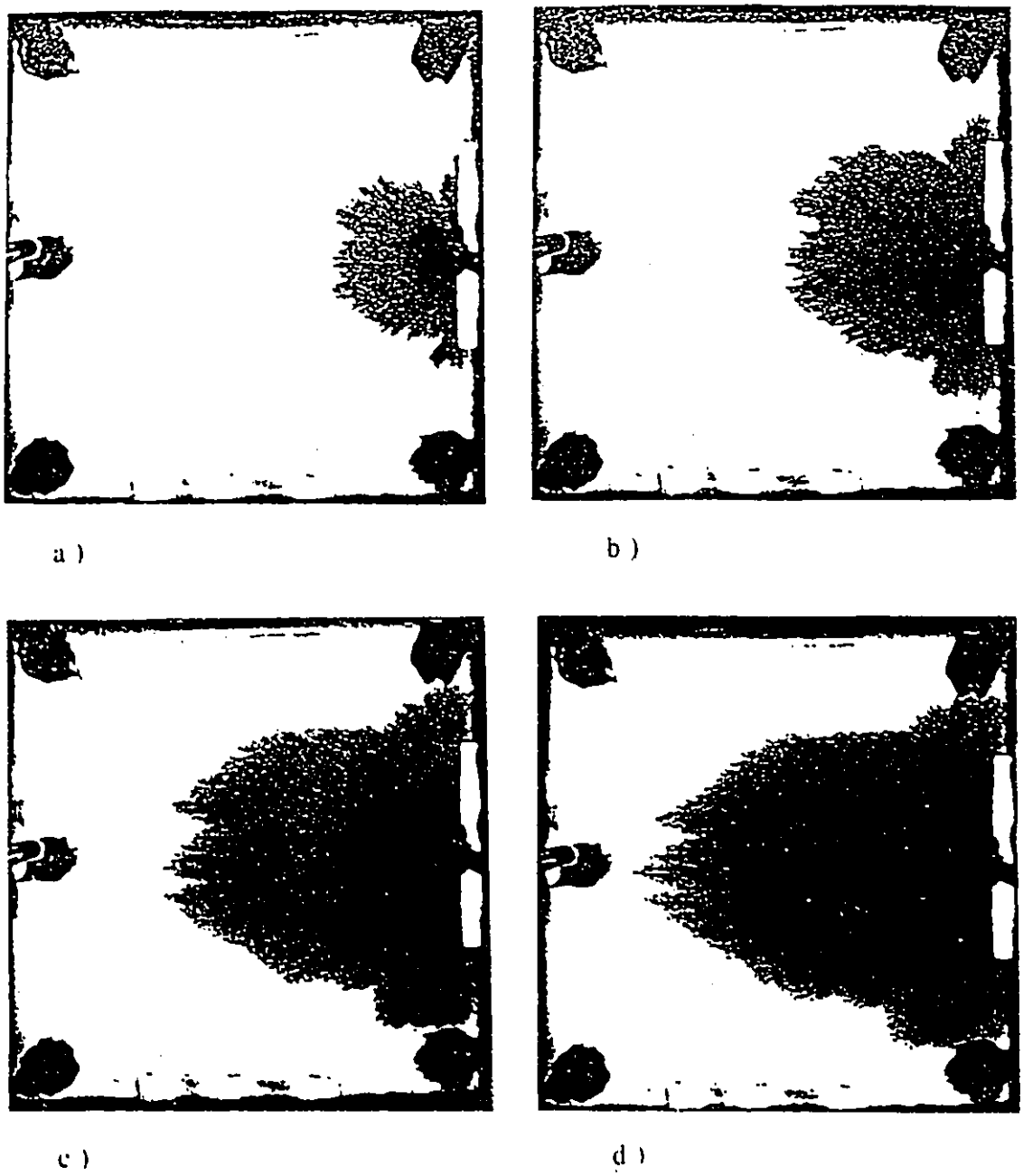

Fig.5.7 The development of the displacement pattern for a low injection flowrate of 38.4 ml/hr. $\mu_o/\mu_w = 7.4$, $\rho_o/\rho_w = 1.14$, (a) time = 45 seconds, (b) time = 109 seconds, (c) time =231 seconds, (d) time = 305 seconds, Recovery = 16.70 %.

HORIZONTAL DISPLACEMENT

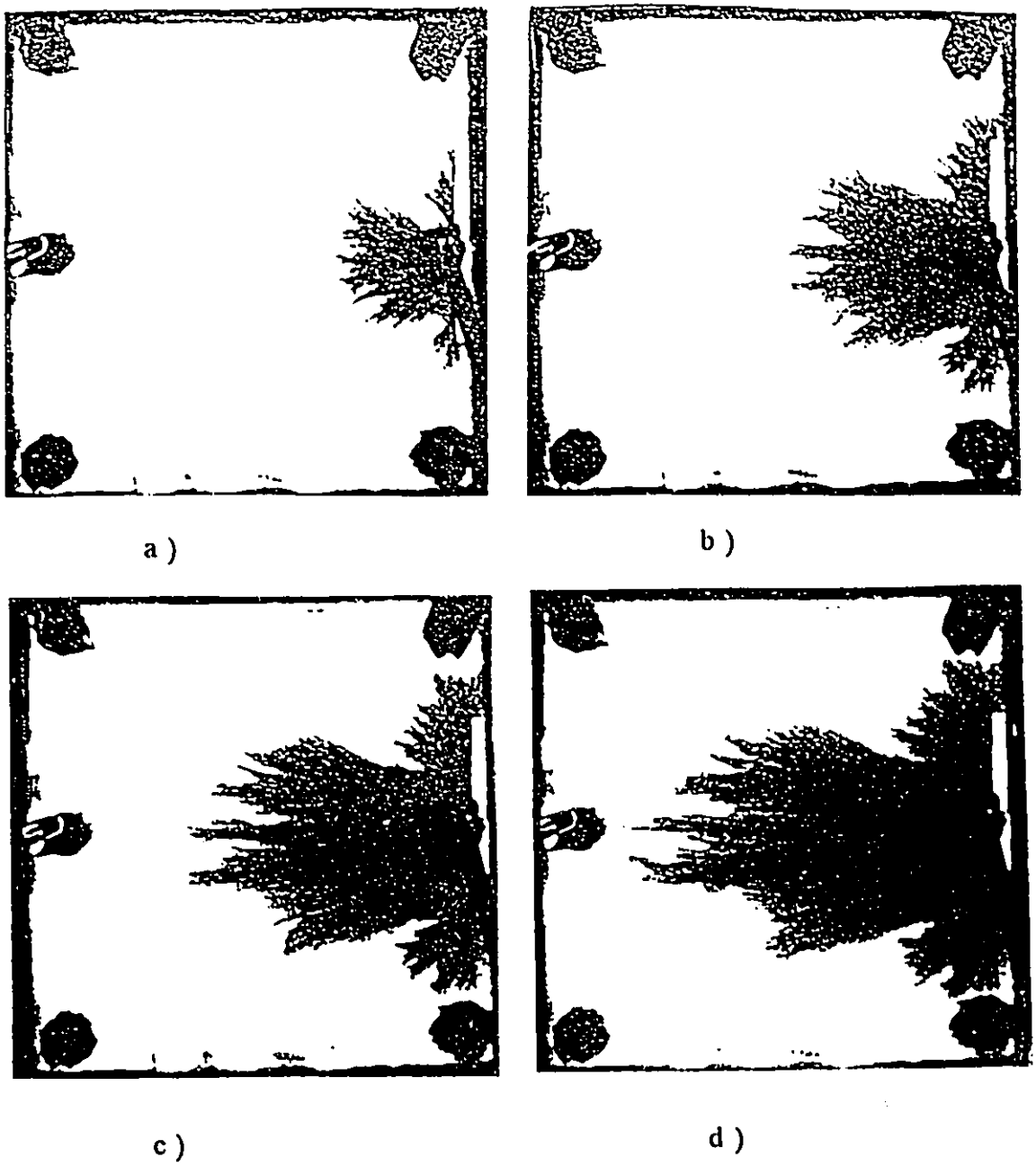

a)

b)

c)

d)

Fig.5.8 The development of the displacement pattern for a low injection flowrate of 38.4 ml/hr. μ_o/μ_w = 23.41, ρ_o/ρ_w = 1.19, (a) time = 33 seconds, (b) time = 76 seconds, (c) time =127 seconds, (d) time = 178 seconds, Recovery = 9.25 %.

HORIZONTAL DISPLACEMENT

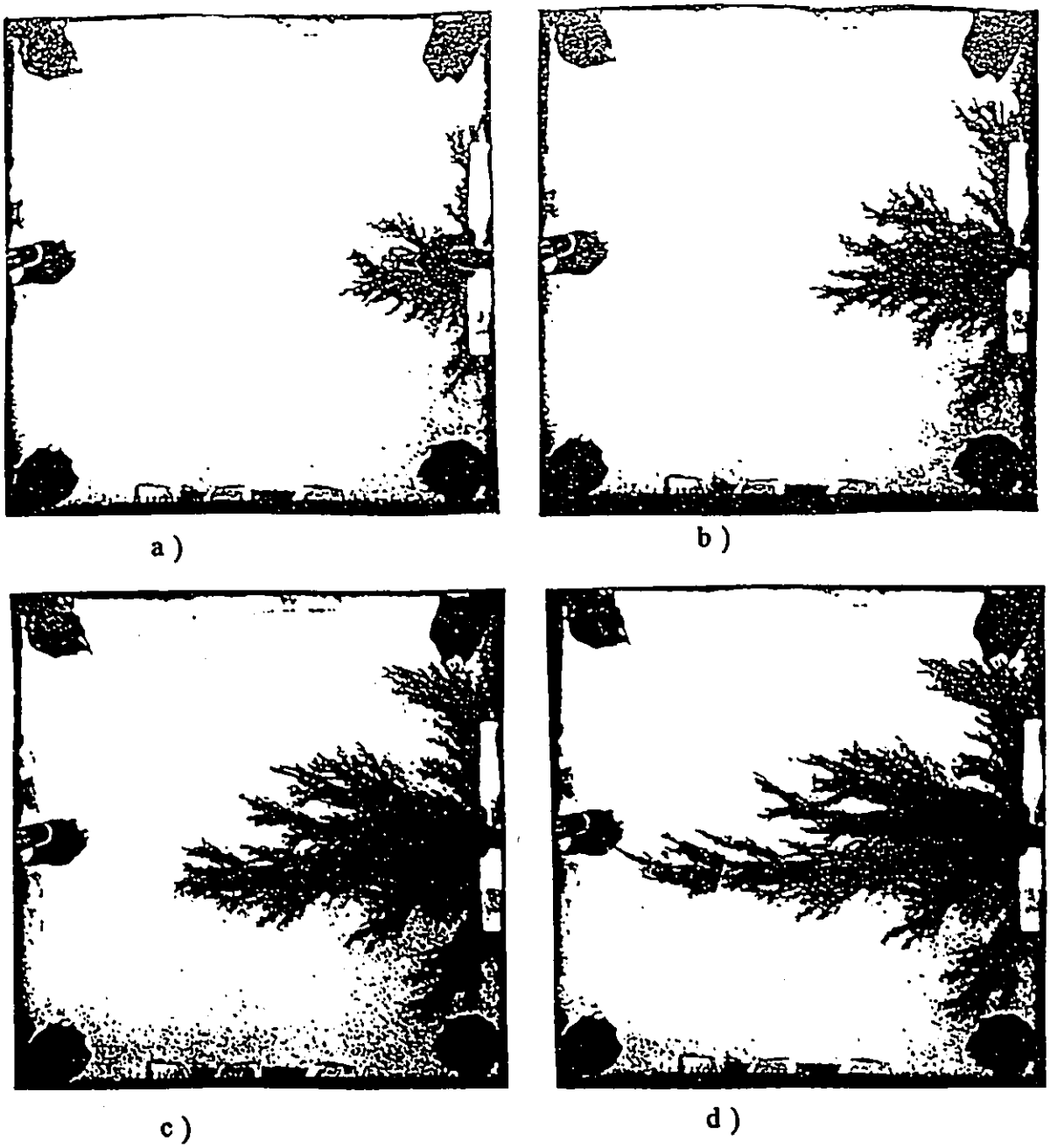

Fig.5.9 The development of the displacement pattern for a low injection flowrate of 38.4 ml/hr. $\mu_o/\mu_w = 147.5$, $\rho_o/\rho_w = 1.23$, (a) time = 19 seconds, (b) time = 44 seconds, (c) time =90 seconds, (d) time = 117 seconds, Recovery = 6.41 %.

HORIZONTAL DISPLACEMENT

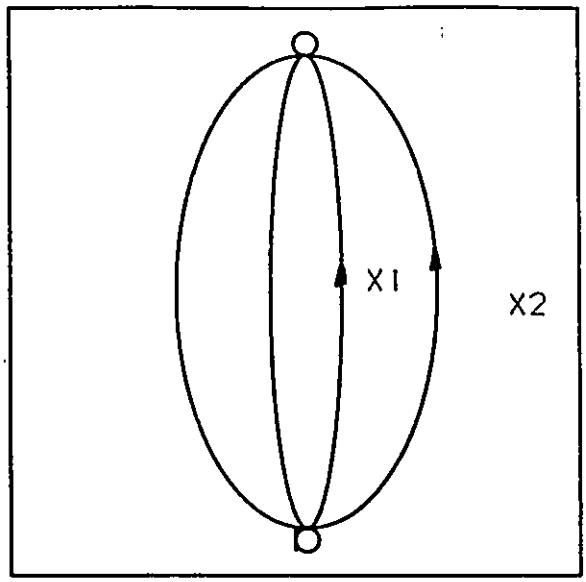

Fig.5.10 Flow stream line in the displacement

HORIZONTAL DISPLACEMENT

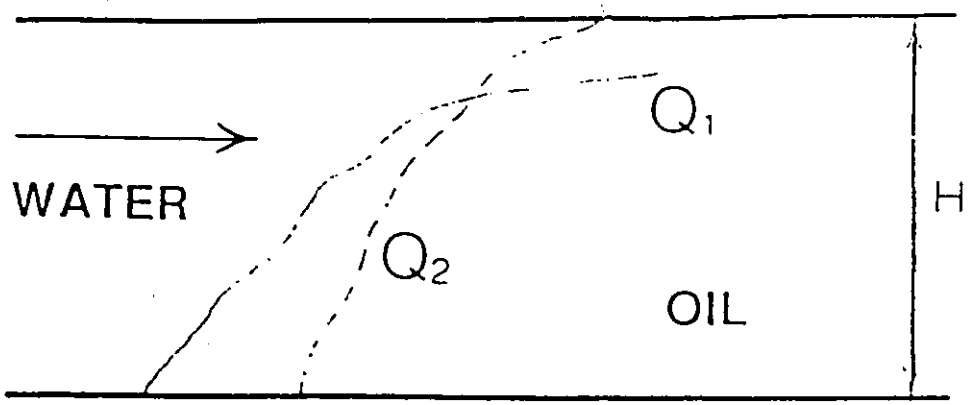

$$\rho w < \rho o$$

$$Q_1 > Q_2$$

Fig.5.11 Gravity over-ride in horizontal displacement

HORIZONTAL DISPLACEMENT

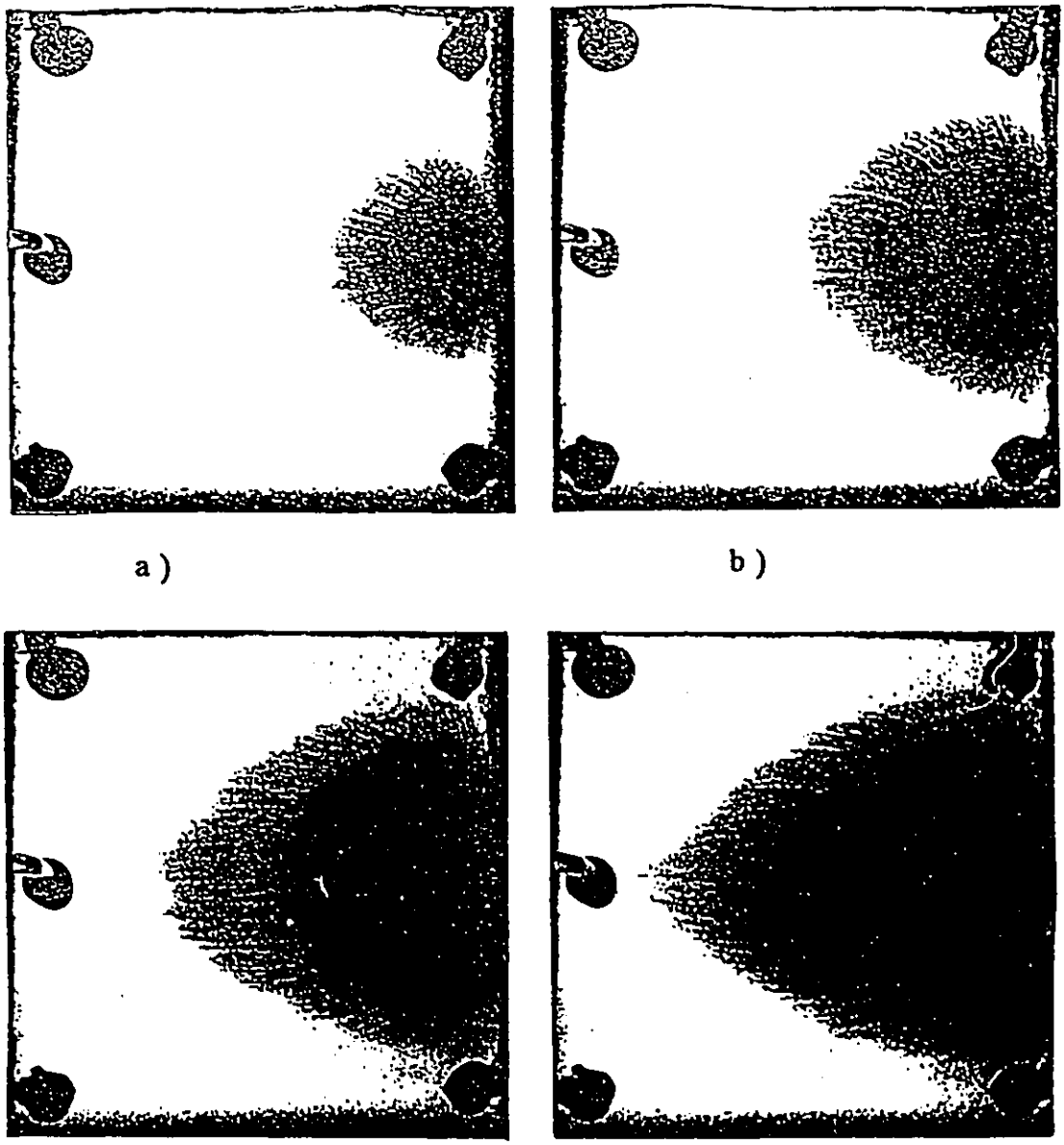

a)

b)

c)

d)

Fig.5.12 The development of the displacement pattern for a high injection flowrate of 169.2 ml/hr. $\mu_o/\mu_w = 1.56$, $\rho_o/\rho_w = 1.03$, (a) time = 30 seconds, (b) time = 69 seconds, (c) time =114 seconds, (d) time = 139 seconds, Recovery = 29.31 %.

HORIZONTAL DISPLACEMENT

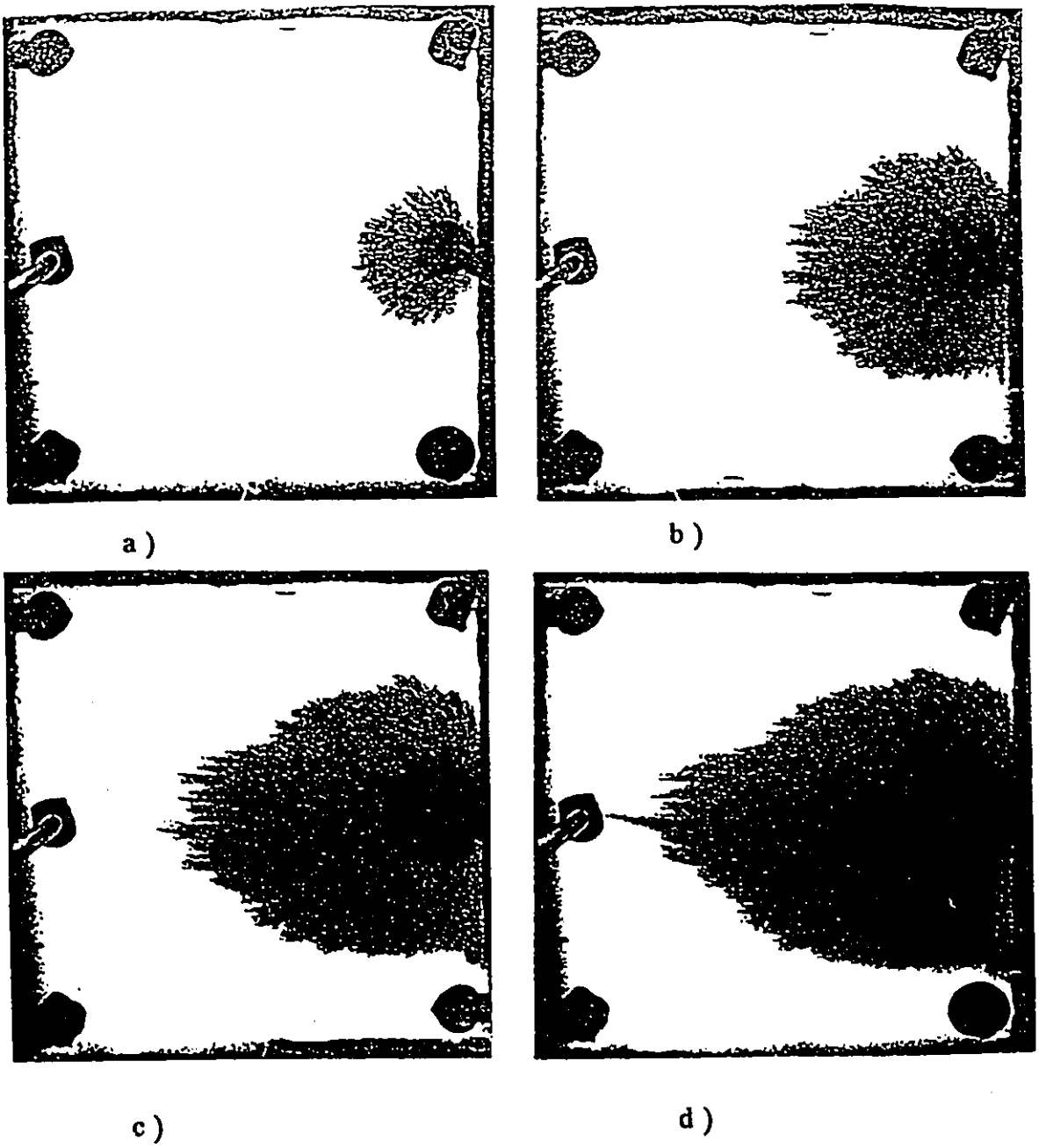

Fig.5.13 The development of the displacement pattern for a high injection flowrate of 169.2 ml/hr.. $\mu_o/\mu_w = 3.1$, $\rho_o/\rho_w = 1.09$, (a) time = 23 seconds, (b) time = 41 seconds, (c) time =78 seconds, (d) time = 92 seconds, Recovery = 22.20 %.

HORIZONTAL DISPLACEMENT

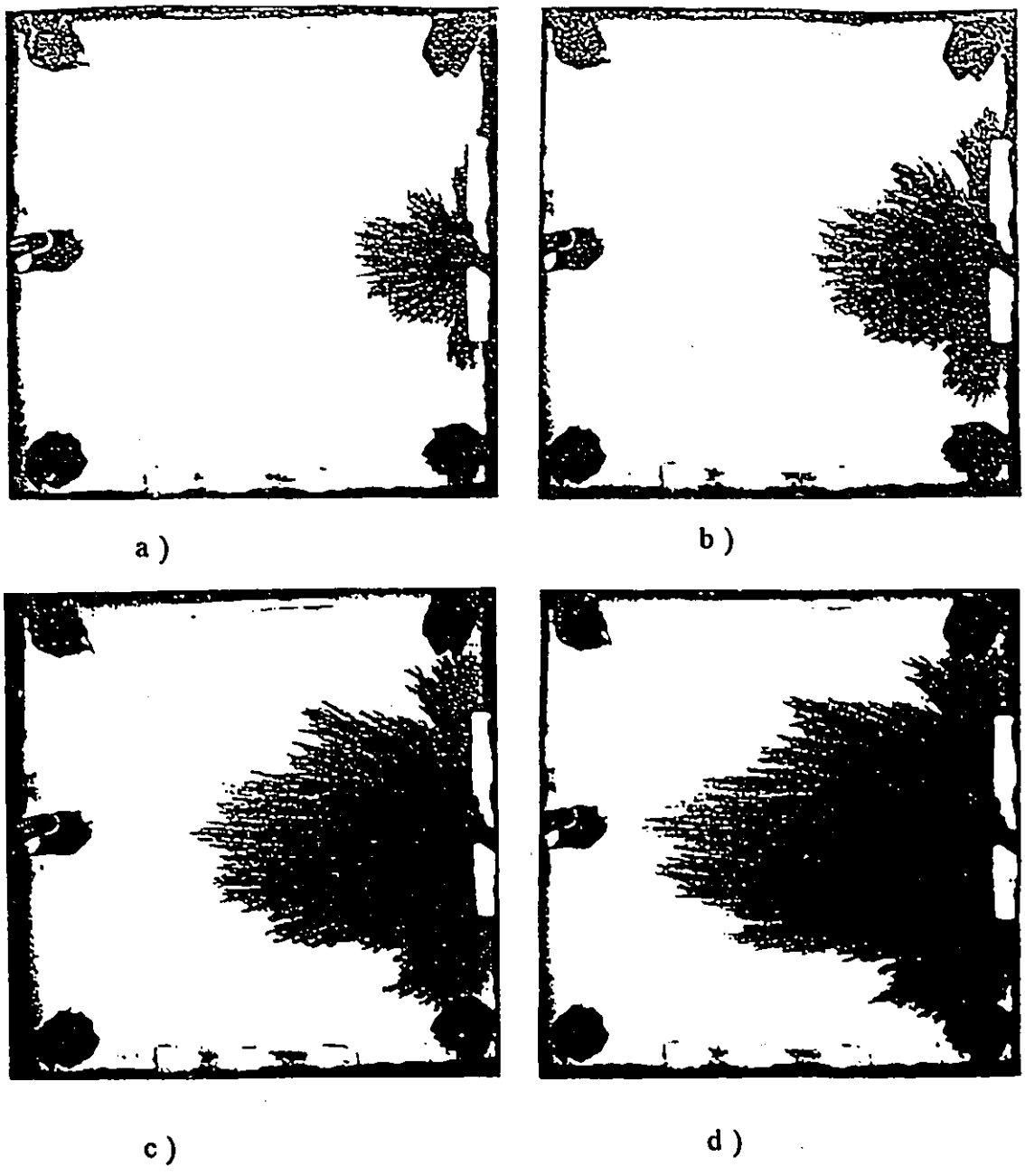

a)

b)

c)

d)

Fig.5.14 The development of the displacement pattern for a high injection flowrate of 169.2 ml/hr. $\mu_o/\mu_w = 7.4$, $\rho_o/\rho_w = 1.14$, (a) time = 18 seconds, (b) time = 28 seconds, (c) time =42 seconds, (d) time = 60 seconds, Recovery = 14.48 %.

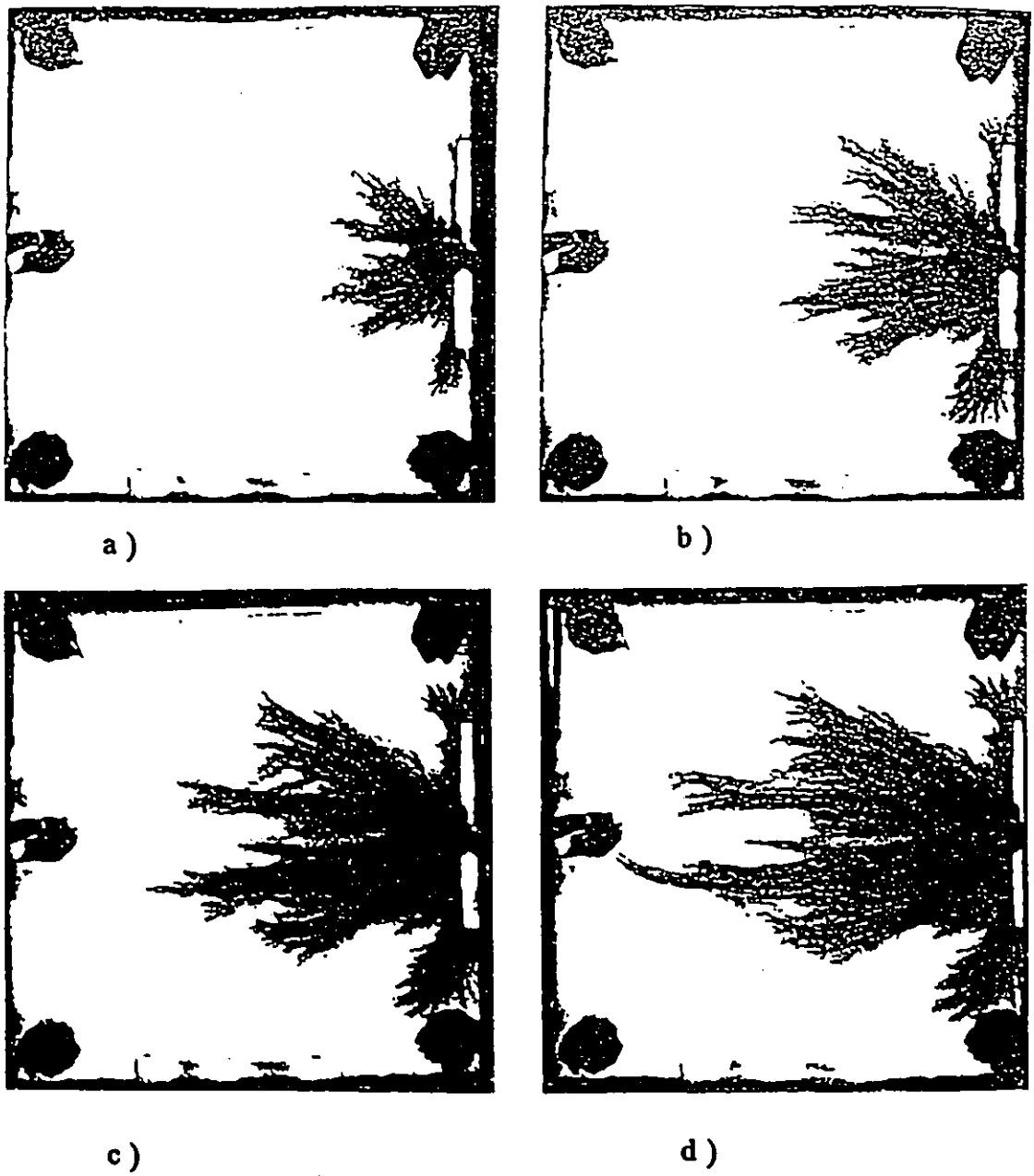

Fig.5.15 The development of the displacement pattern for a high injection flowrate of 169.2 ml/hr. μ_o/μ_w = 23.41, ρ_o/ρ_w = 1.19, (a) time = 9 seconds, (b) time = 18 seconds, (c) time =27 seconds, (d) time = 32 seconds, Recovery = 7.72 %.

HORIZONTAL DISPLACEMENT

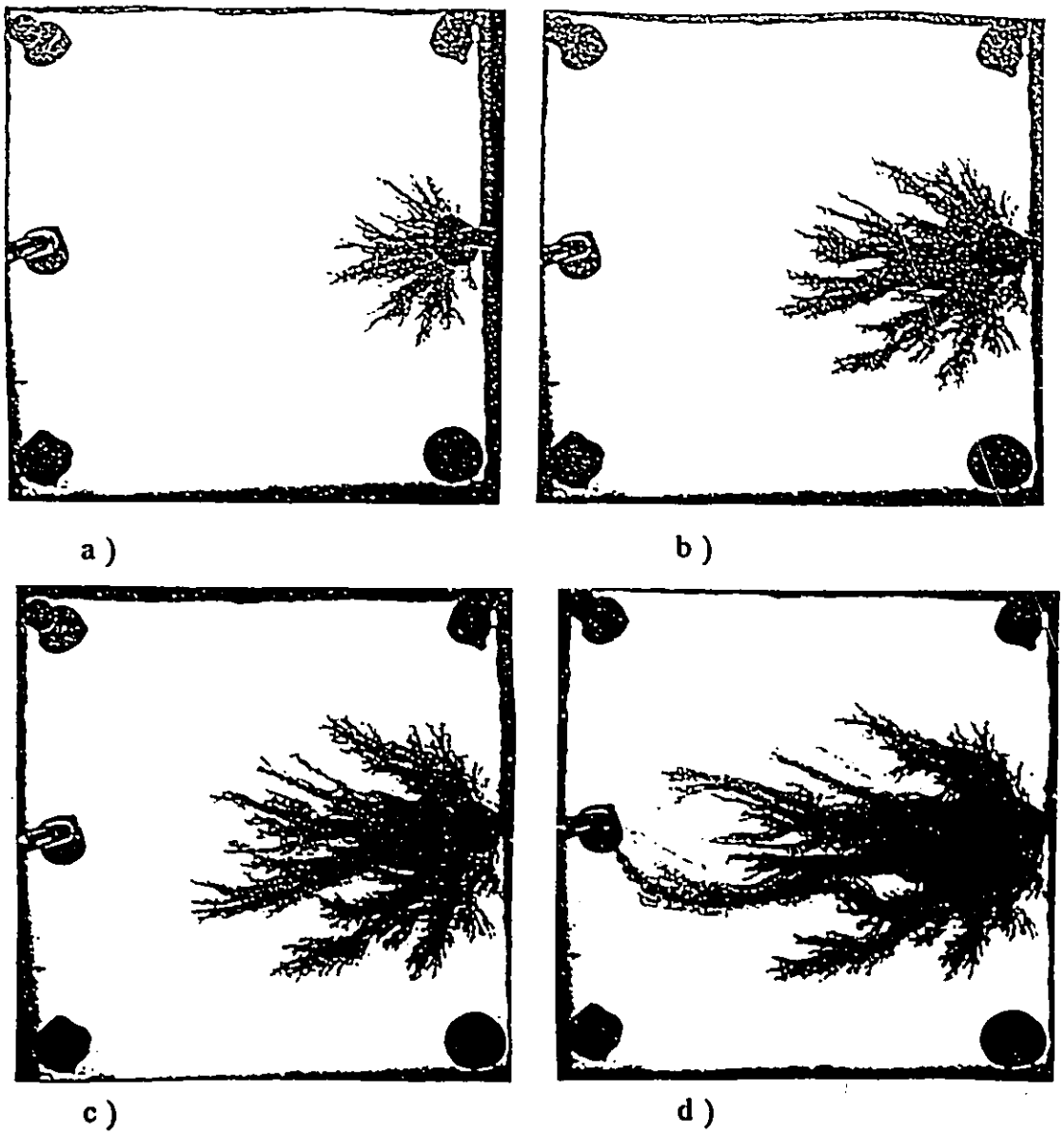

Fig.5.16 The development of the displacement pattern for a high injection flowrate of 169.2 ml/hr. μ_o/μ_w = 147.5, ρ_o/ρ_w = 1.23, (a) time = 7 seconds, (b) time = 16 seconds, (c) time =26 seconds, (d) time = 30 seconds, Recovery = 7.24 %.

HORIZONTAL DISPLACEMENT

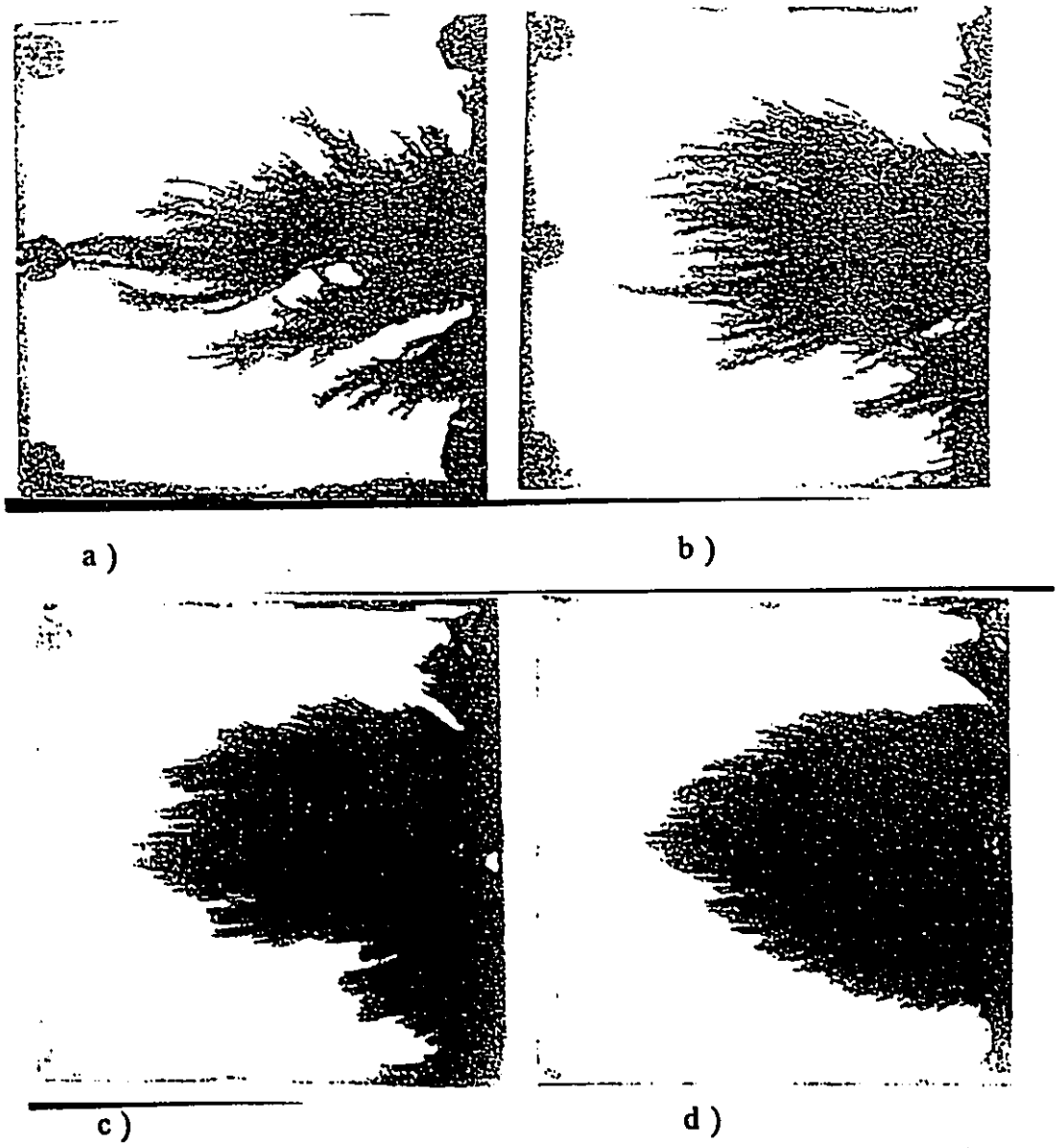

Fig.5.17 The effects of viscous forces. (a) μ_o/μ_w = 147.5, Q = 681 ml/hr., t_{br} = 12 seconds, R= 10.32%; (b) μ_o/μ_w = 23.41, Q = 681 ml/hr., t_{br} = 19 seconds, R = 16.34%; (c) μ_o/μ_w = 7.4, Q = 681 ml/hr., t_{br} = 30 seconds, R = 25.81%; (d) μ_o/μ_w = 3.1, Q = 449.4 ml/hr., t_{br} = 48 seconds, R = 27.25%.

HORIZONTAL DISPLACEMENT

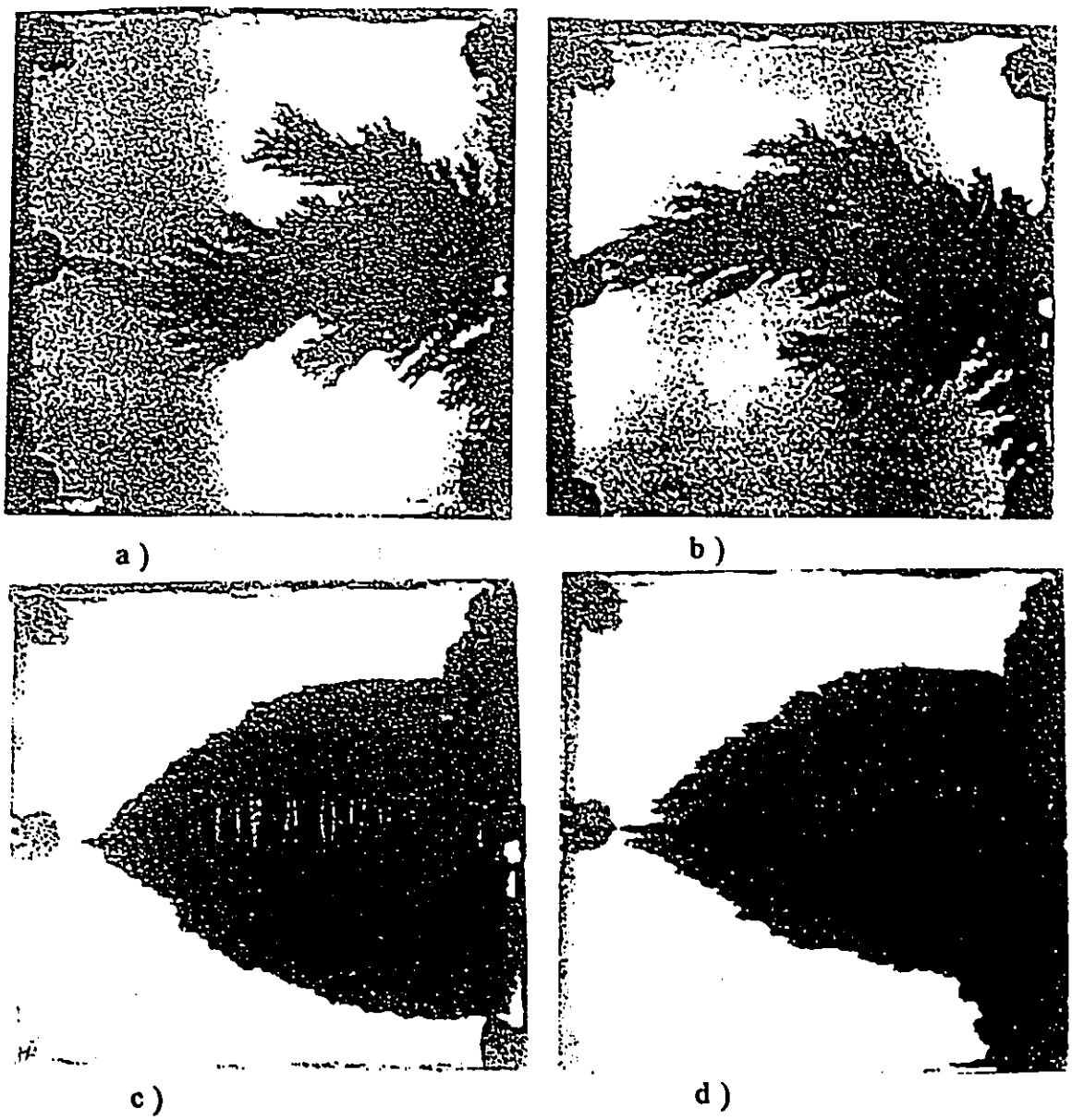

Fig.5.18 The behaviour from gravity region to viscous region. (a) μ_o/μ_w = 147.5, Q = 54.6 ml/hr., t_{br} = 102 seconds, R= 7.04%; (b) μ_o/μ_w = 147.5, Q = 116.4 ml/hr., t_{br} = 50 seconds, R = 7.35%; (c) μ_o/μ_w = 7.4, Q = 16.8 ml/hr., t_{br} = 907 seconds, R = 19.25%; (d) μ_o/μ_w = 7.4, Q = 38.4 ml/hr., t_{br} = 394 seconds, R = 19.11%.

5.4 Discussion for Vertical Downward Displacement

In experiments 6-10, the displacements were conducted in the vertical-downward flow mode. Similarly, the main variables in these experiments, besides wide range of injection flow rates, were the density difference and the viscosity ratio between the displacing and displaced fluids. The results of these experiments are summarized in Fig.5.19, 20, which show the stabilizing effects of gravity (buoyancy) forces on miscible, vertical-downward displacement processes. Meanwhile, the reverse effects of viscous forces can also be observed. Three regions may be identified at different flow rates according to Dumoré's theory [11]. They are (1) stable region; (2) transition (partially stable) region; (3) unstable region. In each of these regions, buoyancy forces and viscous forces play a different role during displacement processes.

5.4.1 The Development of the Displacement Pattern

In the vertical-downward displacements, the fingering pattern is completely different from that in horizontal displacement. The effects of buoyancy forces seem to be very important and vary on different injection flow rates, density differences and viscosity ratios. For a low density difference ($\rho_o / \rho_w = 1.03$) and a low viscosity

ratio ($\mu_o / \mu_w = 1.56$), as shown in Fig. 5.21 (Q= 38.4 ml/hr) , the displacing fluid was uniformly distributed around the inlet port of the cell, and tended to occupy the top of the cell during the first two stages (Fig.5.21a, b), where the time is 153 seconds and 594 seconds, respectively. Due to the low injection flow rates, the effects of buoyancy forces have ample time to influence the displacement, and entire top of the cell was occupied by the displacing fluid. When the time is up to 1100 seconds (breakthrough condition) the front of the displacing fluid arrived at the outlet port of the cell. In this case, the effects of buoyancy forces played a very significant role in displacement and led to a higher oil recovery (Fig. 5.21d).

However, increasing viscosity ratio and density difference, the behaviour of the development pattern gradually showed different. When the injection flow rate was kept the same (Q = 38.4 ml/hr), as shown in Fig.5.22, 5.23, 5.24, 5.25, the area covered by displacing fluid gradually decreased with the change of viscosity ratio and density difference, and fingering started to appear, even at the initial stage. Meanwhile, the number of fingers was increased. This phenomenon indicates that the effects of buoyancy forces gradually diminish and the viscous forces become predominant. Although the viscous forces dominate the whole displacement, the buoyancy forces still have their own effects on the fingering pattern. One can see that the fingers moved much wider rather than went downward directly. Finally, the breakthrough of displacing fluid was approached. From the pictures one can see that the total area covered by the displacing fluid is getting less from a lower viscosity ratio (1.56) and a density difference (1.03) to a higher viscosity ratio (147.46) and

a density difference (1.23). It is also shown in Fig.5.26, in which the oil recovery decreased with increasing viscosity ratio and density difference.

For the high injection flow rate of 169.2 ml/hr, the fingering pattern is totally different from that at low injection flow rates. From Fig.5.27, 5.28, 5.29, 5.30, 5.31 one can observe that viscous forces completely controlled displacement, even at a low viscosity ratio and a low density difference. Some smaller fingers appeared, and displacing fluid no longer occupied the whole top of the cell, fingers moved in all directions. Unlike the phenomena happened at a low injection flow rate, the displacing fluid went very faster, as could be seen in Fig.5.20, the breakthrough time decreased with the injection flow rates. The number of fingers was increased and the width of fingers was decreased. This resulted in less oil (aqueous glycerol solution) being displaced and consequently low recoveries.

5.4.2 The Effects of Injection Flow Rate

According to theory [11, 30], Dumoré defined two characteristic rates, which are

(1) the stable rate:

$$U_{st} = \frac{(\rho_o - \rho_w)\, Kg}{\mu_o(\ln \mu_o - \ln \mu_w)} \qquad \ldots\ldots\ldots\ldots\ldots\ldots (5.12)$$

(2) the critical rate:

$$U_c = \frac{(\rho_o - \rho_w)\, Kg}{(\mu_o - \mu_w)} \qquad \ldots\ldots\ldots\ldots\ldots\ldots \quad (5.13)$$

and the ratio between the stable and critical rates was given by:

$$\frac{U_{st}}{U_c} = \frac{(\mu_o - \mu_w)}{\mu_o(\ln \mu_o - \ln \mu_w)} \qquad \ldots\ldots\ldots\ldots\ldots\ldots \quad (5.14) \text{ or}$$

$$\frac{U_{st}}{U_c} = \frac{(1 - \frac{1}{M})}{lnM} \qquad \ldots\ldots\ldots\ldots\ldots\ldots (5.15)$$

where M is the viscosity ratio μ_o / μ_w. Since M > 1, the ratio of these two characteristic rates is always less than 1. Dumoré also proposed a simple way to judge whether the displacement is stable or not, i.e.,

(1) $U/U_c < U_{st}/U_c$, corresponds to a stable displacement (in stable region);

(2) $U_{st}/U_c < U/U_c < 1$, corresponds to a partially stable displacement (in transition region);

(3) $U/U_c > 1$, corresponds to an unstable displacement (in unstable region).

In this context, at lower injection flow rates, i.e. $U / U_c < U_{st} / U_c$ (stable region), as shown in Fig.5.32, the displacing fluid tended to occupy the entire top of

the cell and remained there due to the effects of the buoyancy forces, and then gradually formed a pronounced gravity tongue [6]. These buoyancy forces stabilized the displacement and no fingers were observed; therefore it resulted a higher recovery. This result is in good agreement with theory [11]. In addition, the agreement between these experiment results and Blackwell et al's experiment results [8] is also excellent. At relatively high injection flow rates, i.e. $U_u / U_c < U / U_c < 1$ (partially stable region), fingers were observed and poor displacement efficiencies resulted. In this range, buoyancy forces were comparable with viscous forces, as mentioned by Dumoré [11]. This process belongs to partly stable displacement, as can be proved by Fig.5.32, in which some fingers appeared, but a big gravity tongue still could be observed, which indicated the buoyancy forces still played a role in these displacements, and at the same time the viscous forces were also destroying the stable situation. In other words, the effects of viscous forces increase with the injection flow rate. Conversely, increasing injection flow rate will drastically increase viscous forces and buoyancy forces will no longer dominate the viscous forces, and more fingers will appear (see Fig.5.28d, Fig.5.29d, Fig.5.30d, Fig.5.31d). This is completely unstable displacement (where $U / U_c > 1$). As shown in Fig 5.33, the recoveries were plotted against a dimensionless parameter U / U_c. One can clearly see that the recovery decreased rapidly after $U / U_c > 1$.

Comparing Fig.5.19 with Fig.5.2, the recovery is higher in vertically-downward displacement than that in horizontal displacement in each corresponding case. In the horizontal mode, for example, the lowest recovery ($\varrho_o / \varrho_w = 1.23$, Q = 54.6 ml/hr) is

7.04% and the highest recovery (ϱ_o / ϱ_w=1.03) is 33.85% (average value); however, in vertical-downward flow mode, the lowest recovery (ϱ_o / ϱ_w=1.23, Q = 38.4 ml/hr) is 9.09%, the highest recovery (ϱ_o / ϱ_w=1.03, Q = 1.8 ml/hr) is 90.25%. This comparison obviously shows that buoyancy forces play a pronounced role and a better recovery can be approached in miscible downward displacements.

5.4.3 The Effects of Viscosity and Density

The dependence of recovery on the viscosity ratio was shown in Fig.5.26, in which the recovery at the breakthrough condition was plotted as a function of the viscosity ratio. At higher viscosity ratios increased instability caused both the breakthrough time and recovery decreasing. The trends of breakthrough recovery in this study are in good agreement with the data published by Blackwell et al. [8]. On the other hand, due to the difference of densities, the dimensionless parameter U_{st} / U_c increased as the densities decreased, as shown in Table 5.4, where ϱ_o / ϱ_w=1.23, and U_{st} / U_c=0.2064, U_c is only 0.1254×10^{-3} cm/s. However, when ϱ_o / ϱ_w=1.03, and U_{st} / U_c=0.8073, U_c is 0.3494×10^{-2} cm/s. From these data, one also can see that because of viscosity ratio increasing, the displacement reached the unstable process earlier; furthermore, the density difference would increase with viscosity ratio (it does not vary independently in this study). Therefore, with the increase of density ratio, the effects of buoyancy forces to stabilize the fingering process was diminished, and viscous forces predominated the displacement, resulting

in a lower recovery.

Table 5.4. Dimensionless parameter U/U_c versus concentration.

Conc. (%)	86%	67%	50%	30%	10%
U_c (cm / s)	0.00013	0.00055	0.0015	0.0028	0.0035
U_{st}/U_c	0.21	0.30	0.43	0.60	0.81
U / U_c	0.89 *	0.20	0.07	0.04	0.03
	2.29 *	0.52	0.20	0.10	0.08
	3.54 *	0.81	0.30	0.16	0.13
	8.27 *	1.89*	0.71	0.37	0.30
	18.89 *	4.32*	1.62*	0.84	0.68
	43.10 *	9.86*	3.70*	1.91*	1.55*
	57.27 *	13.10*	4.92*	2.54*	2.06*
	83.24 *	19.04 *	7.15*	3.69 *	2.99*
	137.56*	31.47*	11.82*	6.10*	4.94*
	221.10*	50.58*	19.00*	9.80*	7.94 *

* indicates data in the viscous region.

• in this study, K = 72.36 μm^2 [3].

It should be noted that there is no stable region when μ_o/μ_w=147.46 in this study because the viscosity ratio is very high and the injection flow rate is not low enough. From Fig.5.21, one can see that more fingers exist in the entire displacement , which confirms that the viscous forces completely control the displacements when the viscosity ratio is high and the injection flow rate is not very low.

VERTICAL DOWNWARD DISPLACEMENT

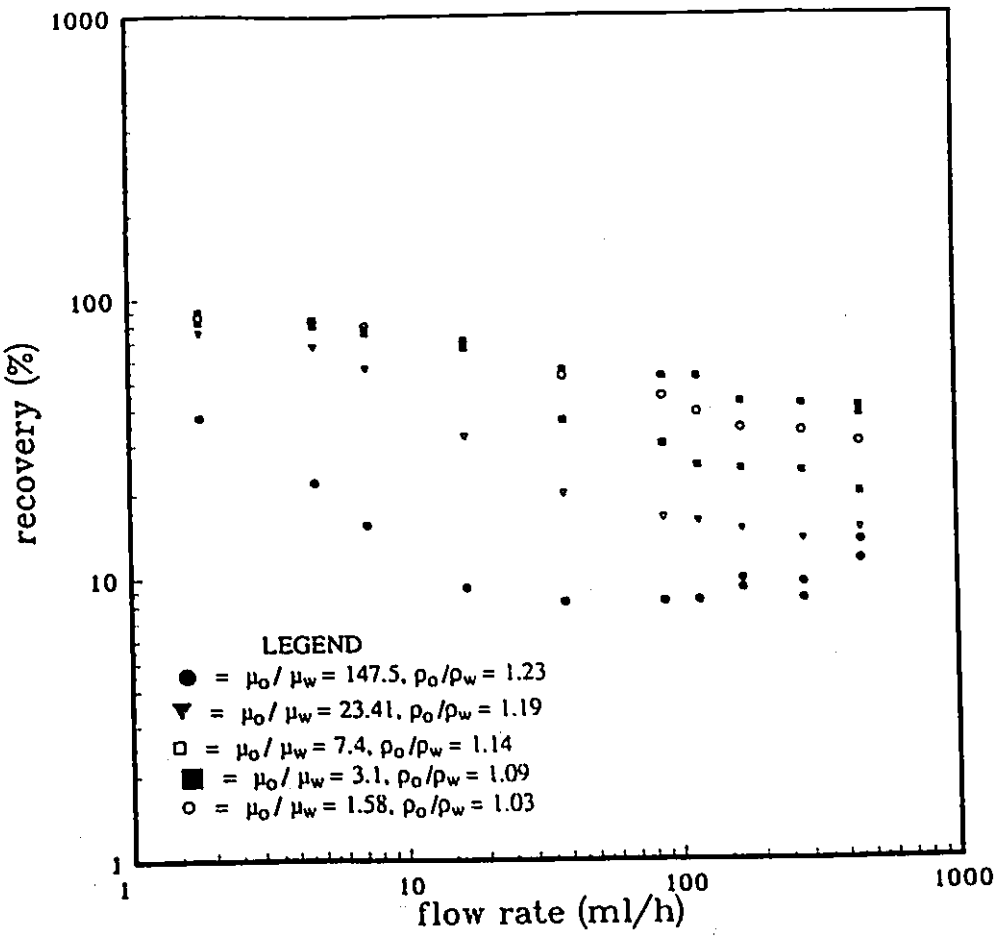

Fig.5.19. Vertical Downward Mode, the relationship between flowrate and breakthrough recovery.

VERTICAL DOWNWARD DISPLACEMENT

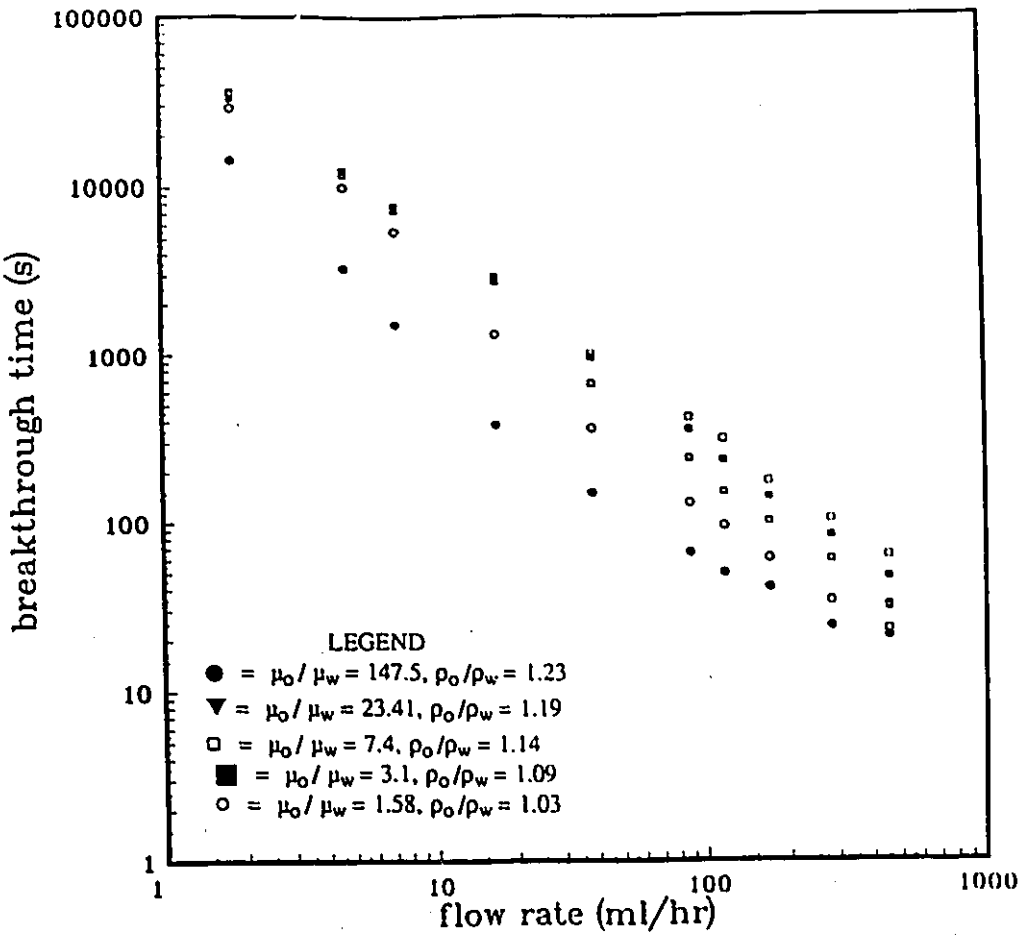

Fig.5.20. Vertical Downward Mode, the relationship between injection flowrate and breakthrough time.

VERTICAL DOWNWARD DISPLACEMENT

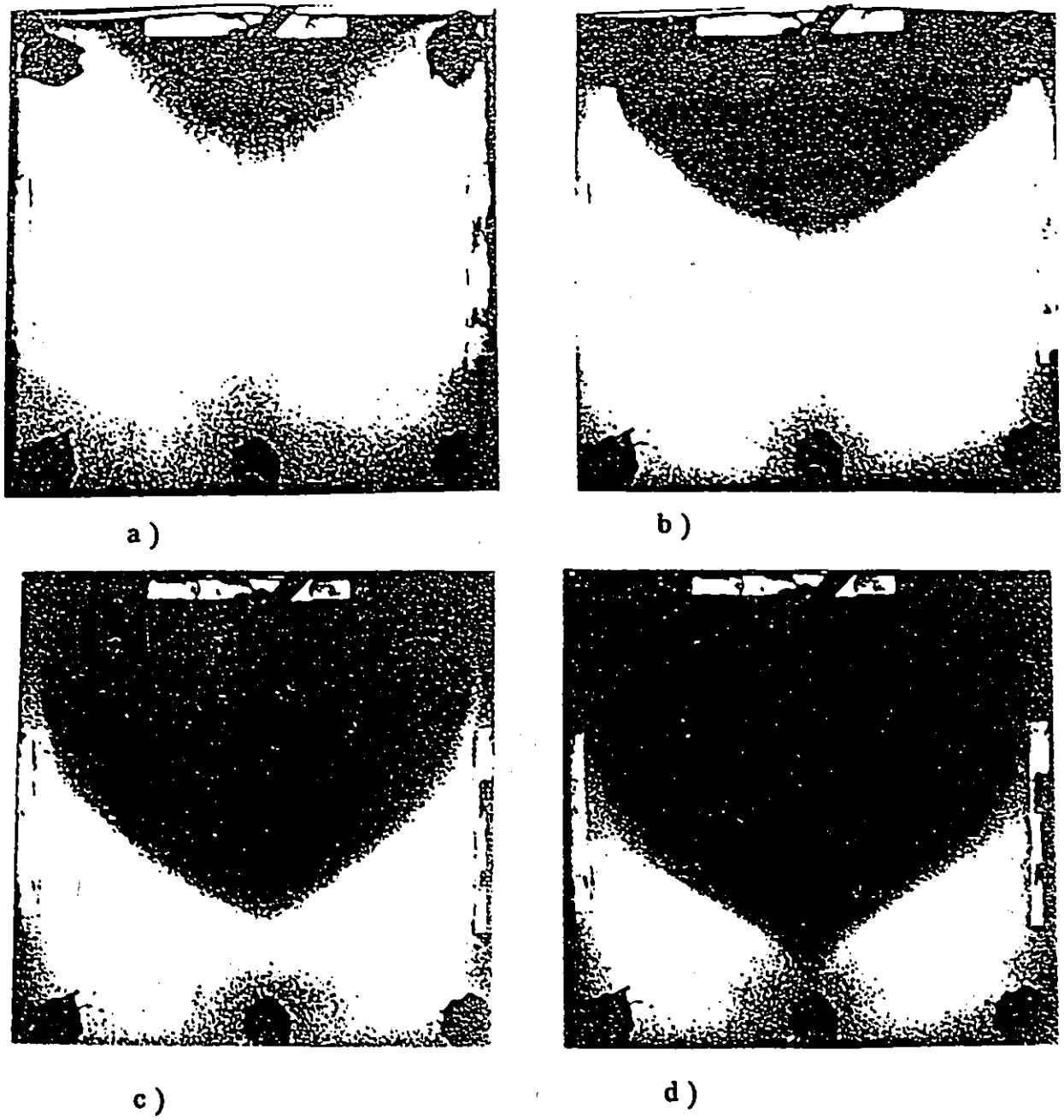

a)

b)

c)

d)

Fig.5.21. The development of the displacement pattern for a low injection flowrate of 38.4 ml/hr. $\mu_o/\mu_w = 1.56$, $\rho_o/\rho_w = 1.03$, (a) time = 153 seconds, (b) time = 594 seconds, (c) time =1100 seconds, (d) time = 1294 seconds, Recovery = 70.86 %.

VERTICAL DOWNWARD DISPLACEMENT

a)

b)

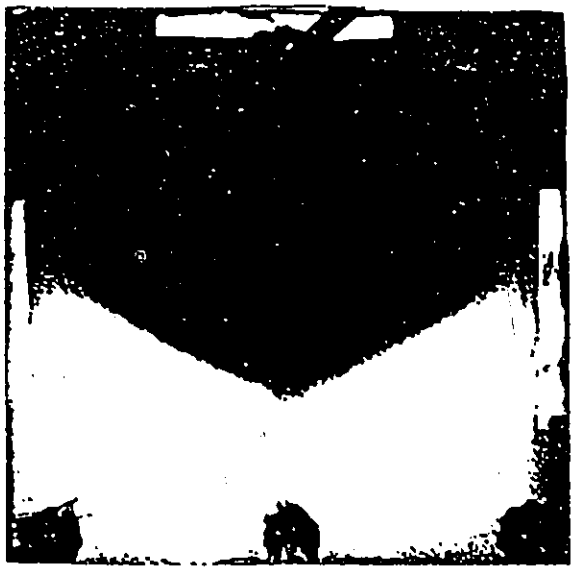

c)

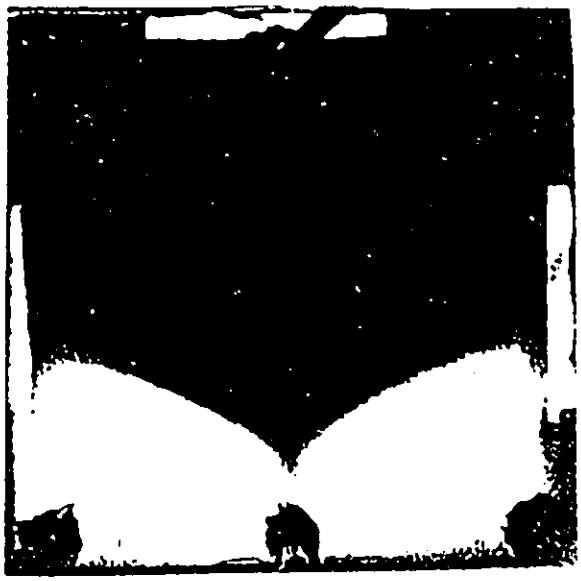

d)

Fig.5.22 The development of the displacement pattern for a low injection flowrate of 38.4 ml/hr. $\mu_o/\mu_w = 3.1$, $\rho_o/\rho_w = 1.09$, (a) time = 145 seconds, (b) time = 530 seconds, (c) time =930 seconds, (d) time = 1116 seconds, Recovery = 61.11 %.

VERTICAL DOWNWARD DISPLACEMENT

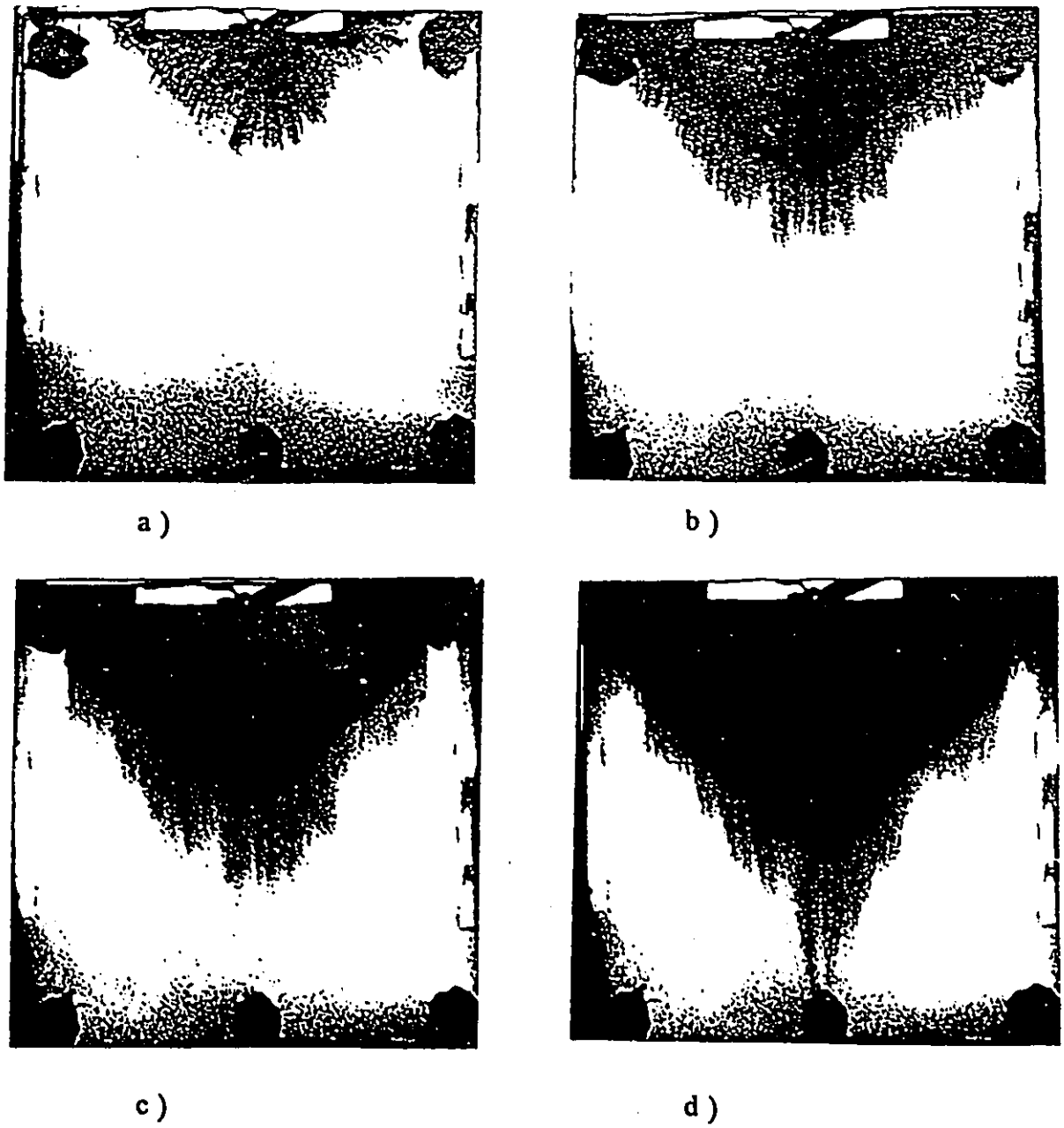

a)

b)

c)

d)

Fig.5.23. The development of the displacement pattern for a low injection flowrate of 38.4 ml/hr. μ_o/μ_w = 7.4, ρ_o/ρ_w = 1.14, (a) time = 96 seconds, (b) time = 327 seconds, (c) time =606 seconds, (d) time = 760 seconds, Recovery = 41.62 %.

VERTICAL DOWNWARD DISPLACEMENT

a)

b)

c)

d)

Fig.5.24 The development of the displacement pattern for a low injection flowrate of 38.4 ml/hr. $\mu_o/\mu_w = 23.41$, $\rho_o/\rho_w = 1.19$, (a) time = 59 seconds, (b) time = 118 second, (c) time =183 seconds, (d) time = 257 seconds, Recovery = 14.07%.

VERTICAL DOWNWARD DISPLACEMENT

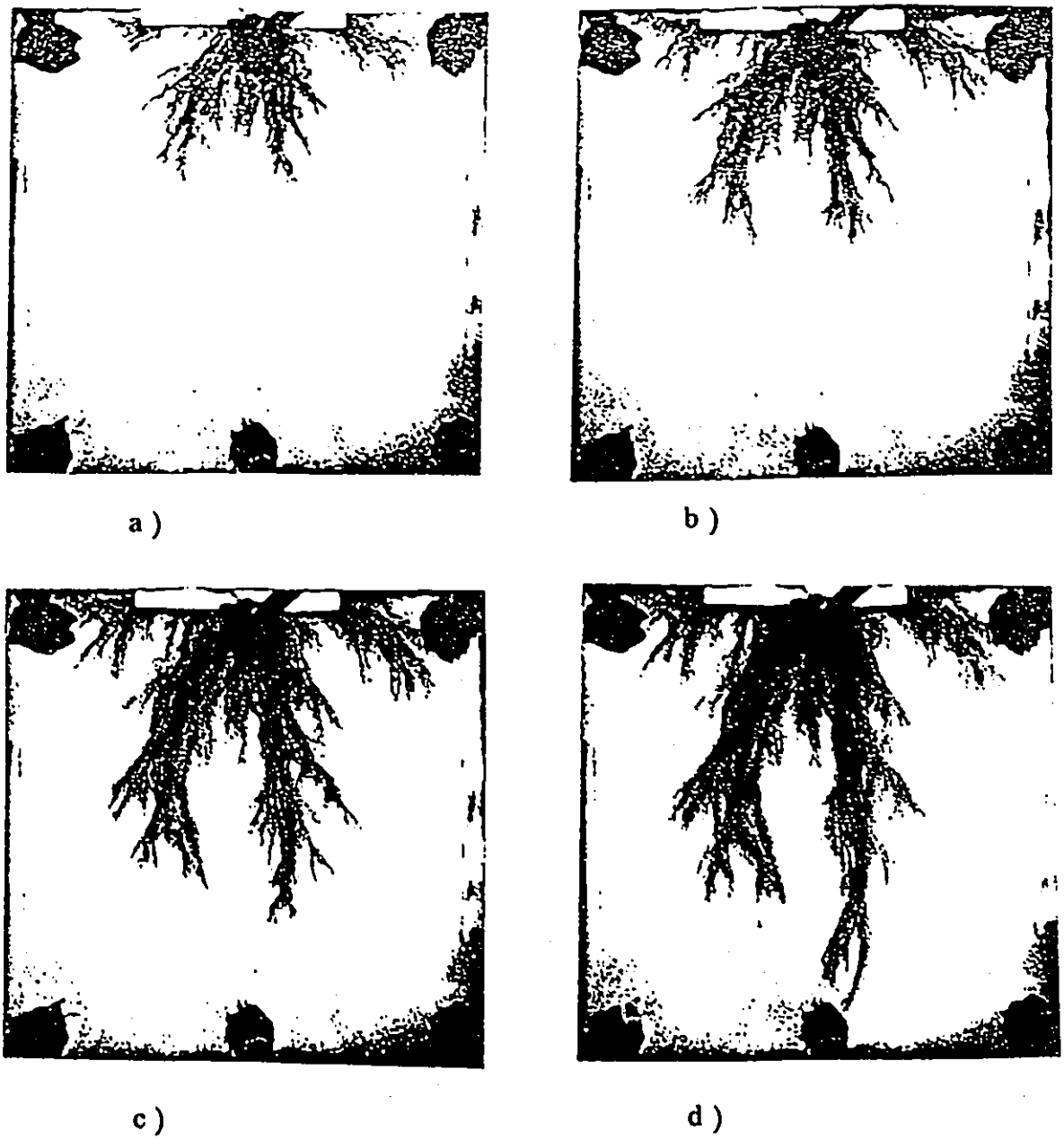

a)

b)

c)

d)

Fig.5.25 The development of the displacement pattern for a low injection flowrate of 38.4 ml/hr. μ_o/μ_w = 147.5, ρ_o/ρ_w = 1.23, (a) time = 52 seconds, (b) time = 90 seconds, (c) time =137 seconds, (d) time = 166 seconds, Recovery = 9.09%.

VERTICAL DOWNWARD DISPLACEMENT

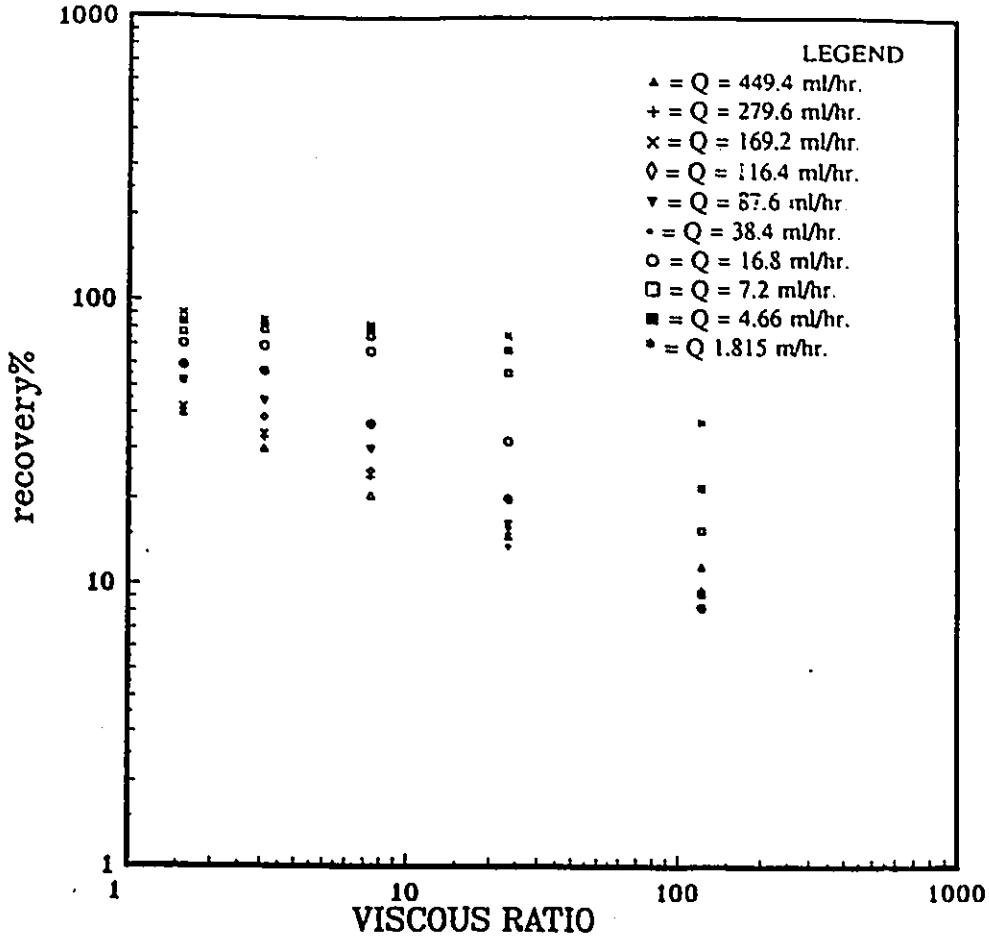

Fig.5.26. Oil recovery versus viscosity ratio

VERTICAL DOWNWARD DISPLACEMENT

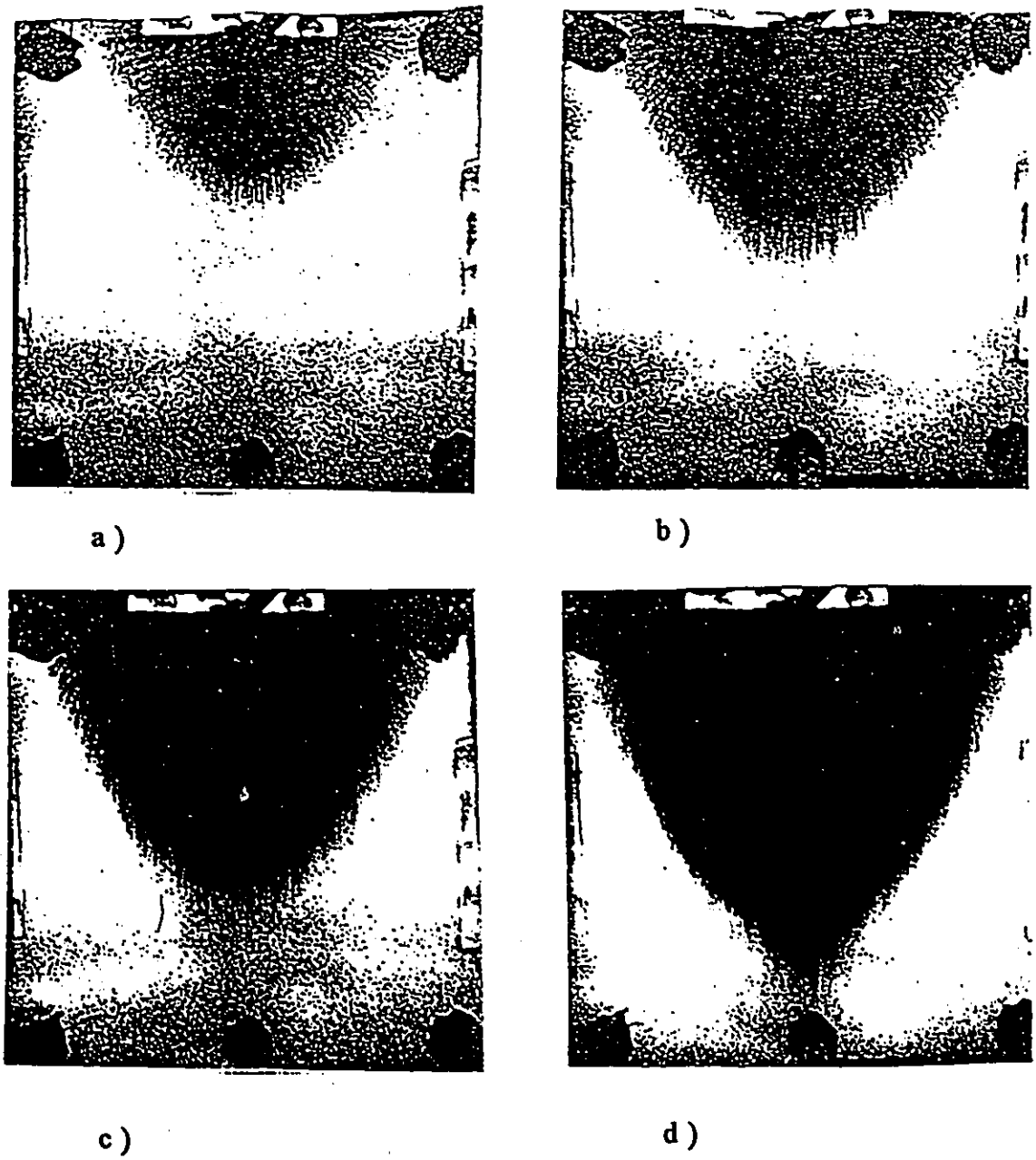

a)

b)

c)

d)

Fig.5.27 The development of the displacement pattern for a high injection flowrate of 169.2 ml/hr. $\mu_o/\mu_w = 1.56$, $\rho_o/\rho_w = 1.03$, (a) time = 31 seconds, (b) time = 46 seconds, (c) time =98 seconds, (d) time = 178 seconds, Recovery = 41.73 %.

VERTICAL DOWNWARD DISPLACEMENT

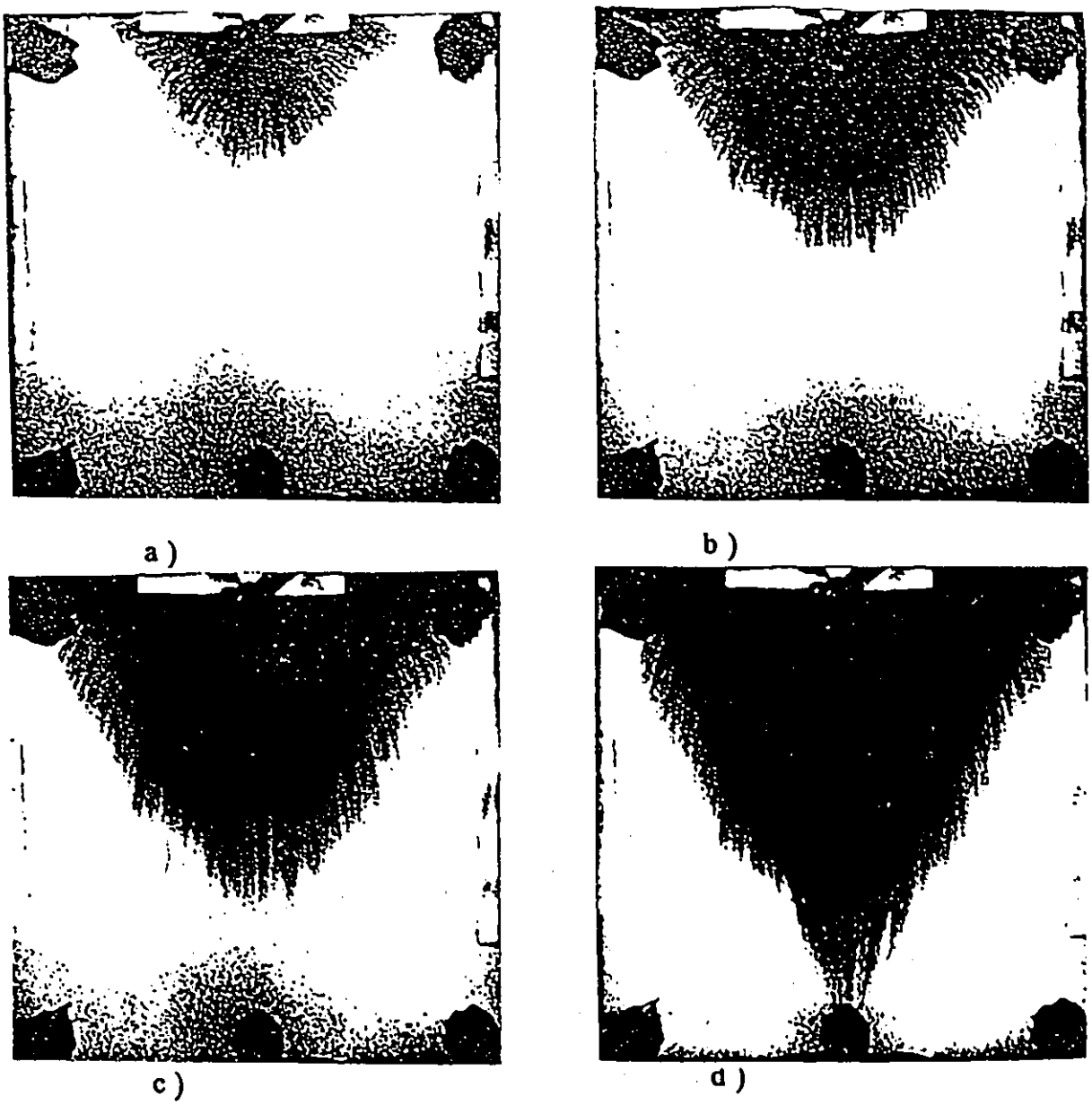

Fig.5.28 The development of the displacement pattern for a high injection flowrate of 169.2 ml/hr. $\mu_o/\mu_w = 3.1$, $\rho_o/\rho_w = 1.09$, (a) time = 21 seconds, (b) time = 68 seconds, (c) time =120 seconds, (d) time = 168 seconds, Recovery = 40.53 %.

VERTICAL DOWNWARD DISPLACEMENT

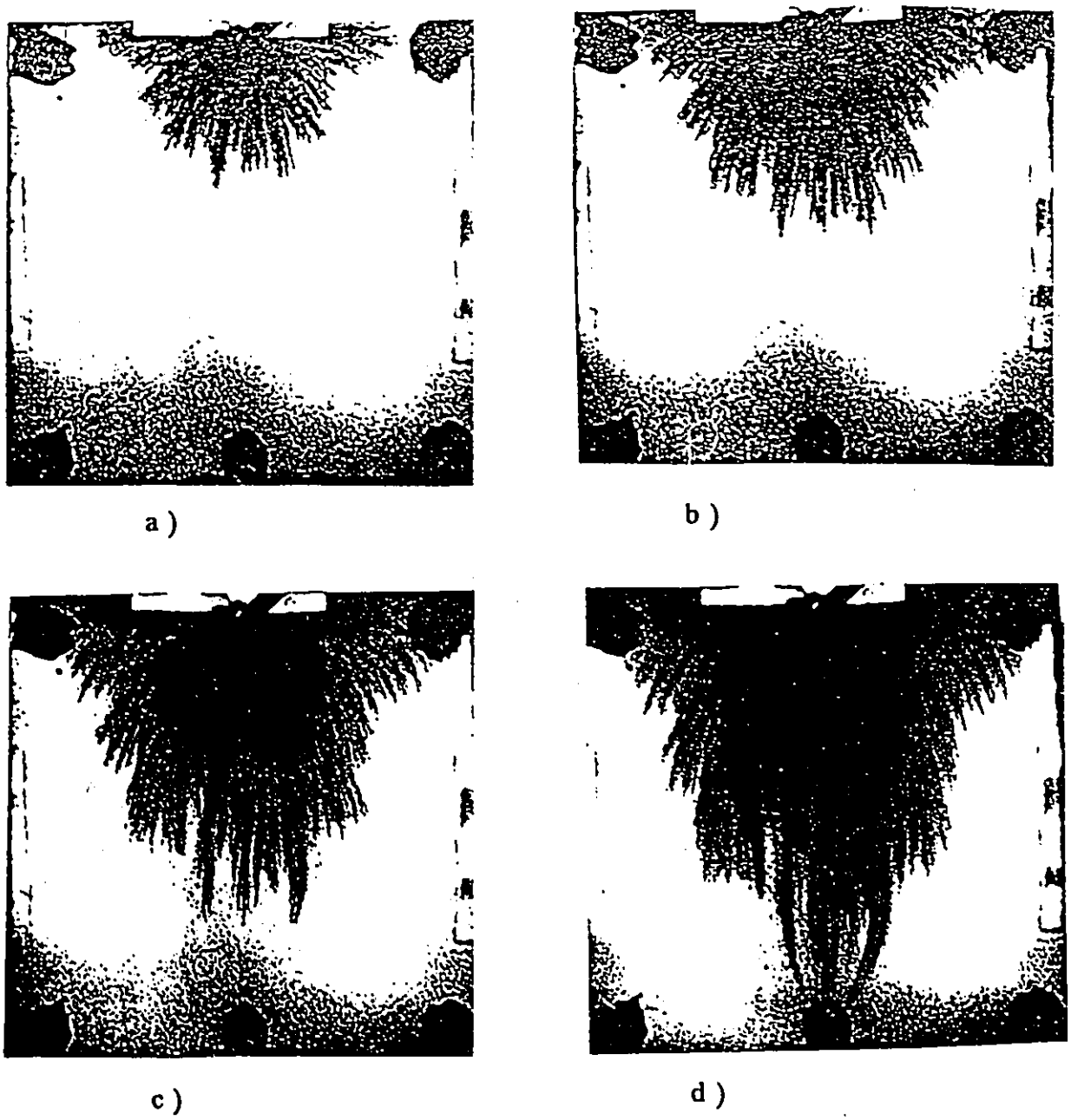

a)

b)

c)

d)

Fig.5.29 The development of the displacement pattern for a high injection flowrate of 169.2 ml/hr. μ_o/μ_w = 7.4, ρ_o/ρ_w = 1.14, (a) time = 16 seconds, (b) time = 43 seconds, (c) time =74 seconds, (d) time = 101 seconds, Recovery = 24.37 %.

VERTICAL DOWNWARD DISPLACEMENT

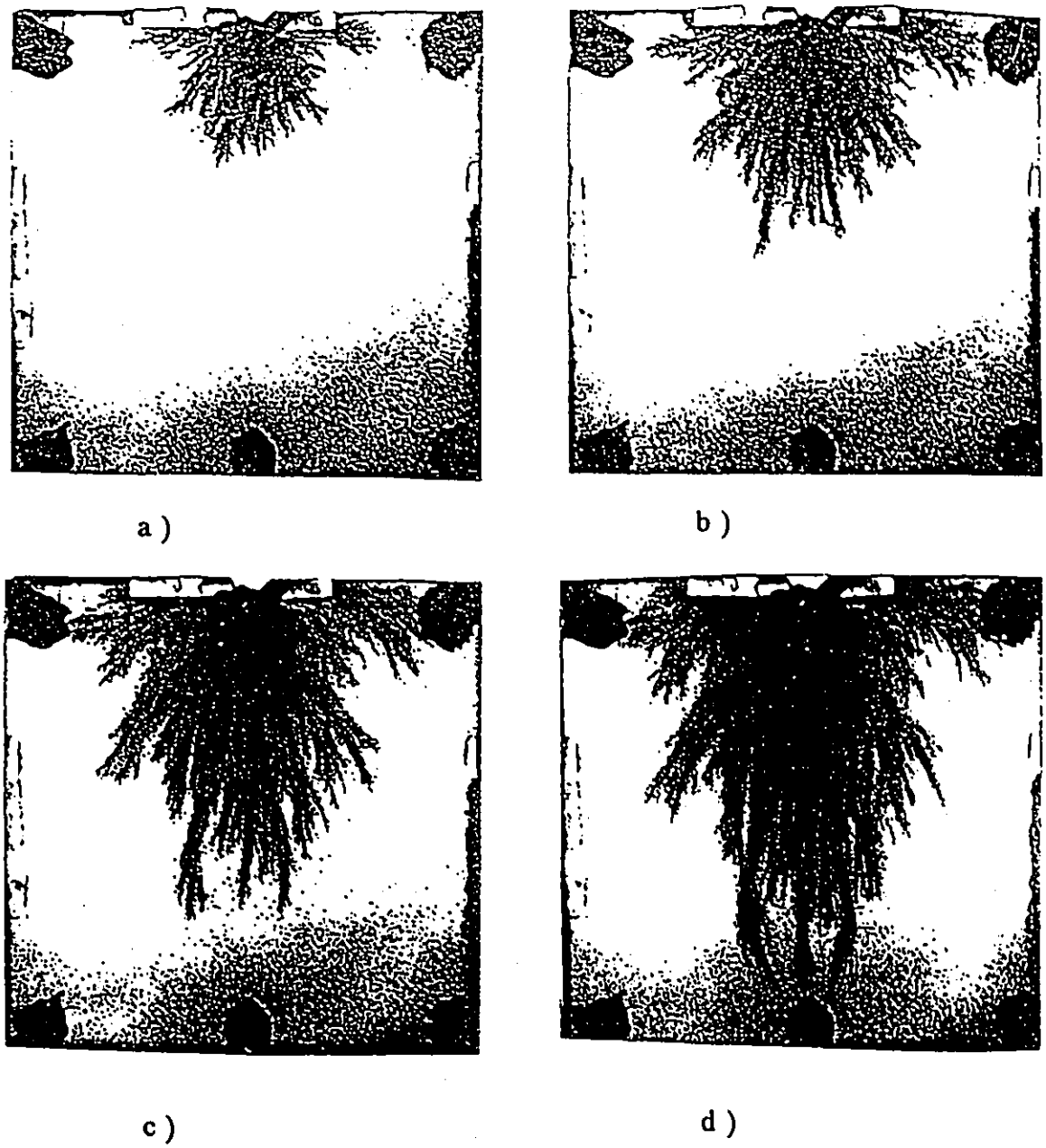

a)

b)

c)

d)

Fig.5.30 The development of the displacement pattern for a high injection flowrate of 169.2 ml/hr. $\mu_o/\mu_w = 23.41$, $\rho_o/\rho_w = 1.19$, (a) time = 10 seconds, (b) time = 24 seconds, (c) time =40 seconds, (d) time = 55 seconds, Recovery = 13.27%.

VERTICAL DOWNWARD DISPLACEMENT

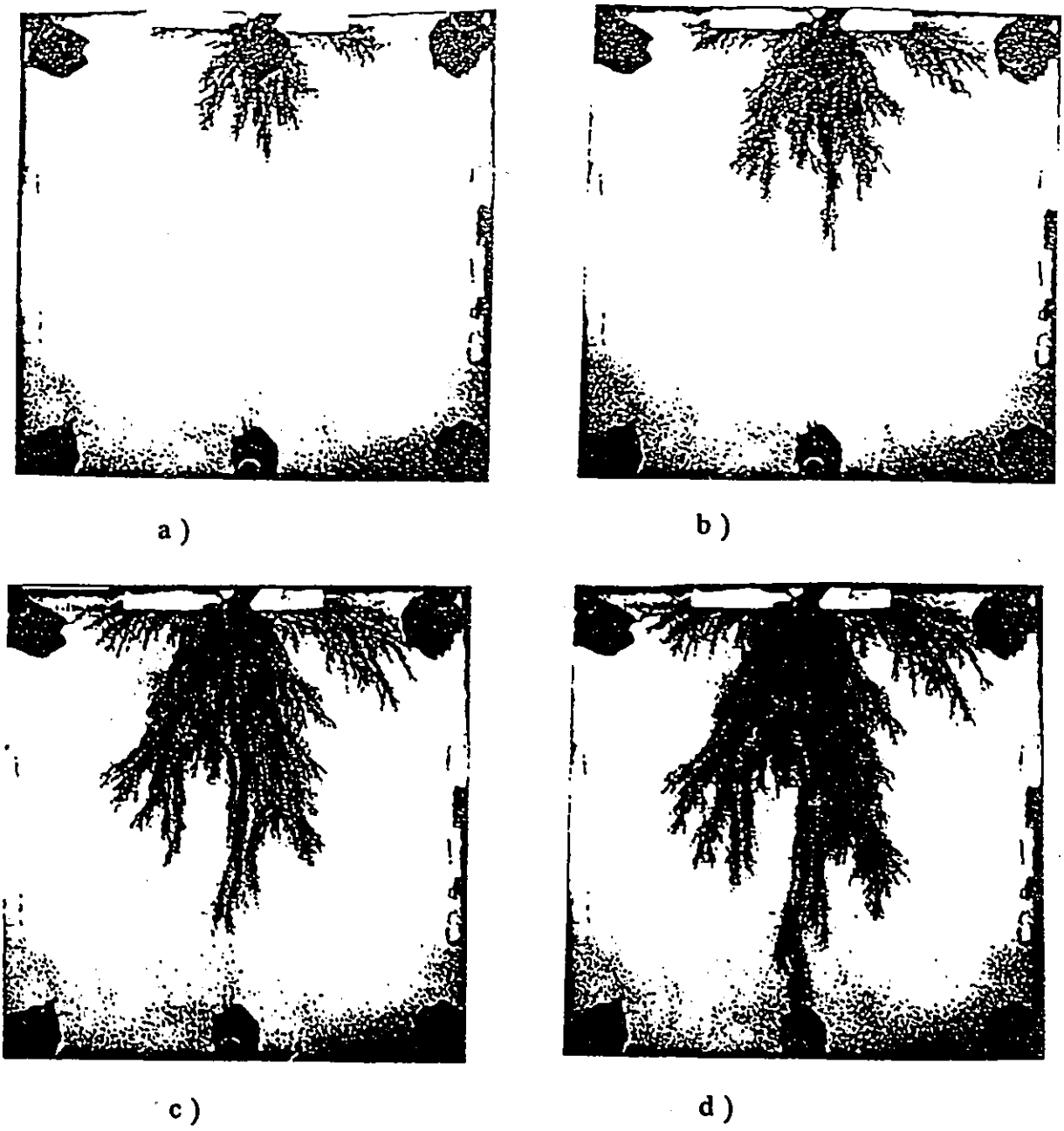

a)

b)

c)

d)

Fig.5.31 The development of the displacement pattern for a high injection flowrate of 169.2 ml/hr. μ_o/μ_w = 147.5, ρ_o/ρ_w = 1.23, (a) time = 8 seconds, (b) time = 17 seconds, (c) time =31 seconds, (d) time = 39 seconds, Recovery = 9.41 %.

VERTICAL DOWNWARD DISPLACEMENT

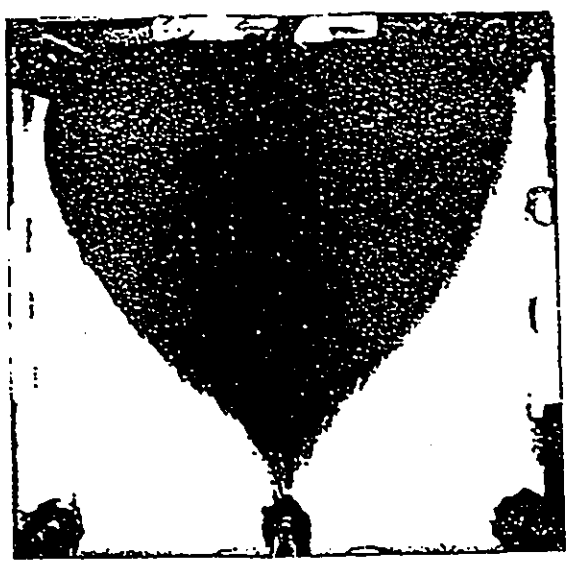

a)

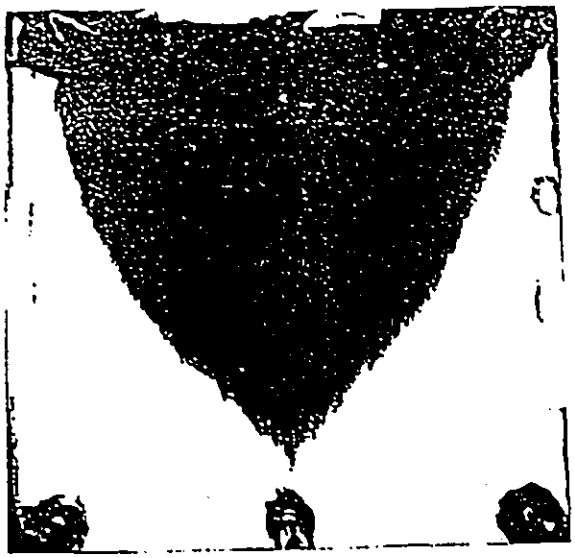

b)

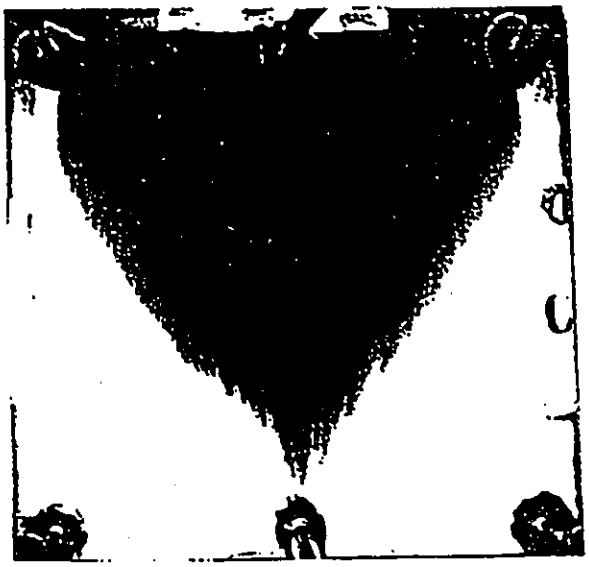

c)

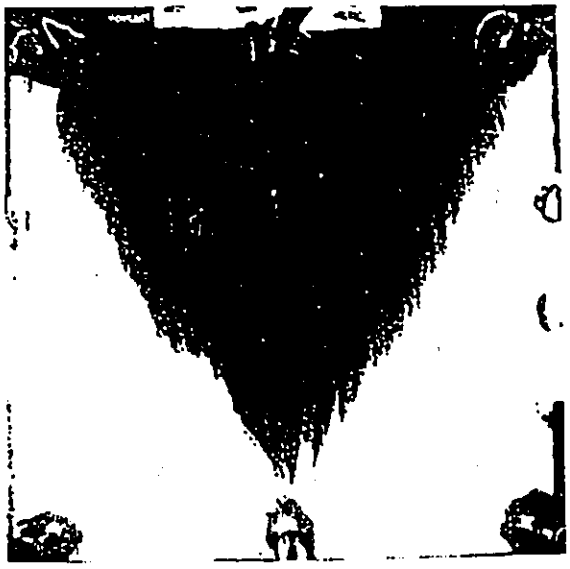

d)

Fig.5.32 In the partial stable region, the fingering pattern show the different effects of gravity forces and viscous forces. For μ_o/μ_w =1.58, (a) Q = 87.6 ml/hr.; (b) Q = 116.4 ml/hr.; for μ_o/μ_w = 3.1, (c) Q = 87.6 ml/hr.; (d) Q = 116.4 ml/hr..

VERTICAL DOWNWARD DISPLACEMENT

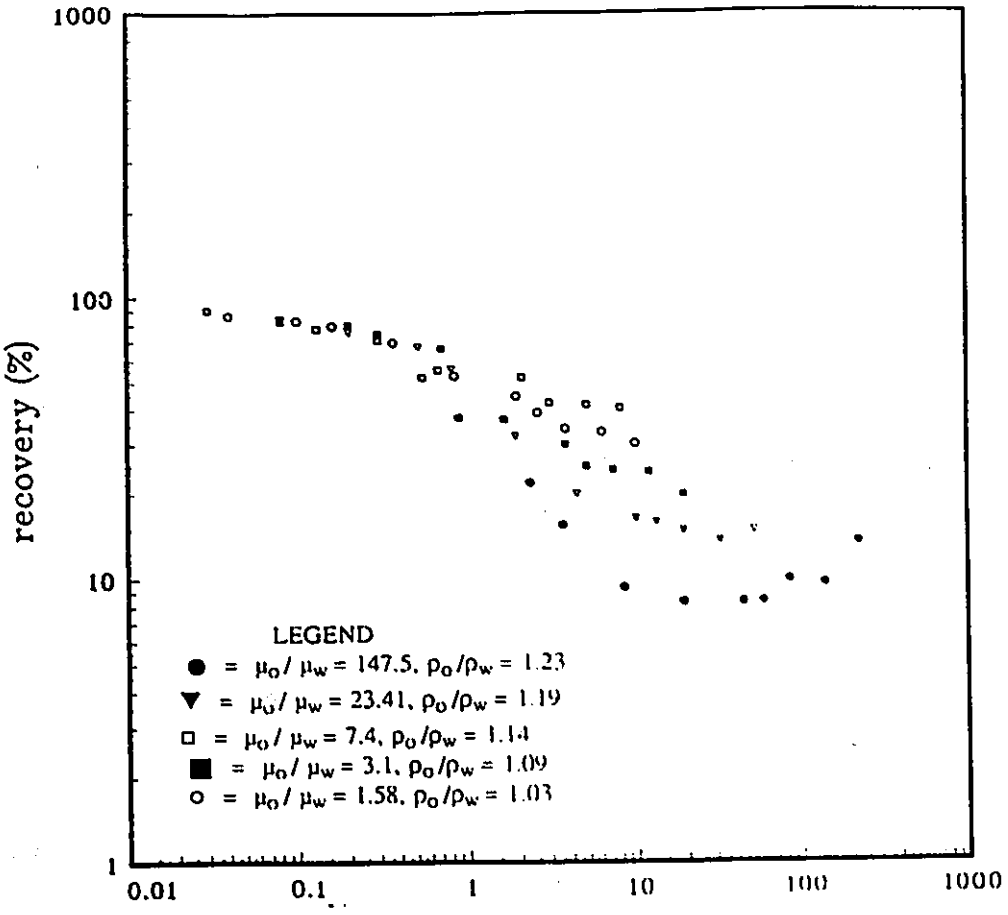

dimensionless velocity U/U_c

Fig.5.33. Vertical Downward Mode, the relationship between oil recovery and dimensionless parameter U / U_c.

5.5 Discussion for Vertical Upward Displacement

In experiments 11--15, the experiments were conducted in the vertical-upward flow mode. Injection of displacing fluid (water dyed with methylene blue) with a low viscosity into a vertically oriented cell that contained oil (glycerol solution) more dense than the displacing fluid tends to lead to the formation of a gravity tongue if the flow rate is low enough that vertical transport by gravity segregation dominates the viscous forces that induce instability. However, if the viscosity ratio is high, the result will be totally different. On the other hand, unlike the phenomena that occurred in vertical-downward displacement, (in which the buoyancy forces can suppress viscous fingers developing), the buoyancy forces can promote viscous fingers developing and magnify the size of viscous fingers. The results of these experiments are shown in Fig.5.34, 35. As the flow rate increases, gravity forces play a diminishing role, and eventually viscous forces dominate the buoyancy forces. This can also be seen from Fig.5.36, in which the oil recovery is plotted as a function of the viscous/gravity ratio, N_{gr}. The oil recovery increases as this ratio increases, which also means that viscous forces play a very important role in vertical-upward displacement.

5.5.1 The development of the displacement pattern

Fig.5.37, 38, 39, 40, 41 show the development of the displacement pattern for a low injection flow rate of 4.7 ml/hr. Time intervals were measured starting from the moment that the displacing fluid first entered the porous medium. During the early stages of displacement for a low viscosity ratio (1.56), as shown in Fig.5.37a, the displacing fluid invaded the displaced fluid in only one direction, gradually forming a small gravity tongue. This gravity tongue moved upwards and no fingering occurred under this condition. During the next 700 s, as shown in Fig.5.37b, the gravity tongue grew only in the longitudinal direction rather than transverse direction. This indicates that the buoyancy forces promote upwards motion of the displacing fluid and suppress it from moving transversely. After approximately 1165 s, the top of the gravity tongue was getting a little wider and the bottom part near the inlet port still kept the same shape as shown in Fig.5.37c. In the final interval, the displacing fluid converged at the outlet port. Throughout the whole displacement process one can observe that the displacing fluid was basically filling the invaded area because the gravity tongue was almost displaced by the darker colour (displacing) fluid. Also, due to the effects of buoyancy forces, the width of the gravity tongue was very narrow, as shown in Fig.5.37d, which resulted in a low recovery.

With increasing viscosity ratio, the pattern of the displacements would be different. One could clearly see that at the first stage the viscous fingers gradually appeared as the viscosity ratio increased (Fig.5.38a, 5.39a, 5.40a, 5.41a), especially at

high viscosity ratios. Even though the fingering began during the first stage, the fingers could not get wider because of the effects of buoyancy forces. During the next two stages, as shown in Fig.5.38b ,c, 39b, c, 40b, c, 41b, c, tree-like fingers appeared, but the moving speed of the displacing fluid in the longitudinal direction was still greater than that in the transverse direction. More small fingers were born from the original ones. However, these fingers could not grow wider and bigger because the buoyancy forces suppressed them. This process continued until breakthrough of the displacing fluid, as shown in Fig.5.38d, 39d, 40d, 41d.

Fig.5.42, 43, 44, 45, 46 show the development of the displacement pattern for a high injection flow rate of 169.2 ml/hr. As indicated in Fig. 5.42a, for a given low viscosity ratio (1.56) the initial displacement pattern is completely different from those at low flow rates. At the beginning of the displacement the displacing fluid entered into the porous medium in a radial direction and was uniformly distributed. Some smaller dendritic fingers appeared as shown in Fig.5.42b, c, and could not become bigger fingers due to the very small density difference between these two fluids ($(\varrho_o - \varrho_w) / \varrho_w = 3\%$). At the final stage, as shown in Fig.5.42d, the displacing fluid gradually converged to the outlet port until breakthrough occurred. One can observe from Fig.5.42 that at the front of the displacing fluid there were some smaller fingers, but due to the low density difference, the fingers could not grow bigger, and resulted in a good oil recovery. Comparing this with higher viscosity ratios, it showed that more fingers came out and the width of these fingers increased as the viscosity ratio increased (see Fig.5.43,44, 45, 46). On the other hand, the

darker coloured area was getting smaller, which means the fraction of the porous medium occupied by the displacing fluid became much less and consequently lowered the recovery. Furthermore, increasing the injection flow rate will increase the viscous forces. In this case, the viscous forces completely controlled the displacement, and we can see that more fingers developed and some of them were getting bigger. Therefore, one may conclude that the higher the flow rate, the lower the density difference and viscosity ratio, the higher the oil recovery.

5.5.2 The Effects of Injection Flow Rate

Fig.5.34 shows the effects of the injection flow rate on the oil recovery at the breakthrough time. In the situation of a low injection flow rate, the buoyancy forces still played an important role in displacement, but it was a negative effects because the direction of the buoyancy forces was the same as that of the pressure difference applied in the experiment. When the flow rate was lower, the pressure difference between inlet port and outlet port of the cell was smaller so that the buoyancy forces could be comparable with the pressure difference. As shown in Fig.5.37, 38, 39, 40, 41 one can observe that the pattern of viscous fingering (μ_o/μ_w =147.46) or gravity tongue (μ_o/μ_w =1.56) was very narrow, the displacement pattern developed much more in the longitudinal direction than in the transverse direction. This shows that the inverse effects of the buoyancy forces happened in a low flow rate displacement. As a result of this negative effects, only a lower oil recovery could be obtained. The

lowest recovery in these vertical-upward flow experiments is 3.66% (μ_o/μ_w =147.46, ϱ_o/ϱ_w =1.23, Q = 0.91 ml/hr). However, these phenomena were completely different from those when the injection flow rate was increased. The buoyancy forces no longer played an important role in these displacements, and viscous forces completely controlled the displacement. One can see from Fig.5.42, 43, 44, 45, 46 that more fingers appeared and the pattern of the viscous fingers was much wider compared with what happened at low injection flow rates, and the fingers not only developed in the longitudinal direction, but also in the transverse direction. Comparing these patterns with those in horizontal displacements, one can observe that the patterns of the fingers (Fig.5.47a, b) are totally different from each other at lower injection flow rates. The same phenomena happened at high viscosity ratios. The recovery, for example, is 11.43% for μ_o/μ_w =147.46, ϱ_o/ϱ_w =1.23, and Q =1.8 ml/hr in horizontal displacement but is only 3.74% for μ_o/μ_w =147.46, ϱ_o/ϱ_w =1.23, and at the same flow rate in vertical-upward displacement (see Fig.5.47c, d). This indicates that buoyancy forces played a negative role in vertical-upward displacement at lower injection flow rates, and this point can also be seen from the comparison of oil recoveries, i.e. 5.71% for the vertical-upward displacement (μ_o/μ_w =1.56, ϱ_o/ϱ_w =1.03, Q=1.8 ml/hr) and 32.13% for the horizontal displacement (μ_o/μ_w =1.56, ϱ_o/ϱ_w =1.03, Q=1.8 ml/hr). When the injection flow rate is high, the patterns of the fingers are very close to each other (see Fig.5.48a, b). For a given low viscosity ratio and density ratio (μ_o/μ_w =1.56, ϱ_o/ϱ_w =1.03, Q = 449.4 ml/hr), the recovery is 33.49% for the horizontal displacement and 34.72% for the vertical-upward displacement.

For a given high viscosity and density ratio (μ_o/μ_w =147.46, ϱ_o/ϱ_w =1.23, Q = 449.4 ml/hr) the recovery is 10.22% for the horizontal displacement and 8.96% for the vertical-upward displacement (see Fig.5.48c, d). This also proves that the viscous forces dominate the gravity forces and control the entire displacement process. In addition, the breakthrough recoveries in this study (Fig.5.34) are in good agreement with data published by Araktingi et al. [14] in miscible displacements. Those results discussed above can be proved by comparing the results of Fig.5.2 and Fig.5.34.

The dependence of recovery on the viscosity ratio is shown in Fig.5.49. In this figure the recovery at the breakthrough condition is plotted as a function of viscosity ratio. The recovery at the breakthrough condition decreased from 10.64% for a viscosity ratio of 1.03 to values as low as 4.26% for a viscosity ratio of 147.5 at the injection flow rate of 4.66 ml/hr. Similar trends were observed for other injection flow rates. In addition, early breakthrough of displacing fluid was obtained when the viscosity ratio was high because at high viscosity ratios increased instability caused both the breakthrough time and recovery decreasing [8]. The lowest values of the breakthrough recovery were observed when adverse viscosity ratio augmented the negative effects of buoyancy forces, i.e. when the viscosity ratio is high and the injection flow rate is low.

VERTICAL UPWARD DISPLACEMENT

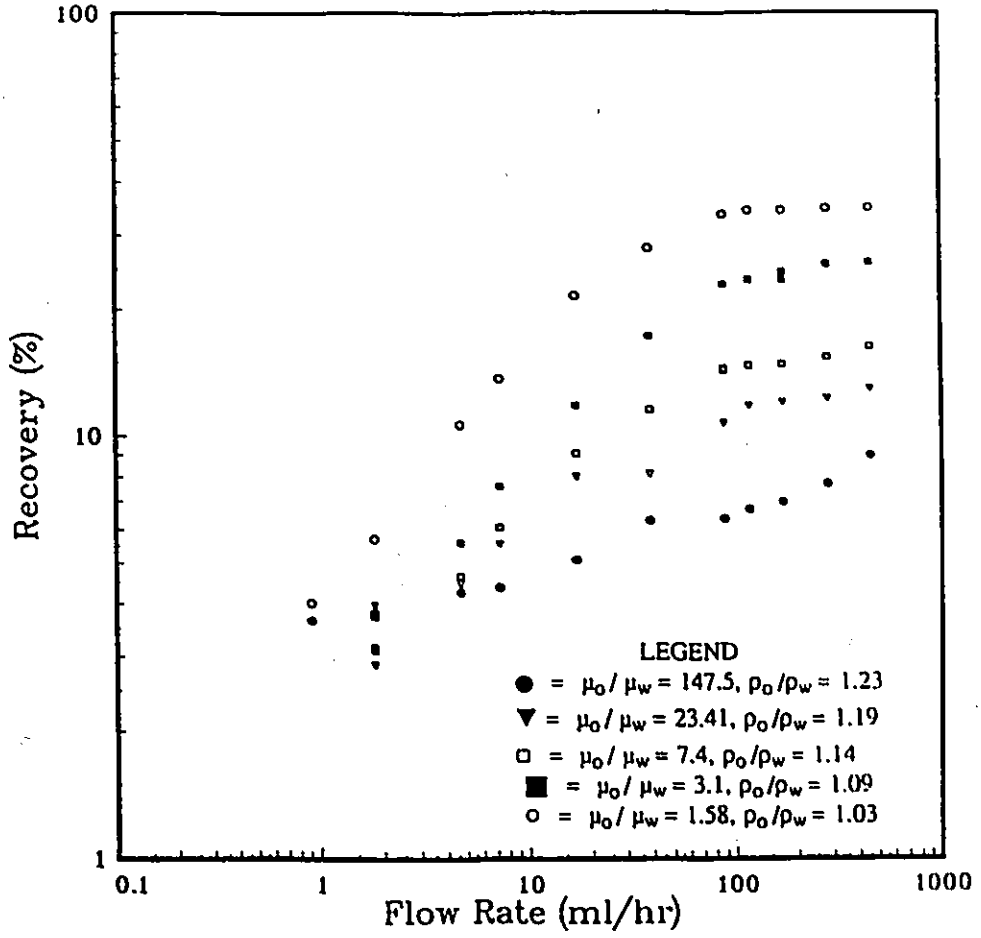

Fig.5.34. Vertical Upward Mode, the relationship between flowrates and breakthrough recovery.

VERTICAL UPWARD DISPLACEMENT

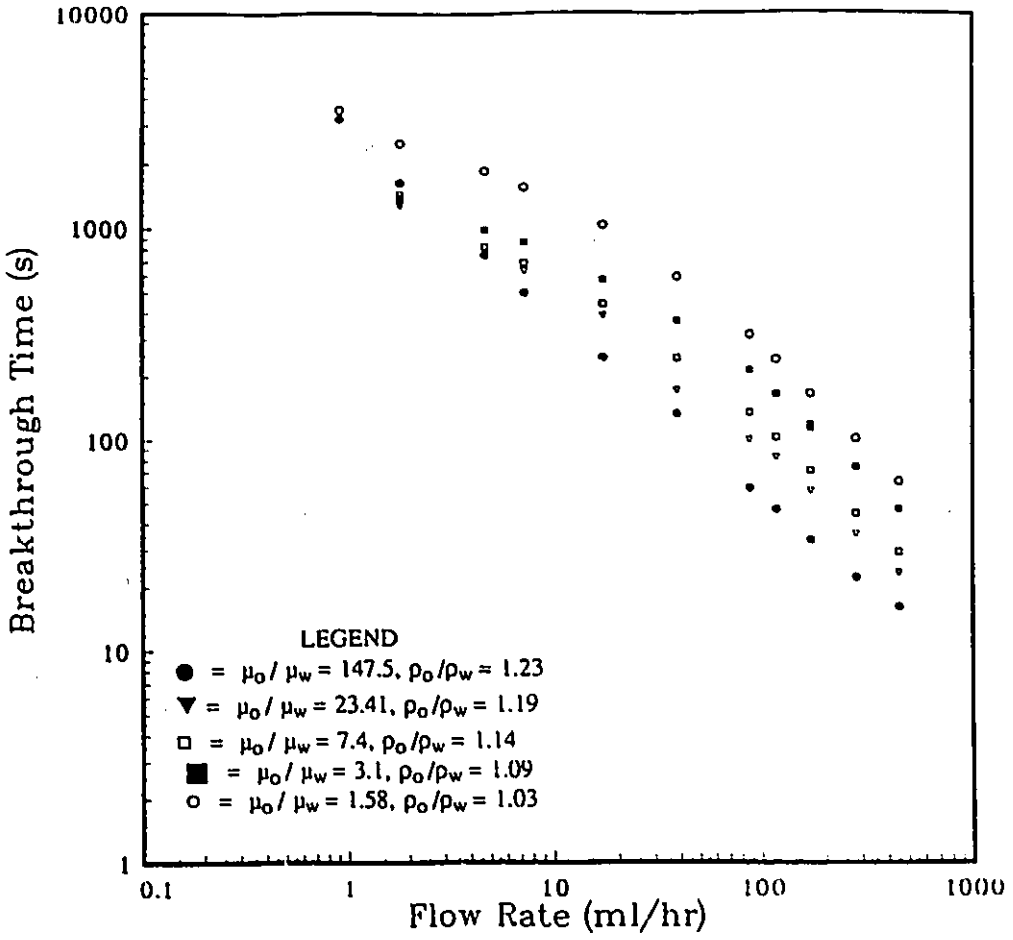

Fig.5.35. Vertical Upward Mode, the relationship between injection flowrate and breakthrough time.

VERTICAL UPWARD DISPLACEMENT

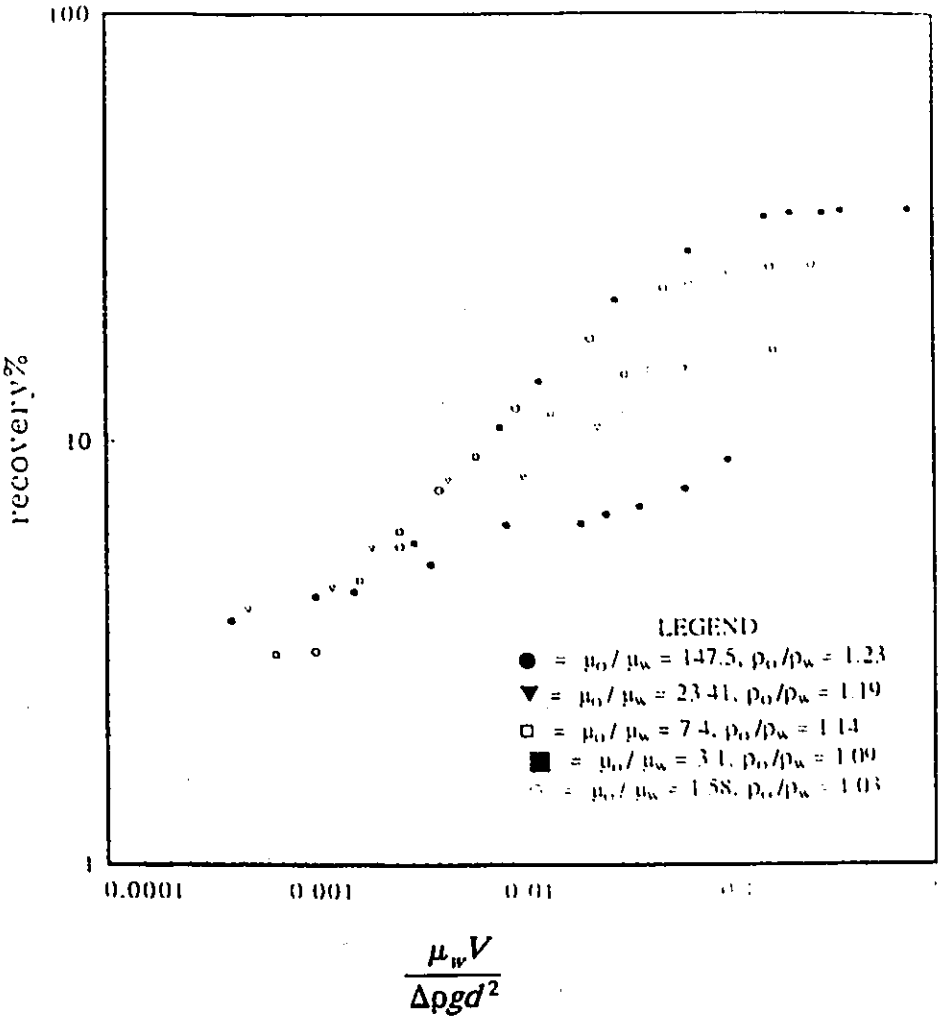

Fig.5.36. Vertical Upward Mode, the relationship between breakthrough recovery and viscous/gravity ratio.

VERTICAL UPWARD DISPLACEMENT

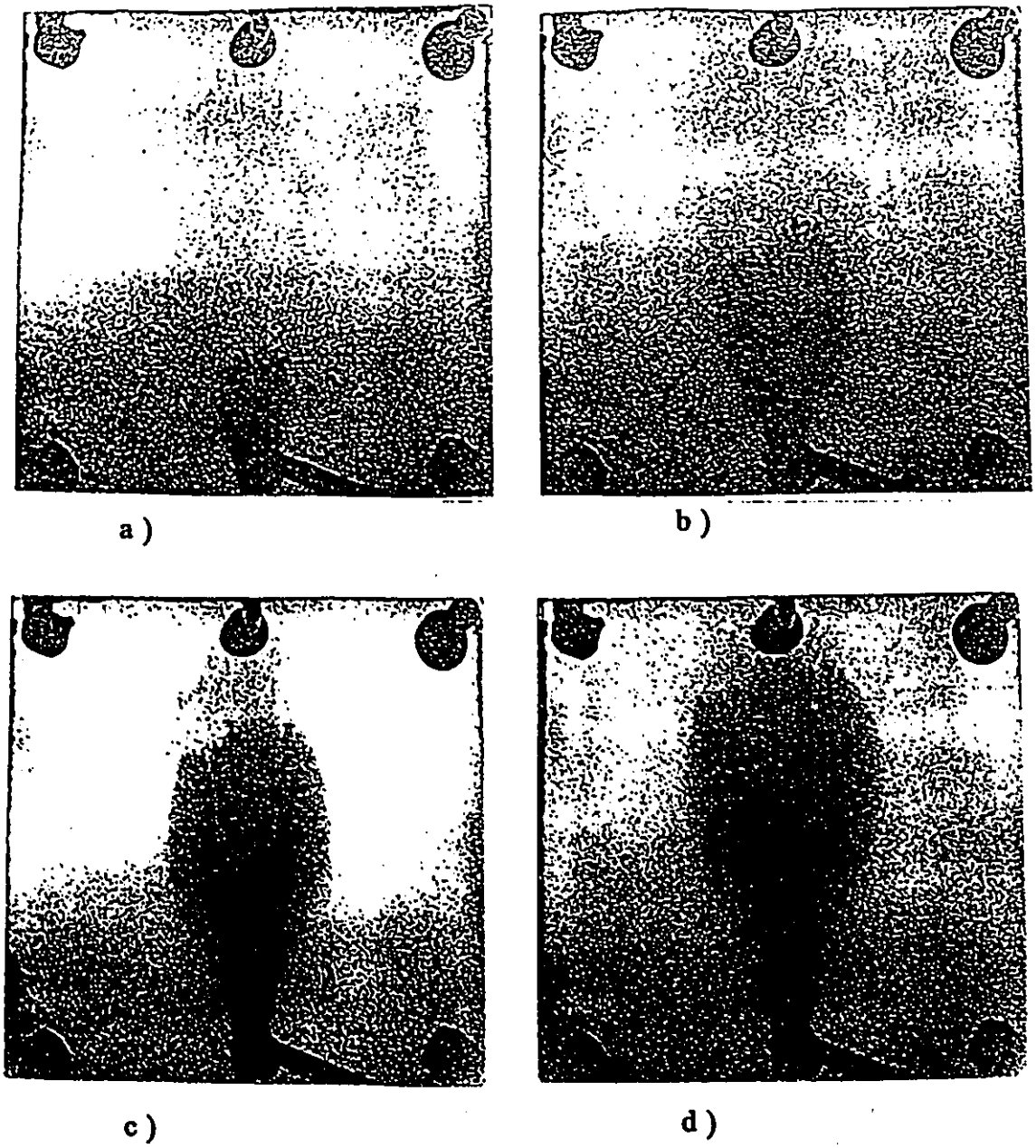

a)

b)

c)

d)

Fig.5.37. The development of the displacement pattern for a low injection flowrate of 4.66 ml/hr. $\mu_o/\mu_w = 1.58$, $\rho_o/\rho_w = 1.03$, (a) time = 260 seconds, (b) time = 700 seconds, (c) time =1165 seconds, (d) time = 1503 seconds, Recovery = 8.73%.

VERTICAL UPWARD DISPLACEMENT

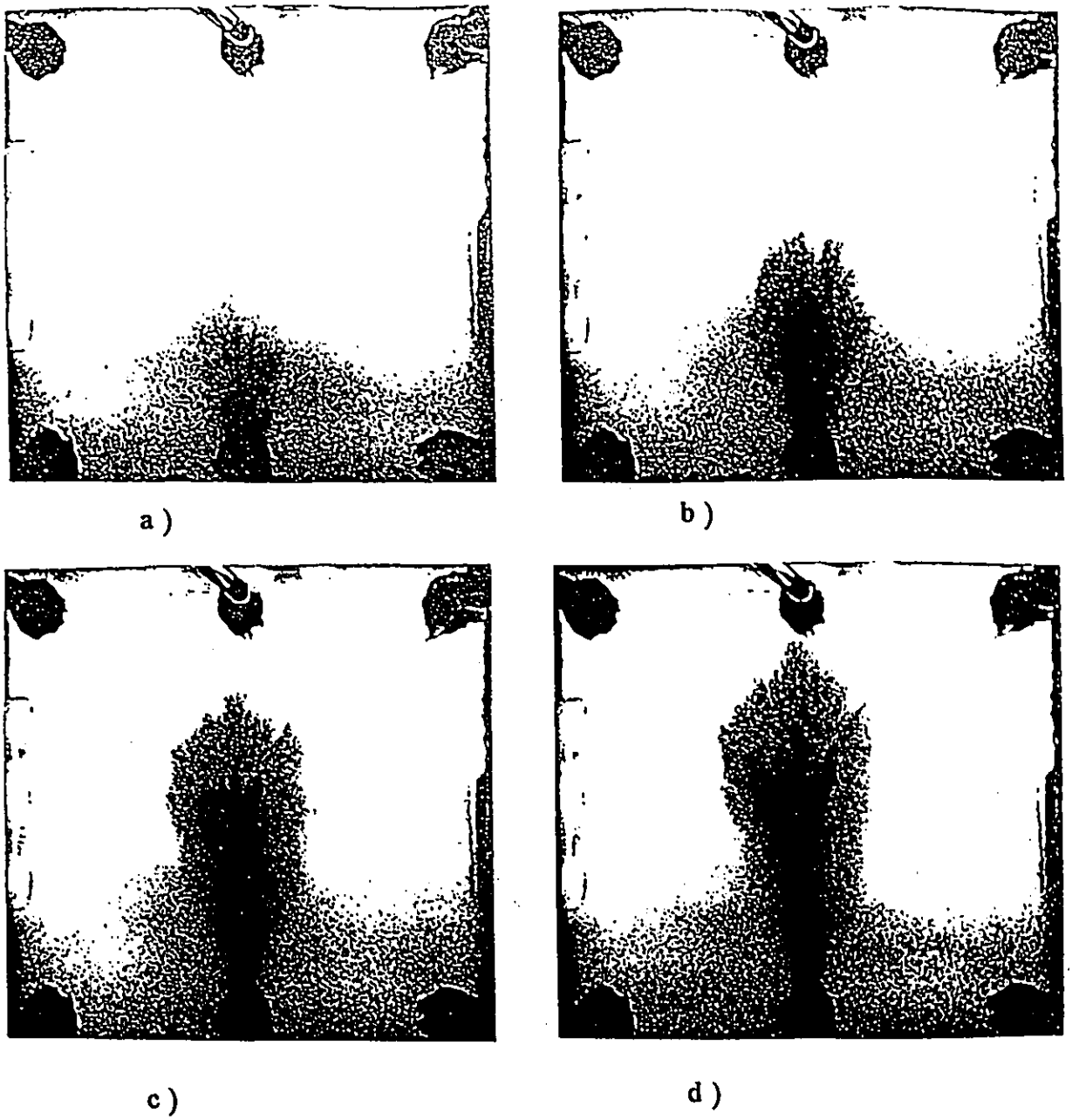

Fig.5.38 The development of the displacement pattern for a low injection flowrate of 4.66 ml/hr. $\mu_o/\mu_w = 3.1$, $\rho_o/\rho_w = 1.09$, (a) time = 186 seconds, (b) time = 419 seconds, (c) time =689 seconds, (d) time = 841 seconds, Recovery = 5.59%.

VERTICAL UPWARD DISPLACEMENT

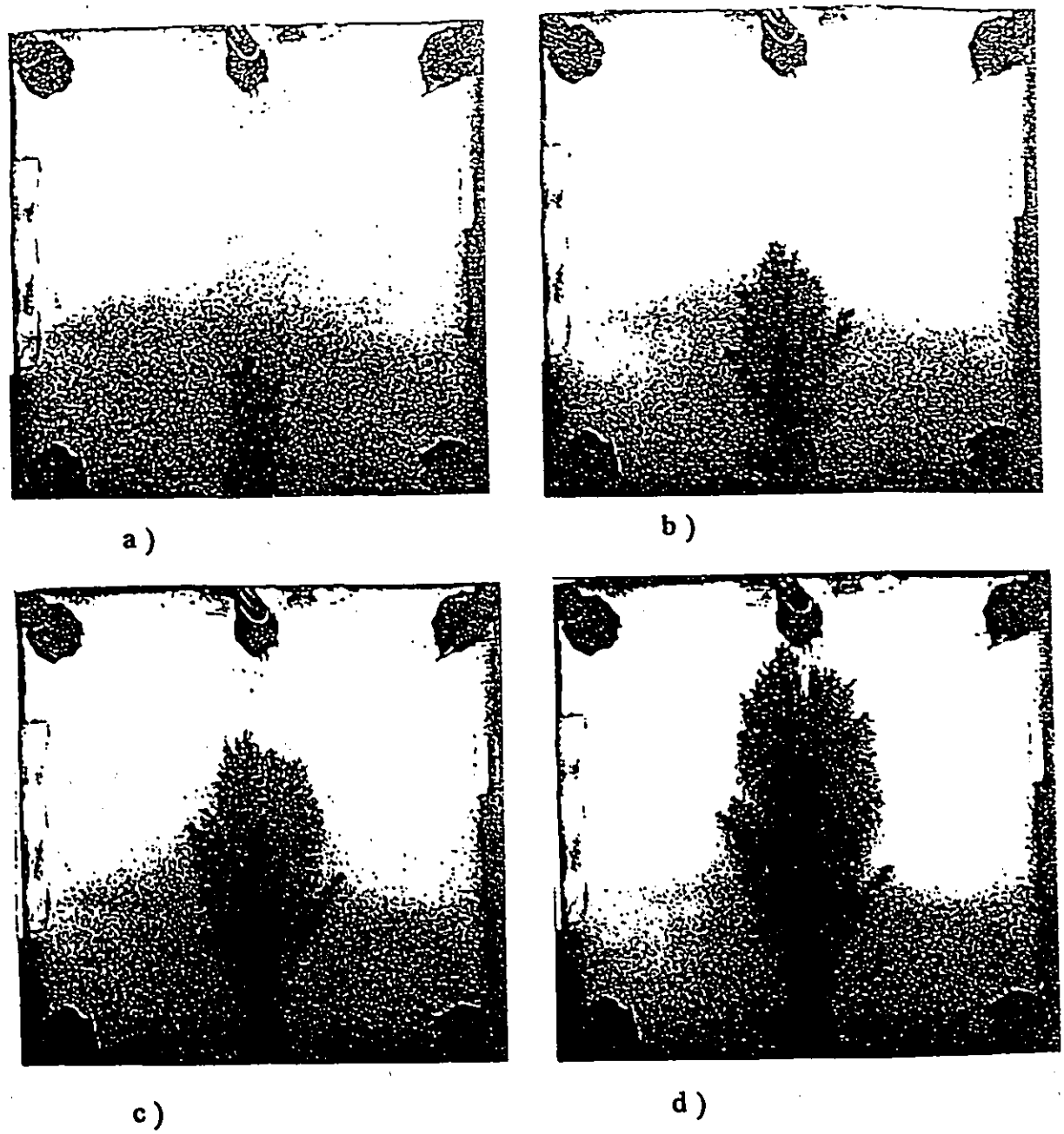

Fig.5.39. The development of the displacement pattern for a low injection flowrate of 4.66 ml/hr. $\mu_o/\mu_w = 7.4$, $\rho_o/\rho_w = 1.14$, (a) time = 135 seconds, (b) time = 317 seconds, (c) time =582 seconds, (d) time = 788 seconds, Recovery = 5.24%.

VERTICAL UPWARD DISPLACEMENT

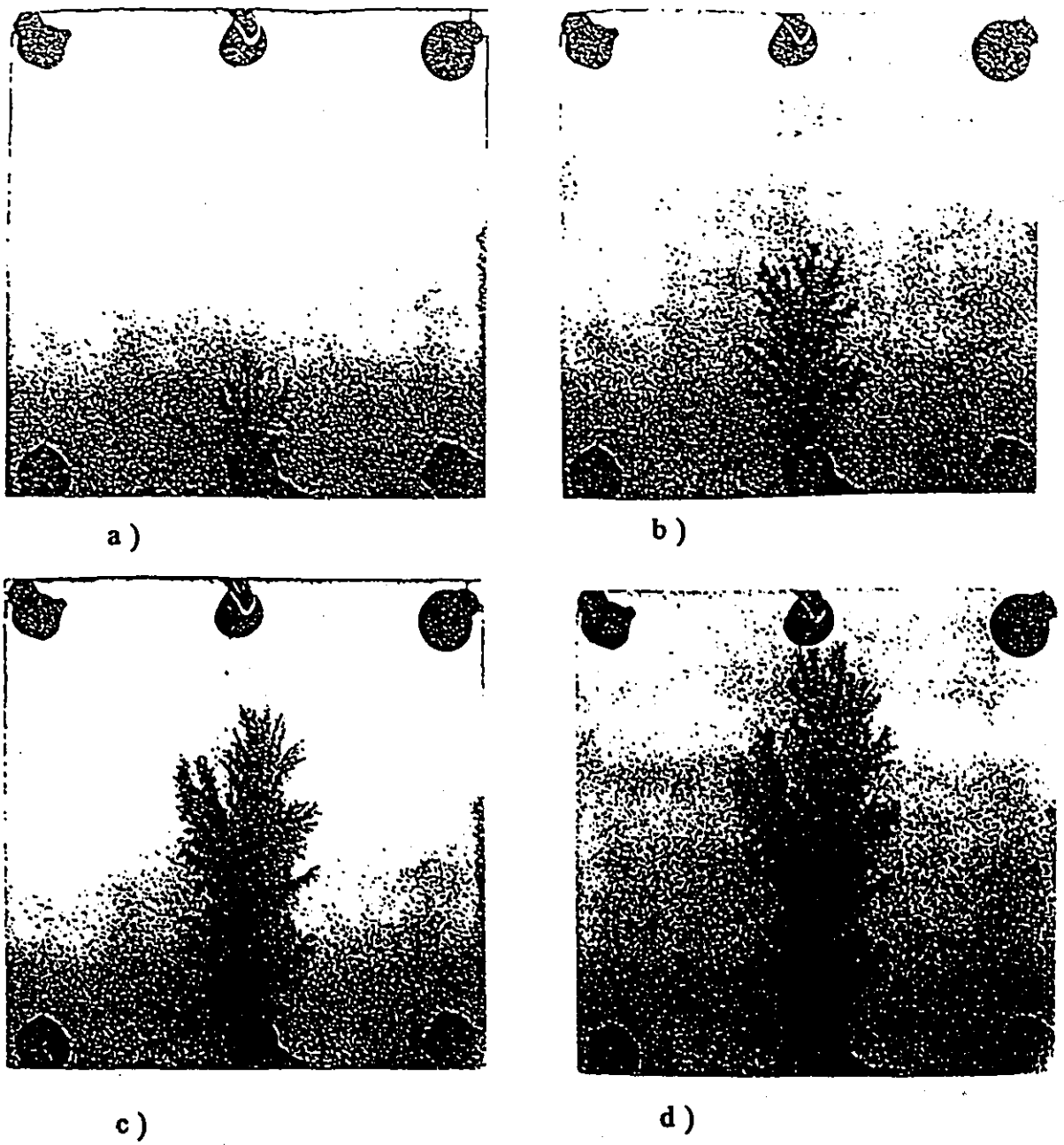

Fig.5.40 The development of the displacement pattern for a low injection flowrate of 4.66 ml/hr. $\mu_o/\mu_w = 23.41$, $\rho_o/\rho_w = 1.19$, (a) time = 101 seconds, (b) time = 204 second, (c) time =466 seconds, (d) time = 638 seconds, Recovery = 4.24%.

VERTICAL UPWARD DISPLACEMENT

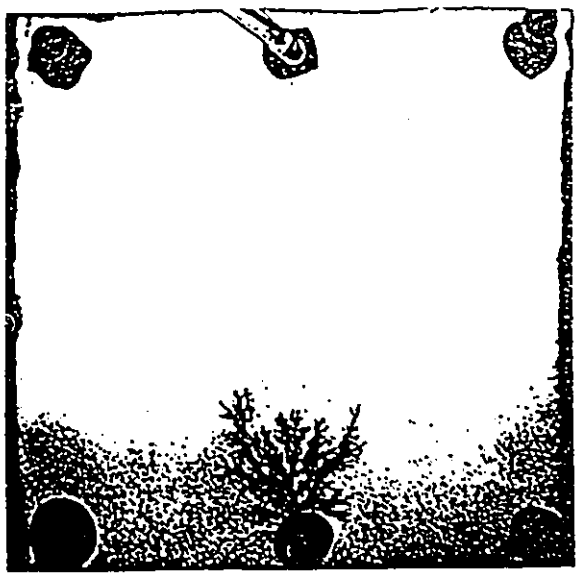

a)

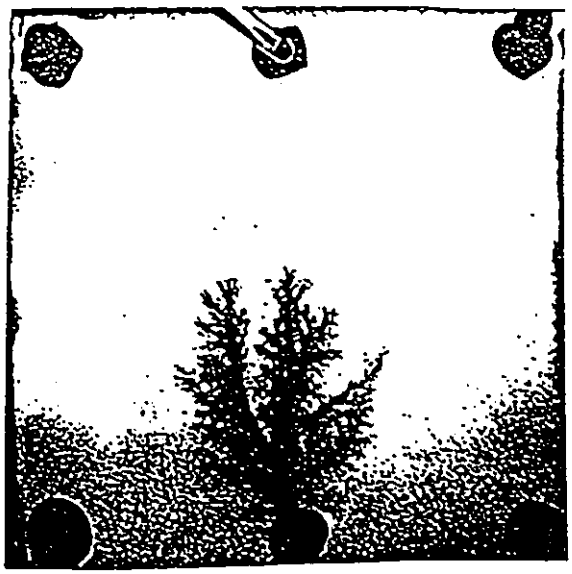

b)

c)

d)

Fig.5.41 The development of the displacement pattern for a low injection flowrate of 4.66 ml/hr. μ_o/μ_w = 147.5, ρ_o/ρ_w = 1.23, (a) time = 80 seconds, (b) time =194 seconds, (c) time =355 seconds, (d) time = 598 seconds, Recovery = 3.97%.

VERTICAL UPWARD DISPLACEMENT

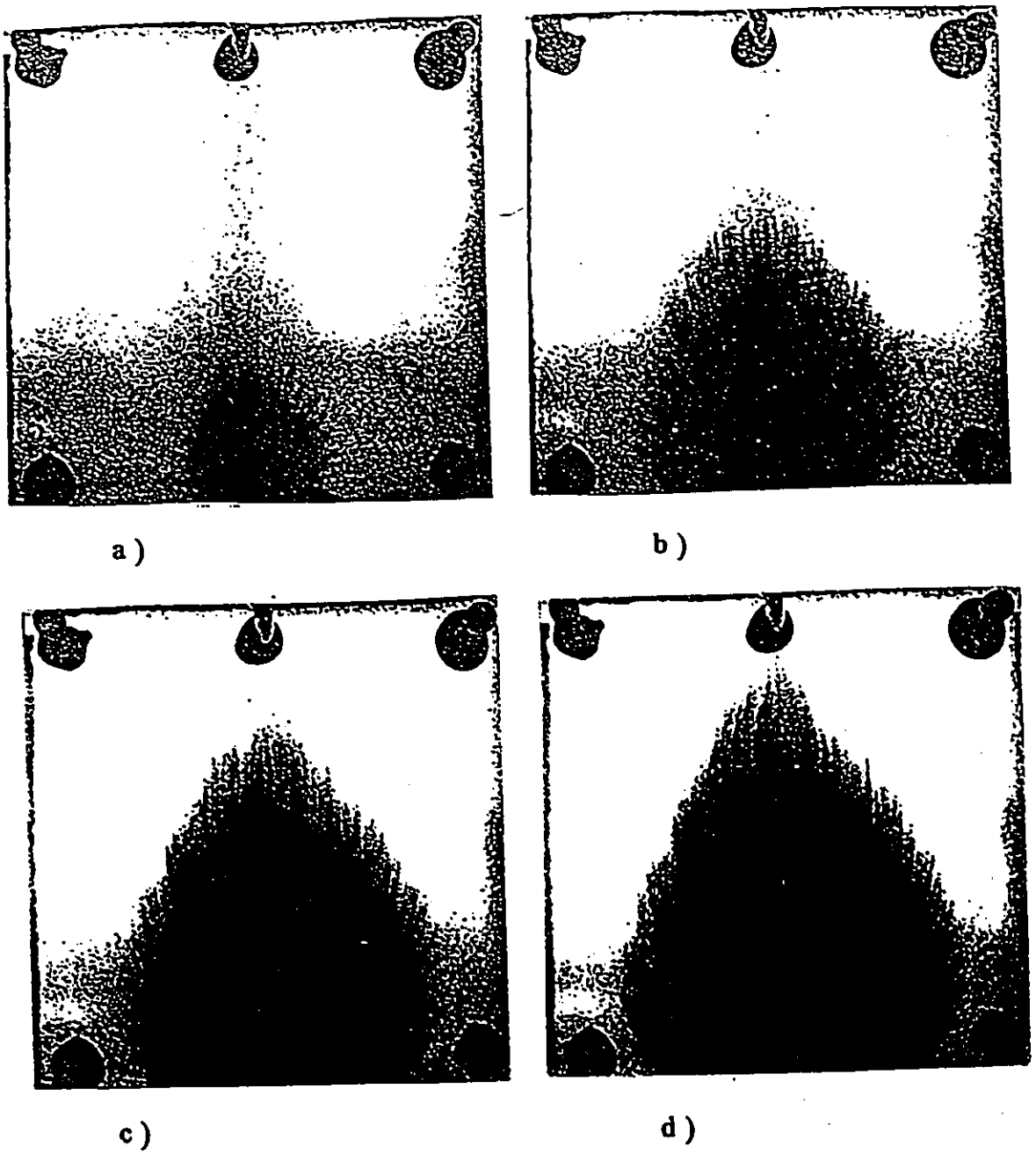

a)

b)

c)

d)

Fig.5.42 The development of the displacement pattern for a high injection flowrate of 169.2 ml/hr. $\mu_o/\mu_w = 1.58$, $\rho_o/\rho_w = 1.03$, (a) time = 22 seconds, (b) time = 87 seconds, (c) time =139 seconds, (d) time = 161 seconds, Recovery = 33.95%.

VERTICAL UPWARD DISPLACEMENT

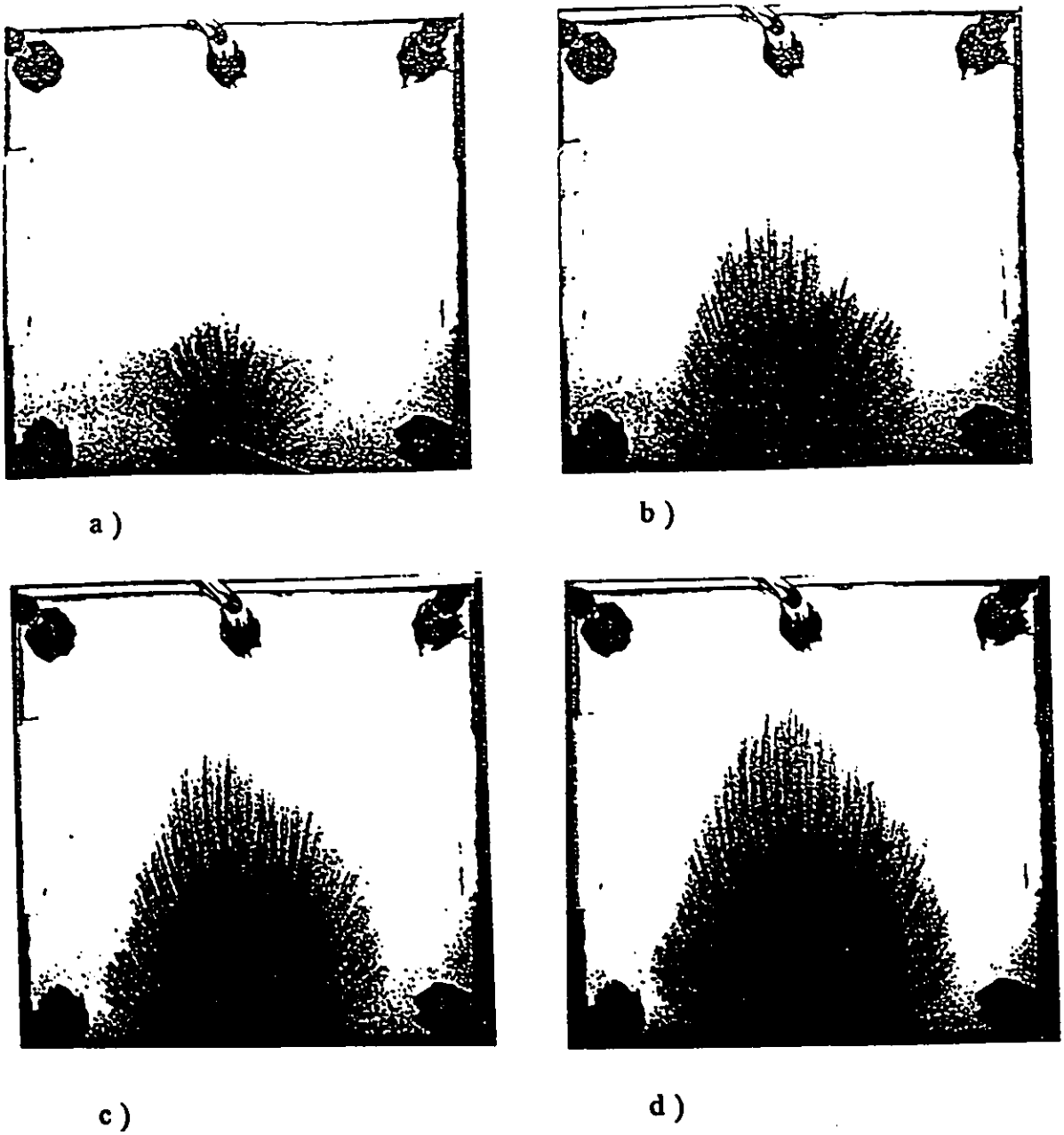

a)

b)

c)

d)

Fig.5.43 The development of the displacement pattern for a high injection flowrate of 169.2 ml/hr. $\mu_o/\mu_w = 3.1$, $\rho_o/\rho_w = 1.09$, (a) time = 17 seconds, (b) time = 43 seconds, (c) time =62 seconds, (d) time = 76 seconds, Recovery = 18.34%.

VERTICAL UPWARD DISPLACEMENT

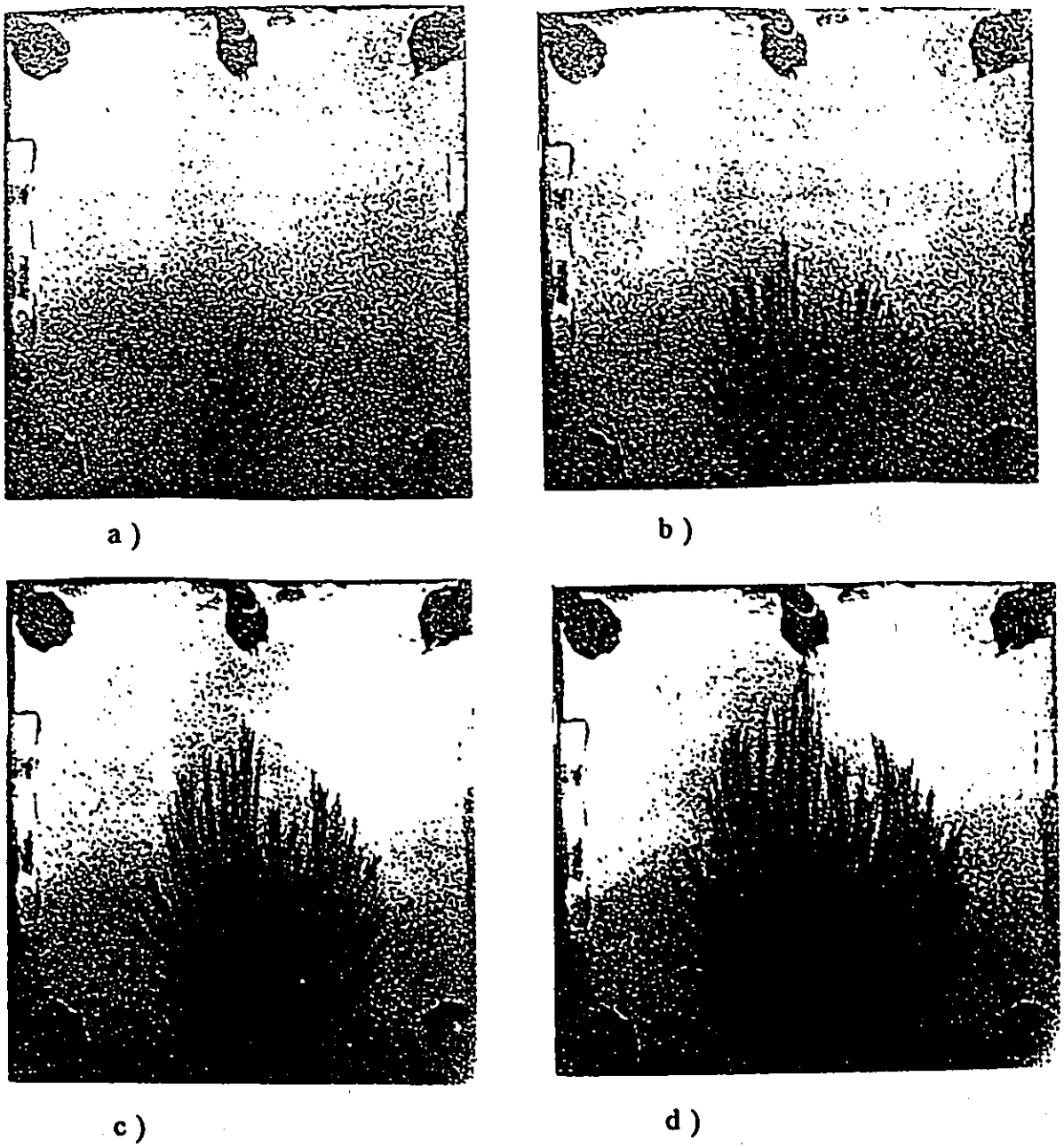

a)

b)

c)

d)

Fig.5.44 The development of the displacement pattern for a high injection flowrate of 169.2 ml/hr. $\mu_o/\mu_w = 7.4$, $\rho_o/\rho_w = 1.14$, (a) time = 11 seconds, (b) time = 25 seconds, (c) time =43 seconds, (d) time = 55 seconds, Recovery = 13.27%.

VERTICAL UPWARD DISPLACEMENT

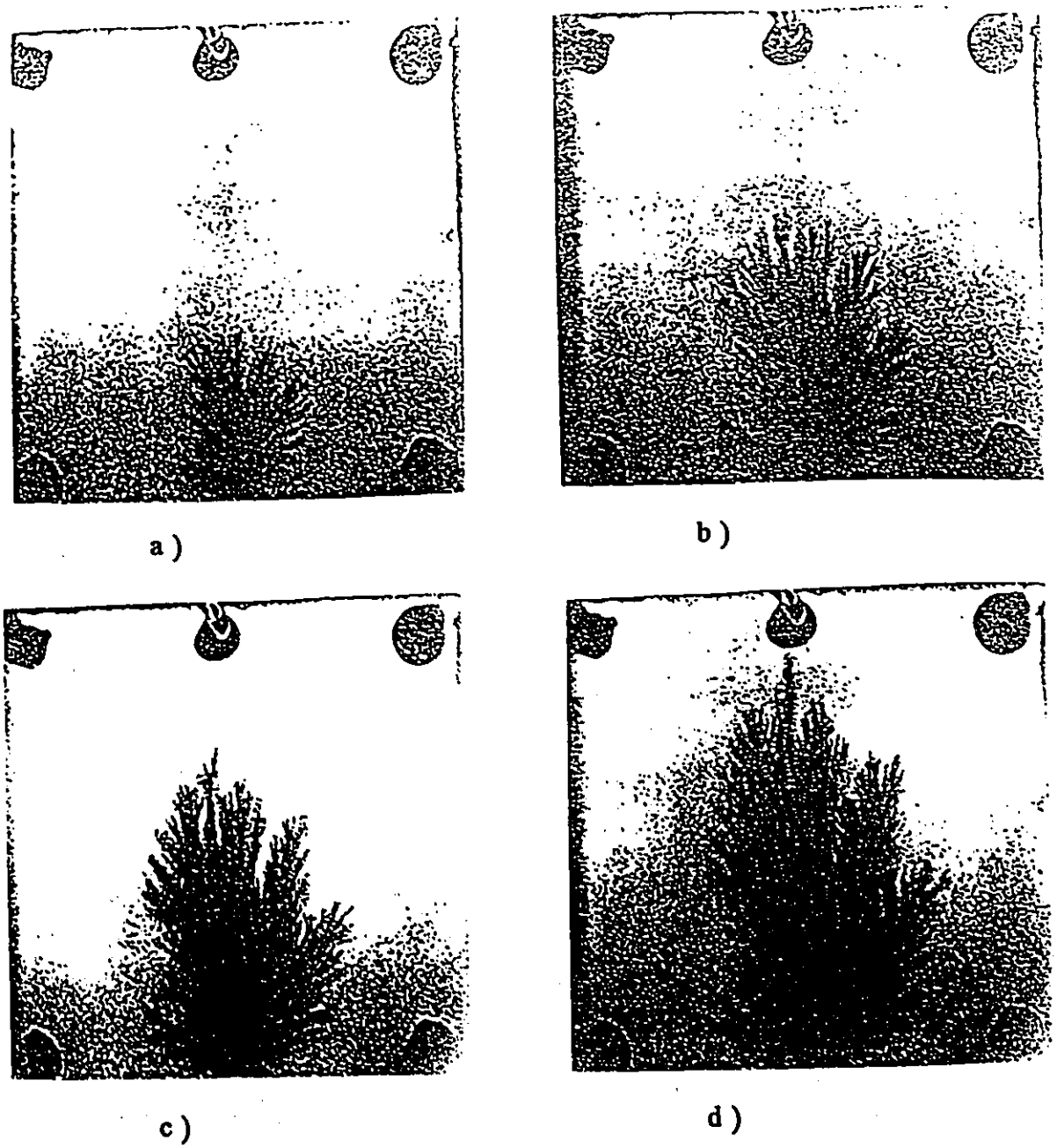

a)

b)

c)

d)

Fig.5.45 The development of the displacement pattern for a high injection flowrate of 169.2 ml/hr. $\mu_o/\mu_w = 23.41$, $\rho_o/\rho_w = 1.19$, (a) time = 11 seconds, (b) time = 25 seconds, (c) time =39 seconds, (d) time = 50 seconds, Recovery = 12.06%.

VERTICAL UPWARD DISPLACEMENT

a)

b)

c)

d)

Fig.5.46 The development of the displacement pattern for a high injection flowrate of 169.2 ml/hr. $\mu_o/\mu_w = 147.5$, $\rho_o/\rho_w = 1.23$, (a) time = 8 seconds, (b) time = 19 seconds, (c) time =28 seconds, (d) time = 33 seconds, Recovery = 7.96%.

VERTICAL UPWARD DISPLACEMENT

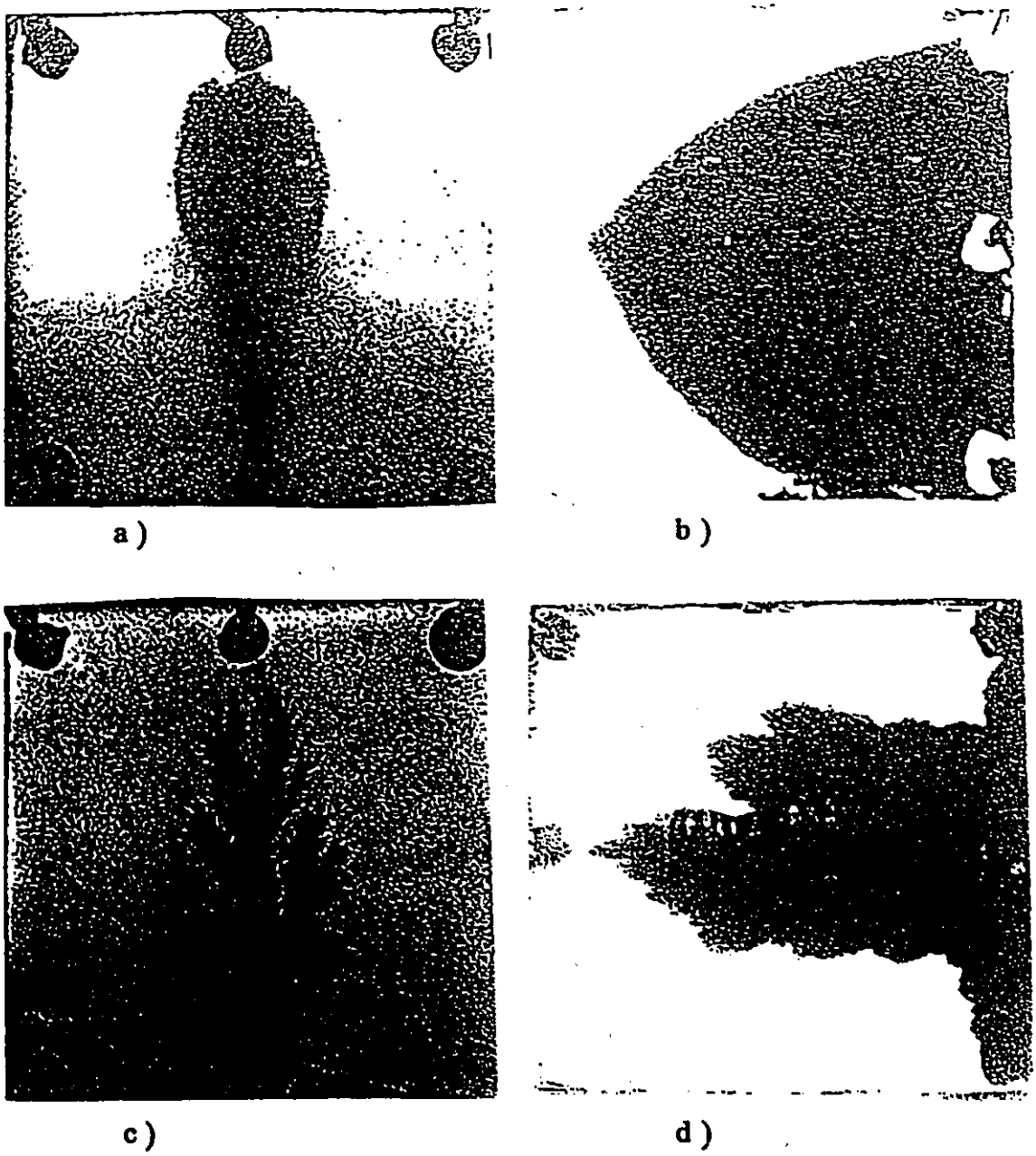

a)

b)

c)

d)

Fig.5.47 Comparison vertical-upward mode (a) and (c) with horizontal mode (b) and (d) at flowrate of 1.815 ml/hr. (a) time = 2523 seconds, R = 5.71%; (b) time = 14016 seconds, R = 32.13%; (c) time =1654 seconds, R = 3.74%; (d) time = 4986 seconds, R = 11.43%.

VERTICAL UPWARD DISPLACEMENT

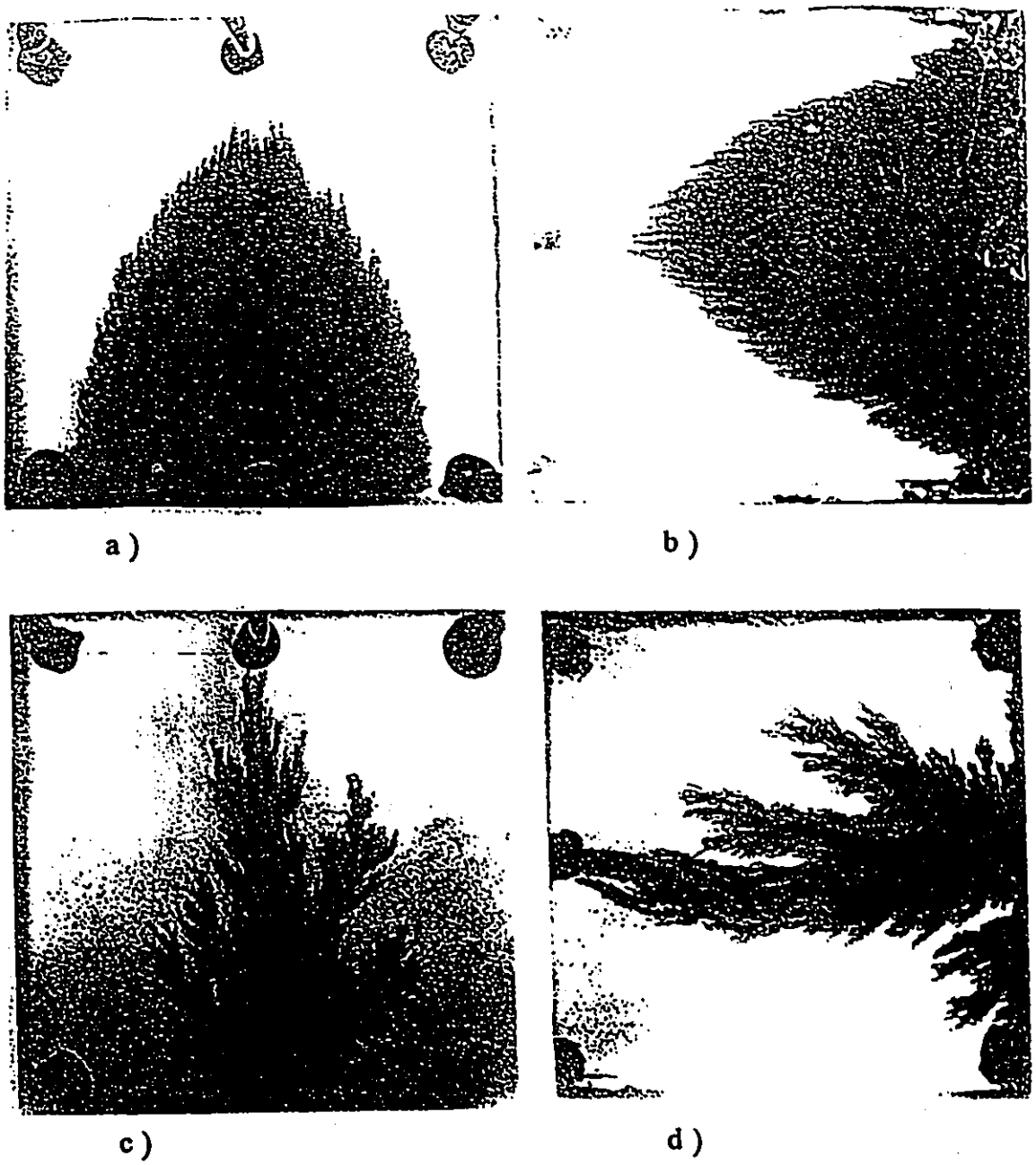

Fig.5.48 Comparison horizontal mode with vertical-upward mode at flowrate of 449.4 ml/hr. (a) time = 62 seconds, R = 34.72%; (b) time = 59 seconds, R = 33.49%; (c) time =16 seconds, R = 8.96%; (d) time = 18 seconds, R = 10.22%.

VERTICAL UPWARD DISPLACEMENT

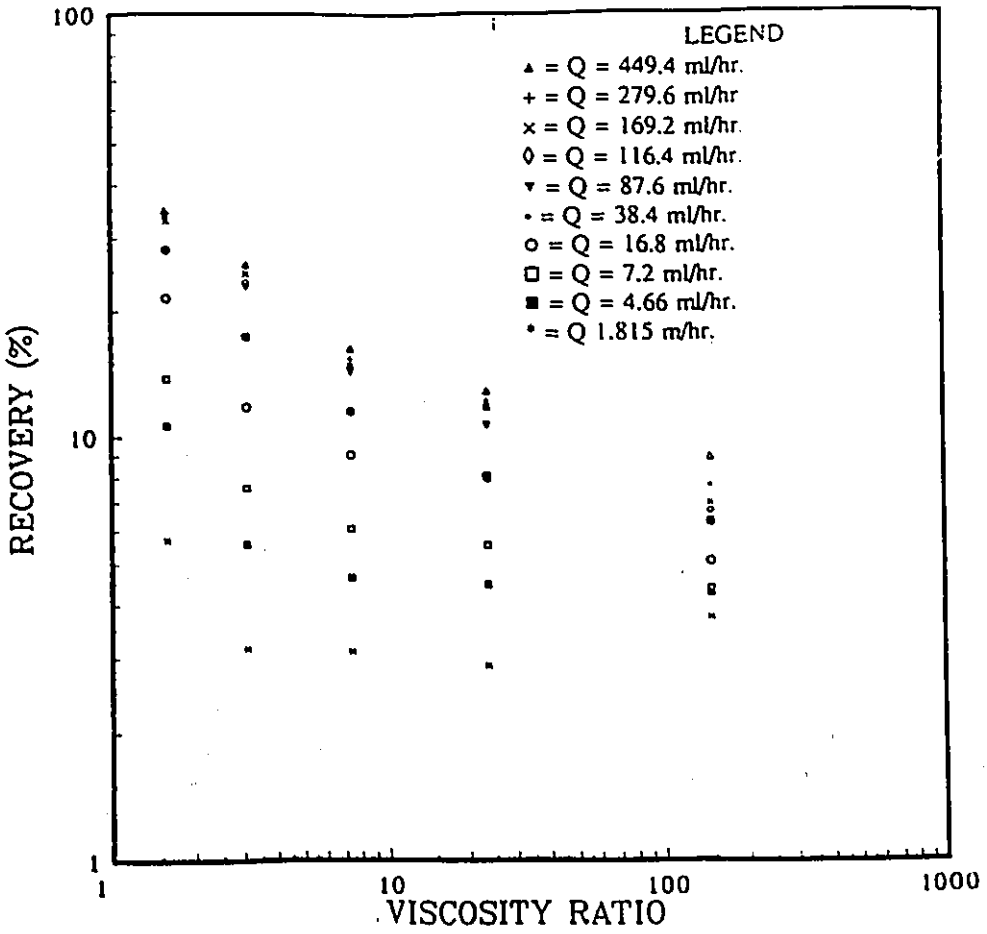

Fig.5.49. Vertical Upward Mode. Relationship between viscosity ratio and breakthrough recovery.

Chapter 6

CONCLUSIONS

1. It is very convenient and useful to study the effects of buoyancy forces by using 2-dimensional consolidated porous medium cells. During the experiments, we can observe the different development of the viscous fingering patterns with various injection flowrates, viscosity ratios and density differences.

2. In the horizontal flow mode, the effects of buoyancy forces can be significant, which cause the displacing fluid to over-ride the displaced fluid.

3. In the vertical flow mode, the effects of buoyancy forces play a very significant role in displacement. In vertical downward flow, $\rho_o/\rho_w > 1$ is favourable to oil recovery efficiency due to the effects of buoyancy forces. In vertical upward flow, the buoyancy forces play a negative role in displacement when $\rho_o/\rho_w > 1$.

4. From the overall point of view, for all flow modes, a small density difference is always favourable for efficient oil recovery.

7.REFERENCES

[1] N. A. Dormani, " Effects of divalent ions in enhanced oil recovery ". M. A. Sc. thesis. Department of Chemical Engineering, University of Ottawa, 1986.

[2] C. A. Page, " Photo-visualization of the effects of buoyancy forces on viscous fingering pattern in vertical aligned porous medium ". B. A. Sc. thesis, 1990.

[3] M. Gholam-Hosseini, " Visualization of water/oil displacement in porous media in the presence of chemical reaction ". M. A. Sc. thesis, Department of Chemical Engineering, University of Ottawa, 1991.

[4] K. N. Jha, Chemistry in Canada, 34, p19, 1982.

[5] J. P. Prince, Canadian Energy Research Institute, Calgary, p9, March, 1980.

[6] F. Stalkup JR, " Miscible Displacement ". Monograph vol.8. Henry l. Doherty Series, Consulting Research Engineer, Arco Oil & Gas Co., 1992.

[7] F. F. Craig. JR, J. L. Sanderlin, D. W. Moore and T. M. Geffen, " A laboratory study of gravity segregation in frontal drives ". Journal of Petroleum Technology, 210, p164-171, 1957.

[8] R. J. Blackwell, J. R. Rayne and W. M. Terry, " Factors Influencing the Efficiency of Miscible Displacement ", Petroleum Transactions, AIME. 216, p1-8, 1959.

[9] F. E. Crane, H. A. Kendall and G. H. F. Gardner, " Some experiments on the

flow of miscible fluids of unequal density through porous media ". Soc. Pet. Eng. J 228, p277-280, 1963..

[10] R. L. Slobod and W. E. Howlett, " The effects of gravity segregation in laboratory studies of miscible displacement in vertical unconsolidated porous media ". Soc. Pet. Eng. J. 231, p1-8, 1964.

[11] J. M. Dumoré, " Stability considerations in downward miscible displacement ".Soc. Pet. Eng. J. 231, p356- 362, 1964.

[12] M. C. Hu, V. Hornof and G. H. Neale, " Visualization of unstable miscible radial displacement in a consolidated porous medium ". Powder Technology, 41, p265-268, 1985.

[13] T. K. Perkins, " Mechanics of viscous fingering in miscible system ". Soc. Pet. Eng. J. 234, p301-317, 1965.

[14] U. G. Araktingi and F. M. Orr Jr., " Viscous fingering, gravity segregation, and reservoir heterogeneity in miscible displacement in vatical cross section ". Chevron Oil Field Research Co. and Stanford University. SPE/DOE 20176, p39-46, 1990.

[15] R. L. Perrine, " The development of stability theory for miscible liquid-liquid displacement ", Soc. Pet. Eng. J. 222, p17-25, 1961.

[16] J. P. Heller, " Onset of instability patterns between miscible fluids in porous media ", J. Appl. Phys. 37, p1566-1579, 1966..

[17] S. T. Lee, G. M. K. Li and W. E. Culham, " Stability analysis of miscible displacement processes ", SPE/DOE preprint 12631, 1984.

[18] H. Siddiqui, " Cluster aggregation and fluid displacement processes in porous

media ", Ph.D thesis, Department of Chemical Engineering, University of Southern California, Dec.1989.

[19] V. Hornof and N. R. Morrow, " Gravity effects in the displacement of oil by sorfactant solutions ". SPE Reservoir Engineering, p627-633, November 1987.

[20] C. A. Page, H. J. Brooks and G. H. Neale, " Visualization of the effects of buoyancy forces on liquid-liquid displacements in vertical aligned porous medium cells ". Experiments in Fluids, 13, p472-474, 1993.

[21] R. Wolfson and J. M. Pasachoff, " Physics " , Little, Brown and Company Boston, Toronto, p382, 1987.

[22] W. S. Francis, M. W. Zemansky and H. D. Young. " University Physics ". Seventh edition, p325-329, 1987.

[23] R. E. Collins, " Flow of fluids through porous materials ", Chapman & Hall Ltd. London, 1961.

[24] M. C. Hu, V. Hornof and G. H. Neale, " Visualization of unstable miscible radial displacement in consolidated porous medium ". Powder Technology, 41 p265-268, 1985.

[25] H. K. Sarma and B. B. Maini, " An experimental evaluation of viscosity grading for controlling fingering in miscible displacements ". Journal of Canadian Petroleum Technology, p36-41, 1992.

[26] H. A. Nasr-el-Din, K. C. Khulbe, V. Hornof and G. H. Neale, " Effects of interfacial reaction on the radial displacement of oil by alkaline solutions ". Revue de l'institut Françis du pétrole, 45, p231-244, Mars-Avril, 1990.

[27] C. Van Der Poel, " Effect of lateral diffusivity on miscible displacement in horizontal reservoirs ". SPE. Reprint Series No.8. p93, 1992.

[28] E. J. Peter, W. H. Broman and J. A. Nroman, " A stability theory for miscible displacement ". Soc. Pet. Eng. J. 279, p1-12, 1984.

[29] L. W. Ni, V. Hornof and G. H. Neale, " Radial Fingering in a Porous Medium ". Revue de l'institut Françis du pétrole, 41, p217-228, Mars-Avril 1986.

[30] T. K. Perkins and O. C. Johnston, " A review of diffusion and dispersion in porous media ". Soc. Pet. Eng. J. 228, p70-84, March 1963.

[31] T K. Perkins and O. C. Johnston, " A study of immiscible fingering in linear model". Soc. Pet. Eng. J. 246, p39-46, 1969.

[32] R. J. Blackwell, " Laboratory study of microscopic dispersion phenomena ". Soc. Pet. Eng. J. 225, p1-8, March 1962.

[33] D. R. Lide, Editor-in-Chief, " Handbook of Chemistry and Physics ". 74th edition, CRC Press, 1993~1994.

[34] H. Nasr-el-din, V. Hornof and G. H. Neale," Radial Fingering in a Water-Wet Porous Medium", Rev. Inst. Franç. du Petrole, 42, p783-796, 1987.

[35] A. L. Pozzi and R. J. Blackwell, " Design of laboratory models for study of miscible displacement ". Soc. Pet. Eng. J. 228, p28-40, March 1963.

[36] F. J. Fayers, " An approximate model with physically interpretable parameter for representing miscible viscous fingering ". SPE Reservoir Engineering, 291, p551-558, May 1988.

[37] F. J. Fayers and M. J. Newley, " Detailed validation of an empirical model for

viscous fingering with gravity effects ". SPE. Reservoir Engineering, 291, p542-550, May 1988.

[38] Brookfield Engineering Laboratories, Inc., " Brookfield synchro-electric viscometer, instruction manual ". August, 1980.

[39] " DMA48 density meter instruction manual ", PAAR in Austria, 1989.

Chapter 8

APPENDIX A

8.1 Viscosity Measurement

The viscosity was measured by using a Brookfield Viscometer with a U.L. adapter (provided by Brookfield Engineering Laboratories). This viscometer operates by measuring the torque necessary to overcome the viscous resistance to the induced movement. The accuracy of this viscometer is about 1--2% of the full scale range employed. Sixteen ml of the solution was placed in the stainless steel tube of the U.L. adapter and then the precision cylindrical spindle was introduced into the cylinder. This assembly was then attached to the viscometer. The measurements were taken after equilibrium was reached [37].

Fig.8.1 shows the relationship between viscosity and concentration of the glycerol solution (at room temperature).

VISCOSITY MEASUREMENT

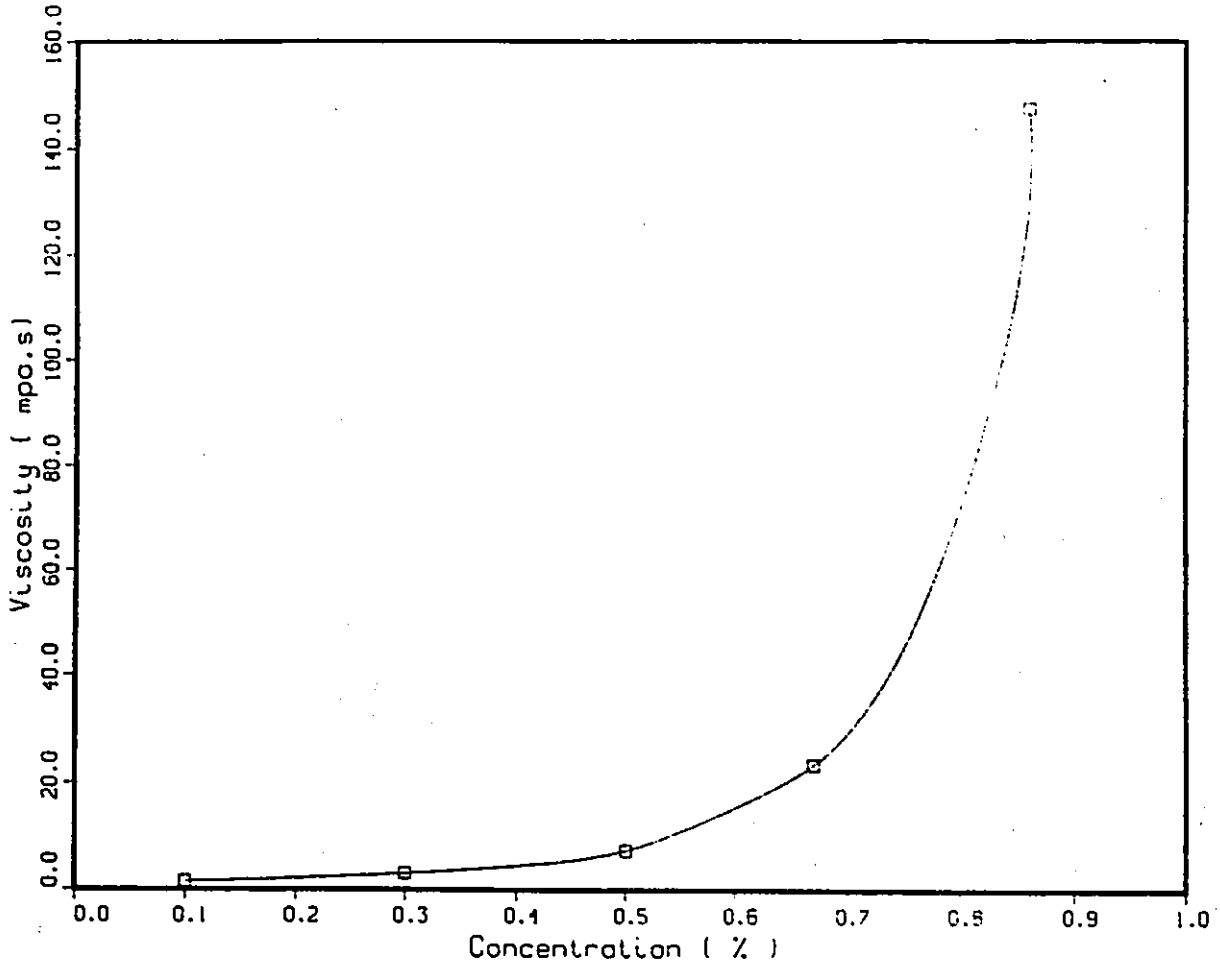

Fig.8.1 The relationship between viscosity and volume concentration of aqueous

8.2 Porosity Measurement

To measure porosity of the cell. the cell was first weighted (M_{cell}) after perfectly drying, then slowly filled the cell with water until the cell was completely saturated and weighted ($M_{cell\text{-}water}$) again; therefore, pore volume and porosity were obtained with the following calculations:

$$M_{water} = M_{cell\text{-}water} - M_{cell} \quad \ldots\ldots\ldots\ldots\ldots\ldots\ldots\ldots \quad (8.1)$$

$$V_{pore} = V_{water}$$

$$= M_{water} / \varrho_{water}$$

$$= (M_{cell\text{-}water} - M_{cell}) / \varrho_{water} \quad \ldots\ldots\ldots\ldots\ldots\ldots\ldots\ldots \quad (8.2)$$

$$V = L \times W \times H \quad \ldots\ldots\ldots\ldots\ldots\ldots\ldots\ldots\ldots\ldots \quad (8.3)$$

$$\varnothing = V_{pore} / V \quad \ldots\ldots\ldots\ldots\ldots\ldots\ldots\ldots\ldots\ldots \quad (8.4)$$

8.3 Density Measurement

The density was measured by using the DMA 48 density Meter manufactured by PAAR in Austria. It determines the density of liquids and gases by electronically measuring the period of oscillation of a glass-U shaped tube. After the sample is injected into this tube, the oscillation is influenced by the mass of the sample. The tube, up to its mounting points on the instrument wall , is called the oscillation cell. The volume of the cell is fixed; therefore, once calibrate with known substances such as air and water. The mass of the sample can be taken as proportional to its density

[38].

Here is the specifications of this Density Meter:

- measuring range is 0 to 3 g/cubic cm. Accuracy is $\pm 1 \times 10^{-4}$ g/cubic cm.
- the temperature accuracy is 0.1 ^{0}C. The temperature range for measurement is usually between -10 to +70 ^{0}C.
- sample size of cell is approximate 0.7 cubic cm.

In this study, the temperature was set at 25 ^{0}C. Fig.8.2 shows the relationship between the density and concentration of the glycerol solution.

DENSITY MEASUREMENT

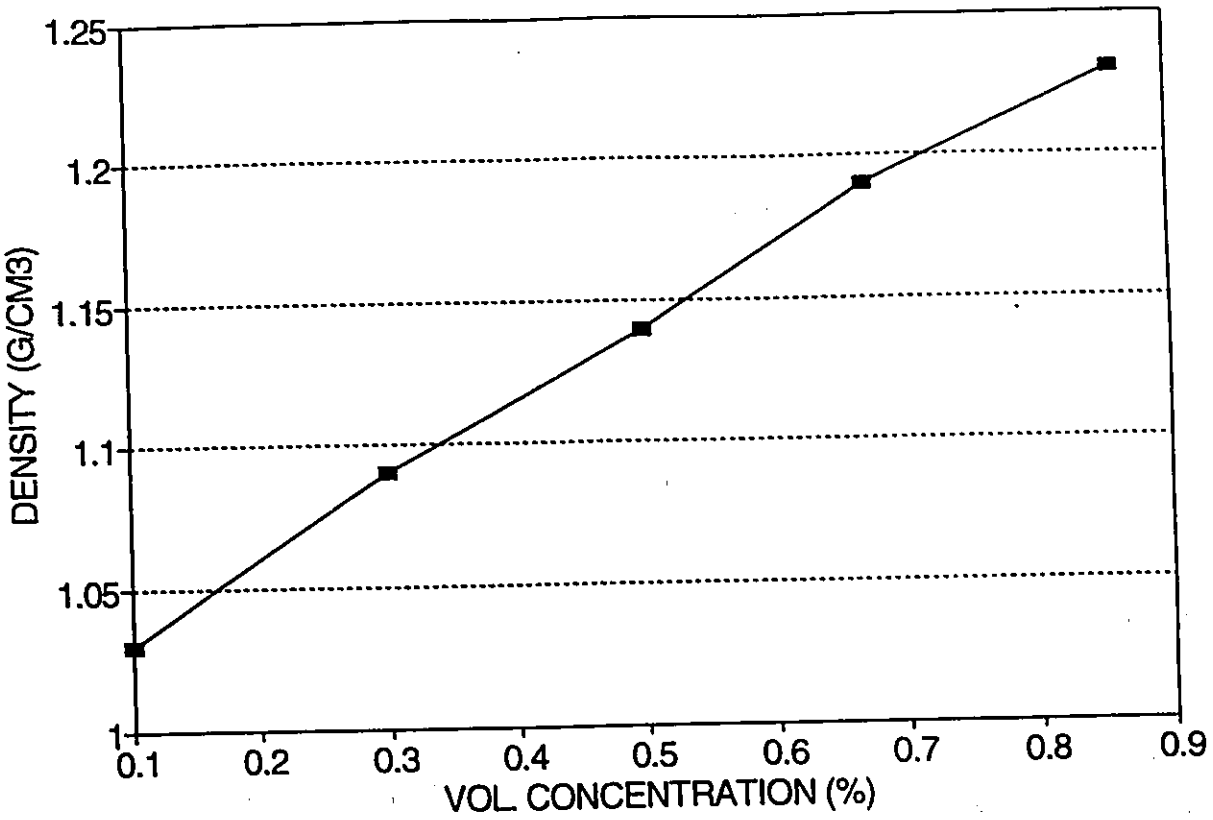

Fig.8.2. The relationship between the density and volume concentration of aqueous glycerol solution at 25°C.